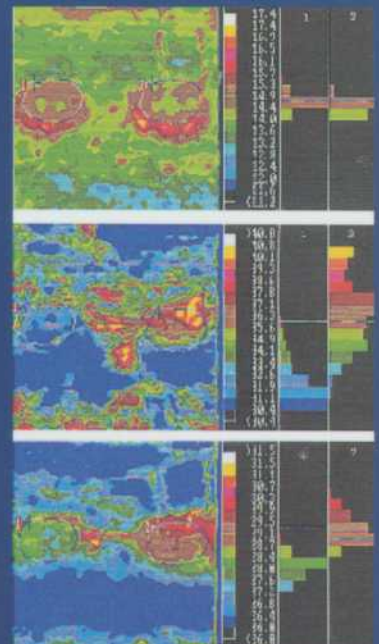
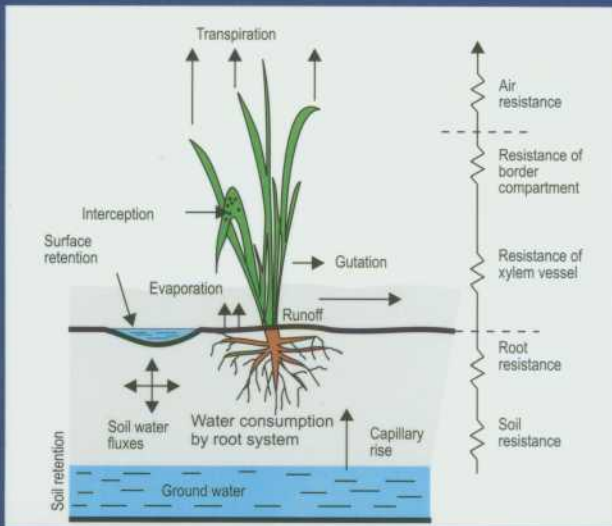


Evapotranspiration into the boundary layer of the atmosphere

Piotr Baranowski, Bogusław Usowicz
Ryszard T. Walczak, Wojciech Mazurek

EDITED BY

Piotr Baranowski, Bogusław Usowicz



Centre of Excellence for
Applied Physics in Sustainable
Agriculture AGROPHYSICS



Institute of Agrophysics Polish
Academy of Sciences



EU 5th Framework Program
QLAM-2001-00428

**EVAPOTRANSPIRATION INTO THE BOUNDARY
LAYER OF THE ATMOSPHERE**

*Piotr Baranowski, Bogusław Usowicz
Ryszard T. Walczak, Wojciech Mazurek*

EDITED BY:
PIOTR BARANOWSKI AND BOGUSŁAW USOWICZ

Lublin 2005



Centre of EC Excellence AGROPHYSICS
Centre of Excellence for Applied Physics
in Sustainable Agriculture QLAM-2001-00428

Reviewed by: Assist. prof. dr hab. Barbara Witkowska-Walczak

ISBN 83-87385-99-9

© Institute of Agrophysics PAS, Lublin 2005

Edition: 180 copies

Project of cover and computer edition: Piotr Baranowski

Printed by: ALF-GRAF, ul. Kościuszki 4, 20-006 Lublin, Poland

PREFACE

The consideration of processes of mass, energy and momentum transfer between the bare soil or crop surface and the atmosphere is crucial in planning and management of water resources and in understanding many phenomena which influence the effectiveness of plant production. The most extensive changes of temperature, humidity and wind occur in the atmosphere region close to the surface, termed the boundary layer. It is defined as extending from the surface to the height at which the wind velocity becomes that of the free air stream.

The exchange of mass, momentum and energy in the atmospheric boundary layer can be described by the state equations and the equations expressing the conservation laws.

Water, which evaporates from the surface of water reservoirs or from the surface of lands, including soil or plant cover surface, becomes unavailable for the use by humans. An important problem for agrometeorology is the ability to determine a consumptive use of water by evaporation, especially in conditions of an unfavourable water balance and limited water resources.

Vaporization is a physical phenomenon, which consists in a phase transition of water from liquid into gaseous state. In case of vaporization from a free water surface or from the soil the term of evaporation is used, whereas vaporization from plants through stomata is called transpiration. Because in some specific measurements and calculations it is difficult to distinguish the evaporation from soil and plants, the summary quantity of vaporization is used, called evapotranspiration. When the evaporation from a large, homogeneous area is considered, such as a catchment or a region, the terms of terrain evaporation and regional evapotranspiration are used.

To make water evaporate continuously from a wet surface, the following conditions should be fulfilled:

- an external source (*e.g.* the Sun) has to deliver energy needed for a phase transition of water in a liquid form into the water vapour, absorbed as the latent heat;
- the water vapour concentration should decrease from the evaporating surface into the surrounding;

These two conditions are closely related to the laws of conservation of energy and mass. The law of energy conservation requires that heat used for

evaporation and other processes was equal to the heat delivered to the surface. The law of mass conservation requires that the intensity of water vapour removal from the evaporating surface was equal to the intensity of its turbulent transfer through the atmosphere.

Potential evapotranspiration and actual evapotranspiration are distinguished. The term potential evapotranspiration was firstly used by Thornthwaite in 1948. This term is commonly used, although some differences of its definition can be found among researchers. The potential evapotranspiration for a given kind of plants is most often defined as a summary evaporation from plants and soil under unlimited availability of soil water for plants under actual values of particular meteorological quantities. According to Brutseart [21] the potential evapotranspiration is a maximum intensity of evapotranspiration from a large surface, covered completely and homogeneously with actively growing plants with unlimited availability of soil water. This definition assumes that the surface is large to eliminate the local advection effect on the course of evapotranspiration. Similarly, according to Kędziora [83], the potential evapotranspiration is the evaporation from a given area covered with short plants, under unlimited availability of soil water.

Biological effects such as the stage of biological development of plants or the resistance of stomata for water vapour diffusion can significantly influence the intensity of evapotranspiration. Therefore, some authors prefer to use the term of potential evapotranspiration, understood as the evaporation from any large uniform surface, wet enough to make the air, contacting with it, be completely saturated with water (*e.g.* a reservoir of stagnant water).

The knowledge of potential evapotranspiration is indispensable in designing irrigation systems because it specifies a necessary amount of water, which should be secured for a given agricultural area.

In the last several years, a generally accepted procedure for determination of potential evapotranspiration of various plant species is, firstly, the evaluation of a reference evapotranspiration for standard surfaces (*e.g.* grass or alfalfa), and then the application of suitable empirical plant coefficients [4, 5, 40, 41, 46, 139, 188].

The actual evapotranspiration is the amount of water transferred into the atmosphere as a result of evaporation from soil or from the plant mass as a result of transpiration under existing meteorological conditions and under the actual water status in the soil [83]. The actual evapotranspiration depends on meteorological, soil, biological and agrotechnical factors.

In the studies of plant water status some indirect methods are used, based on measurements of numerous plant, soil and meteorological parameters. Mutual relations between these measured quantities make it possible to evaluate the water deficiency level in plants. Data collected in chosen measuring points have to be extrapolated into large areas, what is connected with the necessity of considering the spatial variability of these parameters. It is connected with a possibility of occurrence of large errors.

In the last decades a possibility occurred to use remote sensing materials in form of thermal airborne and satellite images in various disciplines of economy, including agriculture problems of plant production. In the conditions of Polish agriculture, where the agrarian structure is dominated by small, cultivated fields, in the high level imaging only large areas of grasslands and forests can be distinguished as a whole.

An enormous number of mono- and multispectral images exist, characterized with a very good geometric and radiometric resolution. They contain lots of information about the studied objects. Together with development of the processing and interpretation systems of airborne and satellite images it is necessary to conduct intensive basic investigations, aimed at explanation of phenomena connected with the reflection of solar radiation, the emission of temperature radiation of natural objects and the relation between the intensity of radiation and the properties of these objects.

This book presents model studies of actual evapotranspiration and plant water stress on the base of remote sensing thermographic data and the knowledge of soil water status and soil thermal properties. The role of water for plants development is described and the physical principles of mass, momentum and energy transport in the boundary layer of atmosphere are presented. The methodology is described for determination the soil thermal properties in relation to soil water content, bulk density of soil, soil temperature, mineralogical composition of soil, soil water potential, atmospheric pressure and soil salinity. The principle of infrared radiation registration with the use of thermographic systems is described as well as the factors influencing the measurement of canopy temperature. The review and analysis of the methods of actual and potential evapotranspiration evaluation are contained as well as the results of laboratory and field investigations, performed on two extremely varied soils with natural meadow plant cover.

CONTENTS

LIST OF USED SYMBOLS	9
1. PLANT WATER RELATIONS	13
1.1. Physiological functions of water	13
1.2. The energetic status and movement of water in soil.....	14
1.2.1. Soil water potential	14
1.2.2. Soil water retention curve	16
1.2.3. Water movement in soil	17
1.3. Water uptake by plants	20
1.4. Plant water stress	22
2. PHYSICAL BASIS OF MASS, MOMENTUM AND ENERGY TRANSPORT IN BOUNDARY LAYER OF ATMOSPHERE.....	24
2.1. Law of mass conservation – continuity equation	24
2.2. Momentum transfer in surface sublayer of boundary atmospheric layer ...	26
2.3. Energy conservation law for atmosphere	27
3. MODELLING OF SOIL THERMAL PROPERTIES	29
3.1. Introduction	29
3.2. Thermal conductivity definition	30
3.3. De Vries model.....	31
3.4. Statistical-physical model of thermal conductivity	33
3.4.1. Model definition.....	33
3.4.2. Basic laws used for construction of the model of thermal conductivity	33
3.4.3. Model construction.....	37
3.4.4. Identification and verification of statistical – physical model	41
3.4.5. Comparison of soil thermal conductivity values obtained from model studies and measurement	46
3.5. Heat capacity determination	48
3.6. Thermal diffusivity determination.....	50
3.7. Thermal characteristics of the studied soil as a function of water content .	51
4. RADIATION TEMPERATURE OF PLANTS	57
4.1. Black body and real bodies radiation.....	57

4.2. Factors influencing the measurement of plant cover radiation temperature	61
4.3. Methods of evapotranspiration determination	67
4.4. Heat balance equation of active surface. Water and heat transport in soil-plant-atmosphere system	73
4.5. Use of radiation temperature of plant cover for determination of actual and potential evapotranspiration as well as plant water stress	80
5. EXPERIMENTAL STUDY ON PLANT WATER STRESS DETECTION AND ACTUAL EVAPOTRANSPIRATION DETERMINATIONI	84
5.1. Aim of the study	84
5.2. Object of the study	85
5.3. Description of measuring system	89
5.3.1. Description of thermographic system AGA 680 SWB	89
5.3.2. AGEMA 880 LWB thermographic system	89
5.3.3. Reflectometric water content measuring device (TDR)	92
5.3.4. Total water potential measuring system	93
5.3.5. Automatic system of agrometeorological data acquisition	94
5.4. Description of laboratory experiment	97
5.5. Description of field experiment	100
5.6. Chosen methods of evapotranspiration determination in field study	101
6. RESULTS AND THEIR INTERPRETATION	104
6.1. Analysis of thermal images	104
6.2. Results of water stress study	110
6.3. Influence of meteorological conditions on measured values of radiation temperature of plants	115
6.4. Determination of hourly and daily values of actual evapotranspiration on the base of heat balance equation of active surface under varying soil water content	126
6.5. Comparison of potential evapotranspiration calculated with various methods with actual evapotranspiration any limitation of soil water availability	132
6.6. Determination of crop water stress index CWSI on the base of radiation temperature of plant cover as well as actual and potential evapotranspiration	136
7. SUMMARY	140

8. REFERENCES	143
9. SUPPLEMENT	153
9.1. A procedure of preparation of basic input data for the model	153
10. ELABORATION OF ALGORITHM OF THE PROGRAMME FOR ESTIMATION OF THERMAL PROPERTIES OF SOIL AND GROUND.....	156
11. ELABORATION OF COMPUTER PROGRAMME FOR CALCULATION OF THERMAL PROPERTIES OF SOIL AND GROUND	157
11.1. Maintenance of thermal.exe programme.....	157

LIST OF USED SYMBOLS

a	absorptance coefficient;
a, b, c	the semi-axes of an ellipsoid;
A_n	density of advection flux into the layer [W m^{-2}];
C	parameter in equation for r_{ah} (Jackson's method); a constant in the equation expressing Wien's displacement law = 2898 [$\mu\text{m K}$];
c	light velocity in vacuum $\approx 3 \cdot 10^8$ [m s^{-1}];
c_p	specific heat of air under constant pressure [$\text{J kg}^{-1} \text{K}^{-1}$];
c_v	heat capacity [$\text{J m}^{-3} \text{K}^{-1}$];
$CWSI$	Crop Water Stress Index;
$D = (e_a^* - e_a)$	vapour pressure deficit [kPa];
d	zero displacement [m]; the depth of the layer [m];
E	density of water vapour flux (evapotranspiration flux) [$\text{kg m}^{-2} \text{s}^{-1}$];
E_a	actual evapotranspiration [$\text{kg m}^{-2} \text{s}^{-1}$];
e_a	actual water vapour pressure in the air [kPa];
e_c^*	saturated water vapour pressure [Pa] in temperature T_c ;
E_p	potential evapotranspiration [$\text{kg m}^{-2} \text{s}^{-1}$];
e_a^*	saturated water vapour pressure in air temperature T_a [kPa];
Δ	slope of the saturation vapour pressure curve in relation to temperature [kPa K^{-1}];
f	a parameter representing the influence of the earth's rotation [rad s^{-1}];
F	vector of water vapour specific flux [$\text{kg m}^{-2} \text{s}^{-1}$];
$f(v)$	function of wind velocity v [m s^{-1}];
f_c	ratio of the surface covered with plants and the total surface;
f_i	the probability of the result "i" in a separate test;
F_p	density of CO_2 flux [$\text{kg m}^{-2} \text{s}^{-1}$];
G	density of the soil heat flux [W m^{-2}];
g	acceleration due to the Earth's gravity ≈ 9.813 [m s^{-1}];
g_{ij}	a coefficient which depends on the shape of particles;
H	density of the sensible heat flux [W m^{-2}];
h	Planck's constant = $6.6256 \cdot 10^{-34}$ [J s];
h_c	crop height [m];

H_R	radiation heat flux [W m^{-2}];
I	thermal value corresponding to temperature T [IU (units of isotherm)]; the current [A];
I_n	intensity of radiation in the direction normal to the surface sending the radiation [$\text{W m}^{-2} \text{sr}^{-1}$];
I_β	intensity of radiation for the angle β between the axle of thermographic device and the emitting surface [$\text{W m}^{-2} \text{sr}^{-1}$];
k	Boltzmann's constant = $1.38054 \cdot 10^{-23}$ [J K^{-1}]; Von Karman's constant ≈ 0.41 ; ration of the specific heat of air for constant pressure and the specific heat of air for constant volume;
k_i	the ratio of mean gradient of temperature within the particle to the mean gradient of temperature in the medium in which the particle is situated;
K	soil water conductivity coefficient [m s^{-1}];
α	thermal diffusivity of the air [$\text{m}^2 \text{s}^{-1}$];
K_v	coefficient of molecular diffusion [$\text{m}^2 \text{s}^{-1}$];
L	latent heat of vaporization (equal to $2448000 \text{ J kg}^{-1}$); the Monin-Obukhov length of stability [m];
$L \cdot E$	density of the latent heat flux (energetic equivalent of evapotranspiration flux) [W m^{-2}];
LAI	Leaf Area Index [$\text{m}^2 \text{m}^{-2}$];
L_p	the thermal conversion factor for fixation of CO_2 [J kg^{-1}];
n	number of serial connections;
p	spectral transmittance of the medium;
P	the probability of occurrence of a given combination of the soil particles;
p_0	standard pressure (1000 hPa);
P_1, P_2	stability corrections for momentum and heat transport, respectively;
p_a	atmospheric pressure [Pa];
\bar{p}	mean atmospheric pressure [Pa];
$q = \rho_v/\rho$	specific humidity of air; the heat flux for the uniform and isotropic medium [W m^{-2}];
Q	heat energy amount [J];
R	gas constant [$\text{J kg}^{-1} \text{K}^{-1}$]; electric resistance [Ω];
R_T	the heat resistance of a given system [KW^{-1}];

r	spectral reflectance of the medium;
r_{ah}, r_{av}	turbulent diffusion resistances for heat and water vapour transport, respectively [$s\ m^{-1}$];
r_c	stomatal diffusion resistance for water vapour transport [$s\ m^{-1}$];
r_{cp}	potential value of stomatal resistance [$s\ m^{-1}$];
r_H	effective aerodynamic resistance for heat and long-wave radiation transfer [$s\ m^{-1}$];
R_i	Richardson's number;
r_k	the internal radius of a sphere [m];
r_z	the external radius of a sphere [m];
R_l	longwave solar radiation flux [$W\ m^{-2}$];
R_{lb}	density of the longwave net radiation flux [$W\ m^{-2}$];
R_n	density of the net radiation flux [$W\ m^{-2}$];
r_s	diffusion resistance of plants for water vapour transport [$s\ m^{-1}$];
R_s	density of the incoming shortwave solar radiation flux [$W\ m^{-2}$];
S	the unit area [m^2];
T	absolute temperature of the object [K];
T_g	soil temperature [K];
T_a	air temperature [K] measured at the reference height z_a ;
T_c	temperature of plant cover [K]; radiation temperature of plant cover under comfort soil water conditions [K];
T_r	radiation temperature a real body [K];
T_s	radiation temperature of plant cover in conditions of limited availability of soil water [$^{\circ}C$];
T_{sf}	total temperature of a crop surface under incomplete cover of soil with plants [K];
T_t	thermodynamic temperature of the body [K];
$(T_c - T_a)_{ll}$	(lower limit of the difference between canopy and air temperatures) [K];
$(T_c - T_a)_{ul}$	(upper limit of the difference between canopy and air temperatures) [K];
u	wind velocity [$m\ s^{-1}$]; number of parallel connections;
u^*	friction velocity [$m\ s^{-1}$];
U	voltage [V];

\mathbf{v}	vector of wind velocity [m s^{-1}];
v_{2m}	wind velocity measured at the height of 2 m above the soil surface [m s^{-1}];
W	energy emitted by the black body in a given temperature [J];
W_a	relative humidity of the air [%];
W_{rz}	energy emitted by the real body in a given temperature [J];
$W_{\lambda b}$	density of the energy flux of black body radiation for a given wavelength [$\text{W m}^{-2} \mu\text{m}^{-1}$];
x_i	content of a selected medium [$\text{m}^3 \text{m}^{-3}$]
z	depth in the soil profile [m];
z_0	aerodynamic roughness of the surface [m];
z_a	reference level for the measurement of wind velocity and air temperature [m];
z_{om}, z_{oh}	roughness parameters of the surface for momentum and sensible heat, respectively [m];
θ	potential temperature [K];
Θ	soil water content [$\text{m}^3 \text{m}^{-3}$];
Ω	angular frequency of rotation vector in a right-hand system
Ψ	water potential expressed as negative value [J kg^{-1}];
Ψ_g	soil water potential [J kg^{-1}];
α_s, α_l	reflection coefficients for shortwave and longwave radiation, respectively;
α	albedo of evaporating surface;
$\delta W/\delta t$	rate of energy storage per unit area in the layer [W m^{-2}];
ε_c	emissivity of the plant cover;
ε_s	soil emissivity;
ε	emissivity of the surface;
ε_a	emissivity of the air;
γ	psychrometric constant [Pa K^{-1}];
η	coefficient of dynamic viscosity [$\text{N m}^{-2} \text{s}$];
λ	wave length [m]; soil thermal conductivity [$\text{W m}^{-1} \text{K}^{-1}$];
ρ	air bulk density [kg m^{-3}];
ρ_d	density of dry air [kg m^{-3}];
ρ_v	actual density of water vapour in the air [kg m^{-3}];
σ	the Stefan-Boltzmann constant = $5.6697 \cdot 10^{-8}$ [$\text{W m}^{-2} \text{K}^{-4}$];

1. PLANT WATER RELATIONS

Plants live and develop in a specific environment. This environment influences plants through the so-called environmental factors, *i.e.* soil, water, temperature, light and air. In fact each external force, substance or conditions acting on living organisms contribute the environmental factors. Not all environmental factors are equally important in a chosen moment. The importance of an individual factor increases and it starts to have a limiting influence when its value tends to exceed limits, within which the organism is able to tolerate its considerable intensity or is able to survive its low concentration. For example, for each plant species there is a maximum and a minimum temperature value, which is tolerated. Between these extreme values there is a range of temperature, which fluctuations have a relatively weak impact on the species survival ability. This range determines the limits of optimum values of a discussed factor. This is a basic rule in ecology. The second rule says, that minimum, maximum and optimum values of a given factor are not constant, but they change depending on other conditions of the organism's growth.

1.1. Physiological functions of water

Water is a fundamental factor in living organisms' life. It is a perfect solvent of numerous substances. The transition of a substance into a solution assures free diffusion of particles and ions, and enables nearing of particles of the reacting compounds, what is necessary for the reaction course. Water is a medium in which the transport of feeding substances takes place from the rooting system to other parts of plant. Water is a substrate in many biochemical reactions, which occur in plants. It is adsorbed in the reactions of hydrolysis, delivers hydrogen in the photosynthesis process and takes part in numerous reactions with various compounds. Water occurring in vacuole, maintains the state of firmness (turgor) of the cells due to the osmotic processes. It has high specific heat and high heat of vaporization, and therefore is a factor participating in regulation of plant temperature. Therefore, water is a universal factor in processes connected with life, because due to its physical and chemical properties, it stimulates the reactions, necessary for proper course of life functions. The lowering of the water content below some level causes such an energetic state, that intensity of many important physiological processes decreases, what can lead to plant's death.

The energetic status of water in plants and in soil decides about the optimum course of physiological processes and about the occurrence of plant water stress.

1.2. The energetic status and movement of water in soil

1.2.1. Soil water potential

Soil can be considered as a multicomponent thermodynamic system, described by a set of macroscopic quantities, such as temperature, pressure, volume, entropy, molar mass of particular components. The way of description of this system depends on processes, which will be considered. For the description of energetic status of water in the soil, a function of state is used, called the thermodynamic potential or the Gibbs' free energy. The quantity that characterizes the change of thermodynamic potential, which is caused by the change of content of a given component, is called a specific partial energy of this i -th component or its chemical potential μ_i . In respect to the soil water as a soil component, it is assumed call the chemical potential μ as the soil water potential. The total derivative of the soil water potential μ is expressed by the formula:

$$d\mu = \left(\frac{\partial\mu}{\partial P}\right)_{T,\Theta,C} dP + \left(\frac{\partial\mu}{\partial T}\right)_{P,\Theta,C} dT + \left(\frac{\partial\mu}{\partial\Theta}\right)_{P,T,C} d\Theta + \left(\frac{\partial\mu}{\partial C}\right)_{P,T,\Theta} dC + g dz \quad (1)$$

where: Θ – the soil water content, p – the pressure, C – the concentration of soil in the soil solute, T – the temperature, g – the acceleration due to gravity, z – the distance from a reference zero point.

For the soil water potential as a thermodynamic function, it is impossible to derive its absolute values. Instead, its values in relation to a conventional state, called the reference state, are determined. It is the potential of the distilled free water, which is under a normal atmospheric pressure, placed at an assumed zero level in gravitational field in reference temperature. According to the definition of the International Soil Society Commission for the Soil Physics Terminology from 1976, the total water potential in the soil at temperature T_0 , is the work amount used per mass unit of free water [J kg^{-1}], which should be done by external forces to transfer irreversibly and isothermally an infinitely small amount of water from the reference state to the liquid phase of the soil in an investigated point.

After integration and expressing the potential in reference to the zero level, equation (1) takes the form:

$$\mu = (\mu_\Theta)_{T_0} + (\mu_p)_{T_0} + (\mu_c)_{T_0} + gz + \int_{T_0}^T s dT \quad (2)$$

where: $(\mu_{\ominus})_{T_0}$ – a component connected with changes of water content (the matric potential), $(\mu_p)_{T_0}$ – a component connected with changes of external pressure – the pressure potential, $(\mu_c)_{T_0}$ – a component connected with concentration of salt in the soil solute – the osmotic potential, $gz = \mu_g$ – a component which characterizes the effect of external forces – the gravitational potential, where z is a distance from a conventional zero level, $\int_{T_0}^T s dT$ – describes

the change of potential as a result of temperature change, s is the partial specific entropy of water. The unit of soil water potential is $[\text{J kg}^{-1}]$, $[\text{J m}^{-3}]$ or $[\text{J mol}^{-1}]$.

Because $[\text{J m}^{-3}] = [\text{N m}^{-2}]$, the soil water potential can be expressed in pressure units, *i.e.* hPa, bar, cm H₂O. Since the potential values, expressed in pressure units, change in a very wide range, it was proposed to introduce the quantity pF of the soil water potential, which is a logarithm with the base 10 of the equivalent pressure expressed in centimeters of H₂O. The values of pF in relation to other soil water potential units are presented in Table 1. In this book the values of soil water potential are expressed in units of pF, cm H₂O and bars.

Table 1. Relations between pF values and equivalent pressure units [13]

pF	J m ⁻³	Pa	cm H ₂ O	bar
0.4	245	246.13	2.51	0.0025
1.0	981	980.60	10.00	0.0098
1.5	3100	3100.66	31.62	0.031
2.0	9810	9806.00	100.00	0.098
2.2	15596	15541.53	158.49	0.155
2.3	19620	19565.91	199.53	0.196
2.7	49050	49146.69	501.19	0.491
3.0	98100	98060.00	1000.00	0.981
3.4	245250	246315.93	2511.89	2.463
4.2	1471500	1554146.08	15848.93	15.541

In practical measurements of the soil water potential, the so called equivalent pressure is measured, *i.e.* the pressure which should be applied to the soil solute to restrain the migration of clean water through the semipermeable medium to the soil solution in which water has lower potential. A negative pressure can be also applied on clean water. The instruments used in these measurements are tensiometers, suction plates or pressure plates (Richards chambers). In the thermodynamic equilibrium state, the total potential of water is the same in all phases; therefore it is possible to determine the potential in any phase. In some cases it is convenient to measure the total soil water potential by determination of the relative water vapour pressure in the sample. The relationship between the soil water potential and the relative water vapour pressure in the sample in the range of 98.5-100% was used for the construction WESCOR instrument.

1.2.2. Soil water retention curve

The basic characteristic of soil water properties is the relation between the soil water potential and the soil water content. In practice, the plot of the relation between the pF and the soil water content is called the pF curve or the water retention curve. Each soil has its characteristic pF curve, which contains, between others, the information about the availability of soil water for plants. In the pF curve the following ranges of the soil water availability can be distinguished (Fig. 1).

Below the pF value of 1.8 we deal with the so-called gravitational water, occurring in the soil after heavy rainfalls or directly after irrigation. In this case, water is excessively moistened and inconvenient aeration conditions for plants exist in it. The ability to retain water in specific conditions contrary to the gravitation force is expressed through the field water capacity in the range of pF from 1.8 to 2.7 or even 3.4 depending on the soil type and the position of soil water surface. From pF 2.0 to pF 3.0, the easily available water is distinguished. The value of pF 3.0 specifies a critical water content value, below which the limitation of soil water availability for plants occurs. From pF 3.0 to pF 4.2 the difficultly available water and above pF 4.2 the unavailable water can be distinguished.

When the soil sample is dried, the soil water potential values are different for any water content value than in the wetting process, so the relation between these two quantities is ambiduous. Similarly as in case of other soil physical characteristics, the hysteresis phenomenon occurs here. The hysteresis is caused by high differentiation and irregularities of pore sizes, by water adsorbed by the

surface of soil solid phase and by the contact angle between the surface of solid phase and the water-air contact surface in soil, called the wetting angle. The way, on which a given soil thermodynamic state was gained has an impact on the water content – potential relation.

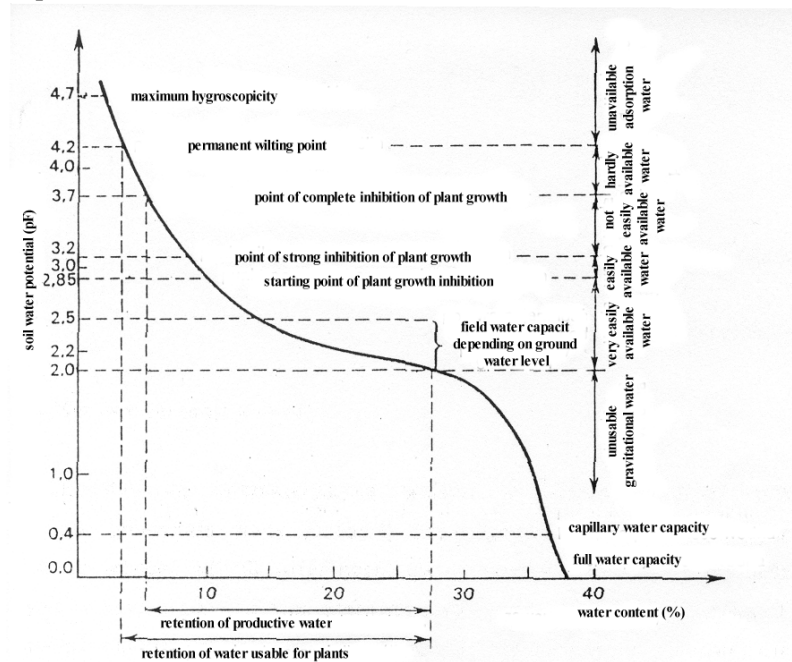


Fig.1. Soil water retention curve after Turski *et al.* [162]

1.2.3. Water movement in soil

The concentration of soil water changes as a result of rainfall water infiltration, evaporation, and water uptake by plants. The soil water constantly moves due to existence of the soil water potential difference and dynamical temperature gradients. The highest soil water changes occur in the subsurface layers, mostly influenced by the external factors and plants through the rooting system. The intensity of water movement in soil in isothermal conditions depends on the grain size distribution of the soil material, its bulk density and potential difference.

A one-dimensional flow of water in the soil is described by Darcy's equation:

$$\vec{q} = -K(\Theta) \frac{\partial \Psi}{\partial z} \quad (3)$$

where: \vec{q} – the water flux (the amount of water flowing in the unit time through the unit surface perpendicular to z direction), Θ – the volumetric soil water content, Ψ – the soil water potential, K – the coefficient of hydraulic conductivity, which is a function of the water content Θ .

In case of the water saturation state, it is generally assumed that K has a constant for a given soil type, however in an unsaturated state K changes even by several orders of magnitude with the change of soil water content. With the decrease of water content, soil pores with the largest sizes, *i.e.* these with best water conductivity properties, are emptied. Water remains in smaller pores, with worse conductivity properties. A violent decrease of water conductivity of the soil, which has large porosity, *e.g.* sandy soil, results in the decrease of soil water content, causing the deepening of plant water stress.

The process of water flow in the soil profile can be described with the use of the mass conservation law, what can be expressed by equation:

$$\frac{\partial}{\partial t} \iiint_V \Theta dV = \iint_S \vec{q} dS \quad (4)$$

where: \vec{q} – the water flux [cm s^{-1}], dS – a surface element [cm^2],
 dV – a volume element [cm^3], t – the time [s].

For a field with sources, the equation (4) can be converted into a differential form, obtaining the continuity equation:

$$\frac{\partial \Theta}{\partial t} + \nabla \cdot \vec{q} = f(\vec{r}, t) \quad (5)$$

where: ∇ – the differential nabla operator, $f(\vec{r}, t)$ – the source function depending on the position and time. The rooting system is just such a negative source of water, which efficiency depends on the external conditions and the stage of plant phonological development. By uptaking soil water, plant strongly reduces water content around the rooting system. A considerable potential difference arises between the plant and the soil water. In spite of the high potential difference,

a limited soil water diffusion under low soil water content values can limit an unlimited consumption of water by plants. Under the smallest values of the soil water content, water diffuses into the rooting system mainly as the water vapour. In this case we deal with water bound by adsorption forces, *i.e.* with hygroscopic water (strongly bound water).

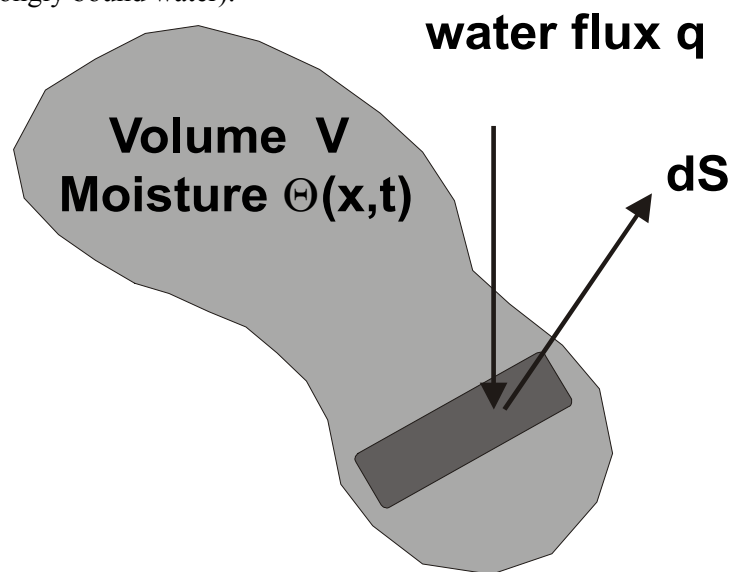


Fig.2. Schematic presentation of mass preservation principle [182]

To describe the vertical water movement in a homogeneous soil profile a one-dimensional Richard's equation is used in the form:

$$\frac{\partial \Theta}{\partial t} = \frac{\partial}{\partial z} \left(K(\Theta) \frac{\partial \Psi}{\partial z} \right) + f(z, t) \quad (6)$$

which combines the Darcy's equation with the continuity equation: The equation (6) is used in numerous one-dimensional hydrological submodels, which are the elements of complex models of plant growth and yielding.

This equation can be used for evaluation of water availability under various soil-climatic conditions, thus it can be helpful in interpretation of thermal images from the point of view of plant water stress detection.

1.3. Water uptake by plants

Plant takes water mainly by the rooting system. In the first stage of water transport it finds its way along the radius to the xylem, *i.e.* the bunch of conducting vessels. Then, water moves in xylem towards leaves. It is evaporated through the cells of mesophyll and cuticula and mainly through stomata into the atmosphere. A part of water taken by plant is transported through phloem into cells, where the photosynthesis takes place.

Two processes, passive and active, are crucial for the movement of water from the soil solute into the plant, and then, as a result of transpiration into the atmosphere. The passive process of water movement in the soil-plant-atmosphere system occurs under the intensive transpiration. The intensity of transpiration is influenced by the difference of water potential in the plant and the water potential in the atmosphere. The water vapour potential in the atmosphere at the relative air humidity of 50% in temperature 20°C is -94.1 MPa. In plant leaves in the same conditions, the water potential can reach values of minus several MPa. So big difference of potentials confirms that the atmosphere is a huge 'pomp', causing the water movement from plants into the surrounding air. Water losses in plants are filled up with water taken from soil, depending on the difference of water potentials between the soil and plant.

Water evaporates from plants by pores in the cell walls of mesophyll and cuticula. In these pores concave menisci are created as a result of surface tension. In this case, the pressure lower than atmospheric arises, causing upward water movement in the xylem of whole plant. The pressure of capillary rise reaches the value of -3 MPa. It is a cohesive mechanism of water uptake and conduction in plants.

The active mechanism of water uptake and conduction in plants is based on the theory of root pressure. The root pressure is the result of water potential difference in the root xylem (higher solution concentration) and in the soil (lower concentration). The osmotic movement is responsible for the water transfer from soil into roots. In case of strong salinisation the concentration of solution in the root can be much lower than in the soil solution. Then, the plant cannot take the soil water.

The soil water uptake is also made difficult in conditions of high potential evapotranspiration at the small coefficient of soil water diffusion. Despite high difference of water potentials in plant and soil, the intensity of water displacement in soil towards roots can be too small, and the actual evapotranspiration can be strongly limited. Such situation leads to the plant water stress.

To explain the phenomenon of root pressure, many models were created, in which the transition into particular anatomical parts of the root, such as epidermis, endodermis or xylem are treated as semipermeable membranes.

Another trial to explain water uptake and conduction in plants is the theory of graviosmosis. It treats the plant xylem as a system of vertically placed compartments filled with solutions of various concentrations, connected with horizontally oriented semipermeable membranes. In this system, the graviosmosis force appears, causing the vertical water movement.

In many models of water flow in the soil-plant-atmosphere system, the resistance theory of water transport is used. According to this theory the flux density of moving water is proportional to the potential gradient between the succeeding elements of the system, and inversely proportional to the resistance within these elements and at their interfaces. The resistance models are constructed as analogs of electrical circuits, and the role of resistors is played by natural barriers of water transport, whereas the role of capacitors by the elements of water storage. In Fig. 3 the water movement from the ground water level through the plant into the atmosphere is presented as well as accompanying resistances. The ground water gets into the unsaturated zone by the capillary rise. In this zone water movement takes place in various directions, depending on the soil water potential gradients. The properties of the soil matrix, such as bulk density of the solid phase, grain size distribution, mineralogical and aggregate composition, water content and water potential, determine soil resistance for water transport in the root direction.

The root resistance for the water transport is determined by the water potential in root, whereas the resistance on the soil root interface by the water potential is soil and root, as well as the quality of the soil-root contact, which is especially important in case of swelling and shrinking soils.

In plants water is conducted by bunches of conducting vessels. In fact they are the passive elements of the water transport, and the resistant of the conducting vessels is mainly influenced by the root pressure and the water potential in leaves. In a special case of some plants, where the root pressure occurs and simultaneously the water potential in leaves is equal to zero, what takes place under the relative air humidity close to 100%, water flows out on the plant's surface. This phenomenon is called guttation.

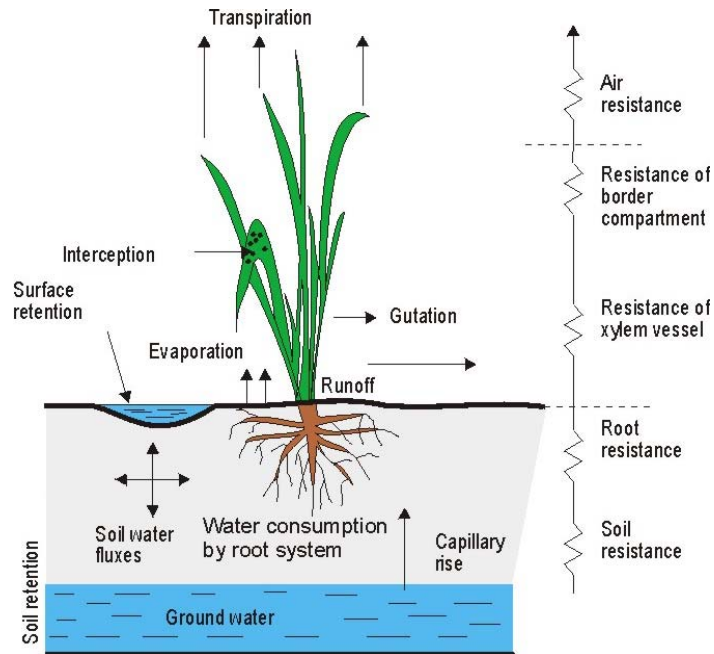


Fig. 3. Water movement in soil-plant-atmosphere system [13]

The resistance of the boundary layer includes the resistance for the water vapour transfer from the inside of the stoma chamber outside, which is determined by the pressure difference within the stoma chamber and on the leaf's surface, and the aerodynamic resistance of the air, determined by the water vapour pressure difference on the leaf's surface and in the atmosphere.

The last of the presented in Fig. 3 resistances – the aerodynamic resistance, depends on the vertical gradients of the wind velocity, the air temperature and the water vapour pressure in the surface layer of the atmosphere.

1.4. Plant water stress

With reference to plants, a term of biological stress exists, which has its analogy to mechanical stress but is difficult to define because most frequently there is not direct action of forces on plants, which would cause some tension or strain, but rather the exchange of energy with the surrounding. Each plant has mechanisms of counteracting the results of negative action of external conditions. The strain caused by biological stress not necessarily projected by the change of

dimensions of particular parts of the plant, but it can be connected with chemical processes in it.

The biological stress can be understood as a physical state of plant, caused by action of an external factor, manifesting itself with distortions of physiological processes. The following kinds of biological stress can be distinguished: the thermal stress caused by too high or too low temperature or a violent change of temperature, the water stress connected with water deficit (drought) or the oxygen stress connected with water excess (flooding), the chemical stress caused by too high concentration of salts and ions in soil or by action of herbicides or insecticides on plants, the stress caused by high intensity of electromagnetic radiation in various ranges of the spectrum and the stress caused by the external factors such as wind, pressure, magnetic field, etc.

This monograph concerns the water stress caused by water deficiency in the plant environment. The water stress occurs when the water content in plant cells decreases to a value which causes the distortion of some physiological functions. It happens, when the transpiration from the plant is higher than the water uptake from the soil. The first symptom of the water stress is the decrease of turgor in plant cells. Longer period of stress situation causes the disruption in cells division, resulting in the inhibition of plant growth. Other consequences of the water stress are: the decrease of the chlorophyll content and the disruption in hormonal and enzymatic equilibrium.

The symptoms of plant water stress, such as the restriction in protein synthesis or metabolic disorders, occur for various plant species at various soil water potential values in the cells. Short plants are more tolerant for the water stress and they are able to survive the period of water deficiency by slowing down the metabolic activity. Cultivable plants, which develop in conditions of constantly repeating or long lasting water stress, give the yield smaller by 15-30%. The plant water stress results in underdevelopment of particular parts of plants, *e.g.* the atrophy of fruits, too early leaf falling, and short rooting system. Simultaneously, each plant defends against the negative effects of water deficiency. It decreases the transpiration rate through closing the stomata. Plants in water stress can respond with subarization of the roots as a mechanism protecting from water loss through the roots into the overdried soil.

Another symptom of the plant water stress is fast accumulation of the abscisic acid, which among other things controls transpiration process through closing stomata. An interdependence exists between the ability of abscisic acid synthesis and the reaction of stomata to water stress [6,13].

2. PHYSICAL BASIS OF MASS, MOMENTUM AND ENERGY TRANSPORT IN BOUNDARY LAYER OF ATMOSPHERE

Evapotranspiration is described by physical processes of mass, momentum and energy exchange. The discussion of these processes is necessary to understand some methods of evapotranspiration determination. They take place in a lower layer of the troposphere, which is called the boundary layer. As opposed to free atmosphere, in which free convection is predominant, in the boundary layer of atmosphere these processes have turbulent nature, what is mainly influenced by the interaction between the air layer and the rough surface. The boundary layer is divided into the outer boundary sublayer, surface sublayer and laminar sublayer. In the outer boundary layer, at the heights from 10 to 2000 meters, the surface hardly affects the transport of mass, energy and momentum. The free-stream velocity is dominant in this sublayer. The pressure gradient and the Coriolis force mainly influence the air mass movement in this layer.

In the surface sublayer of the boundary layer of atmosphere the major process is the exchange of momentum. As a result of friction between the lower layers of air masses and the Earth's surface, a characteristic distribution of wind velocity occurs, achieving zero value at the surface. In this layer, the horizontal component of air movement and the vertical gradients of temperature and water vapour pressure are dominant.

In the laminar layer, which has the thickness of 1 mm and is directly in contact with Earth's surface, the main transport process is the molecular diffusion.

The exchange of mass, momentum and energy in the atmospheric boundary layer can be described by state equations and equations expressing the conservation law concerning mass, momentum and energy.

2.1. Law of mass conservation – continuity equation

In the process of evapotranspiration, water vapour is transported from the active surface to the atmosphere. The continuity equation is fundamental for describing the balance of water vapour mass transported in a given volume.

The continuity equation for the water vapour in air has the form:

$$\frac{\partial \rho_v}{\partial t} + \text{div}\mathbf{F} = 0 \quad (7)$$

where: ρ_v – the actual density of the water vapour in air [kg m^{-3}]; \mathbf{F} – the vector of specific flux of water vapour [$\text{kg m}^{-2} \text{s}^{-1}$].

The movement of water vapour in air takes place by convection and molecular diffusion, therefore the summary specific flux of water vapour \mathbf{F} is determined by the equation [21]:

$$\mathbf{F} = \rho_v \mathbf{v} - K_v \cdot \text{grad} \rho_v \quad (8)$$

where: $\mathbf{v} = \mathbf{i}u + \mathbf{j}v + \mathbf{k}w$ – the vector of wind velocity [m s^{-1}], \mathbf{i} , \mathbf{j} , \mathbf{k} – the unit vectors and u , v , w – the velocity components in the x , y , z directions, respectively; K_v – the coefficient of molecular diffusion [$\text{m}^2 \text{s}^{-1}$].

By combining the continuity equation (7), the equation (8) and the definition of the specific air humidity $q = \rho_v/\rho$, the following general form of the equation expressing the law of mass conservation for the water vapour in air is obtained:

$$\frac{\partial q}{\partial t} + (\mathbf{v} \cdot \nabla)q = K_v \nabla^2 q \quad (9)$$

To solve (9) for q , the suitable boundary conditions should be considered. They usually include the knowledge of the specific air humidity at $z=0$ height, the specific water vapour flux \mathbf{F} or the equation of the heat balance, which combines \mathbf{F} with other energy fluxes. Because in the boundary atmospheric layer the flows are almost invariably turbulent, it is impossible to describe the velocity field and the content of water vapour at any given point of this layer in time and space. Therefore, it is only possible to find the solution of the continuity equation statistically. Usually, the statistics of the mean is used.

The components of velocity \mathbf{v} and specific air humidity q can be decomposed into a mean and turbulent fluctuation:

$$u = \bar{u} + u' \quad v = \bar{v} + v' \quad w = \bar{w} + w' \quad q = \bar{q} + q' \quad (10)$$

By applying the equation (10), the following form of the continuity equation for mean values of the specific air humidity is obtained:

$$\frac{\partial \bar{q}}{\partial t} + \bar{u} \frac{\partial \bar{q}}{\partial x} + \bar{v} \frac{\partial \bar{q}}{\partial y} + \bar{w} \frac{\partial \bar{q}}{\partial z} = \left[\frac{\partial}{\partial x} (\overline{u'q'}) + \frac{\partial}{\partial y} (\overline{v'q'}) + \frac{\partial}{\partial z} (\overline{w'q'}) \right] + K_v \nabla^2 \bar{q} \quad (11)$$

The consecutive terms of this equation express: the rate of change in mean specific air humidity together with the change of the vector of the mean velocity, the components of the diffusion flux caused by the turbulent movement, and the component of molecular diffusion. An analogical form of the continuity equation for fluctuation of the specific air humidity is used for calculation of evapotranspiration in the dissipation method.

2.2. Momentum transfer in surface sublayer of boundary atmospheric layer

In the surface sublayer of the boundary atmospheric layer, an irreversible, viscous process of momentum transfer takes place, connected with friction forces between the atmosphere and the Earth's surface. Due to the Earth's rotation, the Coriolis' force appears. The process of the momentum transfer mostly influences the intensity of evapotranspiration. In this case, the movement equation can be presented as the Navier-Stokes' equation:

$$\frac{\partial \mathbf{v}}{\partial t} + (\mathbf{v} \cdot \nabla) \mathbf{v} = -g\mathbf{k} - \frac{1}{\rho} \nabla p + \frac{\eta}{\rho} \nabla^2 \mathbf{v} - 2\Omega \times \mathbf{v} \quad (12)$$

where: \mathbf{v} – the vector of wind velocity [m s^{-1}]; Ω – the angular frequency of rotation vector in a right-handed system [rad s^{-1}]; g – the acceleration due to gravity [m s^{-2}]; \mathbf{k} – the unit vector in vertical direction; η – the coefficient of dynamic viscosity [$\text{N m}^{-2} \text{s}$]; p – the air pressure [Pa].

Under the Boussinesq's assumption that the air density depends mainly on humidity and temperature, whereas the influence of pressure change is negligible, on the base of decomposition of the velocity vector (10), the equation of horizontal mean movement is obtained:

$$-\frac{1}{\rho} \frac{\partial \bar{p}}{\partial x} + f\bar{v} + \frac{\eta}{\rho} \frac{\partial^2 \bar{u}}{\partial z^2} - \frac{\partial}{\partial z} (\overline{w'u'}) = 0 \quad (13)$$

$$-\frac{1}{\rho} \frac{\partial \bar{p}}{\partial y} - f\bar{u} + \frac{\eta}{\rho} \frac{\partial^2 \bar{v}}{\partial z^2} - \frac{\partial}{\partial z} (\overline{w'v'}) = 0 \quad (14)$$

where: f – the parameter expressing the rotation Earth movement [rad s^{-1}], \bar{p} – the mean air pressure [Pa].

In surface sublayer of the boundary atmospheric layer, the process of momentum transfer is mainly influenced by the vertical profile of wind velocity and the structure of the evaporating surface, which influence latent and sensible heat fluxes. Moving air masses transfer the kinetic energy into the active surface and simultaneously transfer heat and water vapour from it. This way the momentum flux has a considerable impact on the intensity of evapotranspiration.

2.3. Energy conservation law for atmosphere

The change of air temperature during its vertical movement is the result of adiabatic compression and expansion. Considering the vertical movement in the atmosphere, the term of potential temperature is used. This quantity is invariable in adiabatic processes.

The potential temperature θ is the temperature which would be achieved by the air mass under the pressure p and the temperature T , if it were brought adiabatically to a standard pressure $p_0 = 1000$ hPa. It is expressed by the equation:

$$\theta = T \cdot \left(\frac{p_0}{p} \right)^{\frac{k-1}{k}} \quad (15)$$

where: $k = \frac{c_p}{c_v}$ – the ratio of the specific heat of air under the constant pressure to the specific heat of air under constant volume.

The energy exchange in the atmosphere can occur by heat conduction, convection and radiation. The equation expressing the law of energy conservation for incompressible air is as follows:

$$\frac{\partial \theta}{\partial t} + (\mathbf{v} \cdot \nabla) \theta = \alpha \nabla^2 \theta - \frac{1}{\rho c_p} \nabla \cdot H_R \quad (16)$$

where: α – the thermal diffusivity, c_p – the specific air heat under constant pressure, H_R – the radiative heat flux.

Nonlinear differential equations, which express the conservation laws, are difficult to solve. In general, the number of unknowns occurring in these equations for a specific problem is larger than the number of equations. Additionally, turbulent processes of energy and mass transfer between the

atmosphere and the active surface depend on the thermodynamic stability of atmosphere, thus complex functions of the atmosphere state should be considered which require incorporating some empirical coefficients.

To determine the water vapour flux, flowing from the active surface to the atmosphere, on the base of equations expressing the conservation laws, a simplification is used which assumes that flows in the boundary layer are stationary. The application of similarity principles, according to which the turbulent coefficients of mass, momentum and energy transfer are equal in the neutral stability conditions of atmosphere, and the use of semiempirical turbulence theory enable to solve the equations of mass, momentum and energy transfer in the subsurface layer of the atmosphere. This is the base for quantitative description of the evapotranspiration process.

3. MODELLING OF SOIL THERMAL PROPERTIES

3.1. Introduction

Solving the problems of heat exchange can usually be reduced to calculation of the amount of heat flowing through a given system, which has specific physical and geometrical properties. On the other hand these properties determine the flow of heat. Depending on the dynamics of this flow, the processes of steady and unsteady heat exchange can be distinguished. The steady heat exchange is dealt with when the distribution of temperature in the system does not change in time and the amounts of the transferred heat are constant. During the unsteady heat exchange, both the temperature distribution and the amount of the exchanged heat change in time.

In the soil, the unsteady heat flow is the most common. The basic heat properties of soil, which determine and characterize it from the point of view of heat transfer and accumulation, are the thermal conductivity and the heat capacity. The thermal diffusivity of soil, being the ratio the thermal conductivity and the heat capacity per volume unit of the soil is the derivative quantity and it expresses the ability of soil to equalize the temperature in all the points. The highest share of the heat flow in soil or in ground has the thermal conductivity through the mineral and organic components and water. The water or air convection as well as the radiation in soil are of secondary importance. Only in few cases the phase transition (latent heat) of water should be considered, *e.g.* vaporization, condensation, freezing, sublimation and the heat connected with the movement of water and air within the soil. In majority of cases the problem of heat flow can be reduced to solving the equation of heat conductivity with various boundary conditions.

The aim of this chapter is to present a method of evaluation the heat capacity, the coefficient of thermal conductivity and heat diffusivity in soils with differentiated structure on the base of basic experimental data referring to the soil and the statistical model of the thermal conductivity.

The realization of this aim consists in selecting the most important soil factors, which should be measured and in elaborating:

- a theoretical model for estimation of thermal properties of the soil and ground,
- a procedure of preparation of basic input data for the model,

- an algorithm of the programme for estimation of thermal properties of soil and ground,
- a computer programme for calculation of thermal properties.

3.2. Thermal conductivity definition

The result of heat flow from hotter to colder places is equalization of temperature in a studied medium without any macroscopic movements. The ability of a body to conduct the heat is characterized by the thermal conductivity. From macroscopic point of view the thermal conductivity consists in equalization of the energy of heat movements resulting from the collisions between the particles. The coefficient of thermal conductivity λ is a measure of the rate of thermal conductivity. It is equal to the amount of energy Q [J] flowing in a unit of time t [s] through the unit of area S [m²] under the temperature gradient ∇T [K m⁻¹] which equals to one:

$$\lambda = \frac{Q}{t \cdot S \cdot \nabla T} \quad (17)$$

The unit of the thermal conductivity coefficient is W m⁻¹ K⁻¹.

It results from performed investigations that soil water content has the highest influence on its thermal conductivity [29, 30, 37, 39, 52, 54, 64, 69, 78, 84, 88, 89, 142, 170, 178, 179]. The smallest values of the thermal conductivity coefficient are noticed for dry soil. The thermal conductivity of such soil depends mainly on its bulk density and mineralogical composition [29, 39, 167, 168]. After adding even a small amount of water into the dry soil the thermal conductivity increases. This increase is explained by the increase of a heat contact by creation of water film around the solid particles. With the increase of the film thickness the faster and faster increase of the thermal conductivity occurs [88].

The highest increase of the values of thermal conductivity coefficient is between the states corresponding to the maximum molecular water capacity and the capillary water capacity. When the non-capillary spaces are being filled with water, the increases of the thermal conductivity coefficient are smaller. The highest values of the coefficient of thermal conductivity of soil are reached in the state of maximum saturation with water.

There are only few papers referring to the problem of estimation of the thermal conductivity coefficient in a structural soil. It is known that with the

increase of aggregate dimensions the area of the contact between the particles decreases as well as the flow of the heat by conduction through the solid components [55, 56, 88, 142, 168, 170, 179]. The occurrence of water and differentiation of temperature in aggregated soil complicates the problem even more. Because it is impossible to predict the quantitative shares of particular components therefore it is impossible to evaluate the relation between the coefficient of thermal conductivity of soil and soil structure. This problem is investigated indirectly by parameters connected with the structure, *i.e.* shape, sizes and mutual placement of the soil particles or by soil bulk density [36, 37, 38, 39, 170].

3.3. De Vries model

The problem of determination of the coefficient of thermal conductivity in a granular material is mathematically analogical to the problem of determination of the electrical conductivity or the dielectric constant in this material [39]. The coefficient of thermal conductivity in soil in a studied layer as a function of the water content and the bulk density can be determined from de Vries model [39]. It is assumed in this model that soil is a continuous medium (water with dissolved solid particles and air or air with dissolved solid particles and water) possessing the content x_o and the coefficient of thermal conductivity λ_o , in which various solid particles are dispersed with contents $\sum_{i=1}^N x_i = 1 - x_o$ and coefficients of thermal conductivity λ_i and that solid particles do not influence each other.

The thermal conductivity coefficient is calculated from the formula [39]:

$$\lambda = \frac{x_o \lambda_o + \sum_{i=1}^N k_i x_i \lambda_i}{x_o + \sum_{i=1}^N k_i x_i} \quad (18)$$

where: N is a number of types of particles (quartz, other minerals and organic matter), k_i is the ratio of mean gradient of temperature within the particle to the mean gradient of temperature in the medium in which the particle is situated, x_i is the content of i -th component, λ_i is the thermal conductivity coefficient of the i -th component. The value of k_i is calculated from the equation [39]:

$$k_i = \frac{1}{3} \sum_{j=a,b,c} \left[1 + \left(\frac{\lambda_i}{\lambda_o} - 1 \right) g_{i,j} \right]^{-1} \quad (19)$$

where: a , b , c are the semi-axes of an ellipsoid, g_{ij} is a coefficient which depends on the shape of particles and $\sum_j g_{i,j} = 1$.

The values of coefficient g_i for solid particles of soil were estimated by de Vries on the base of experiment and were equal to: $g_a = g_b = 0.144$. and $g_c = (1 - 2 g_a) = 0.712$.

The coefficient thermal conductivity of the mineral soil is calculated on the base of equation (18).

In a completely dry state, the continuous medium can be regarded as air with $\lambda_o = 0.025$ [$\text{W m}^{-1} \text{K}^{-1}$] whereas the value obtained from equation (18) should be multiplied by 1.25 (correction coefficient). In the state of water saturation, the continuous medium can be regarded as water with $\lambda_o = 0.57$ [$\text{W m}^{-1} \text{K}^{-1}$].

For the intermediate states in the range between the state of completely dry soil and the water saturation state, de Vries incorporates the following assumptions:

- the air filling the soil pores is treated as the particles of humid air distracted in the water medium,
- the coefficient of the thermal conductivity of the humid air is equal to 0.238 [$\text{W m}^{-1} \text{K}^{-1}$],
- values of coefficient g_a for the air in the soil pores change linearly between 0.333 for the water content close to saturation and 0.035 for low values of water content, therefore [39]:

$$g_a = g_b = 0.333 - \frac{x_p}{x_w} (0.333 - 0.035) \quad (20)$$

where: x_p is a volume of pores filled with air, and x_w is the volumetric water content under the state of saturation of soil with water.

3.4. Statistical-physical model of thermal conductivity

3.4.1. Model definition

Modelling of physical processes with the use of models, which reflect the reality is commonly accepted in science. It is caused mainly by the complexity of the structure of our Universe, and a wish to express this reality with the use of appropriate mathematical formulas [173].

The physical dictionary [143] gives the following definition of the model ... “model is a set of assumptions simplifying the description of a given physical object, a process or a phenomenon, encompassing the most important properties of the object of study and presenting it in such a way that an object, a process or a phenomenon which in general does not exist in reality, has features sufficiently similar to the real object” ... More general formulation of the model definition is given by Gózdź [53] as: ...“the reflection of the physical reality onto a mathematical formal structure or onto a human controlled physical system, which enables to simulate it”. Taking into account these definitions of a model as well as the present state of knowledge, the description of the heat flow in the soil is presented below, with the use of a statistical model of the thermal conductivity and an empirical model of the heat capacity including a small number of assumptions, and presenting a set of empirical laws as simply, precisely, and completely as it is possible at this stage of solution.

3.4.2. Basic laws used for construction of the model of thermal conductivity

One of the basic physical properties of any body is its ability to conduct heat. It is possible to consider it in terms of the thermal resistance, expressing ability of a body to suppress the conductivity. Understanding of the physical meaning of the thermal resistance can be made easier when considering the following example.

The equation describing the heat exchange shows an analogy with the equation expressing the Ohm's law for the electric current flow. The Ohm's law states that the intensity of the electric current I [A] which flows through the conductor is proportional to the voltage U [V] set to its endings and contrary proportional to the resistance R [Ω] of the conductor:

$$I = \frac{U}{R}. \quad (21)$$

It comes from the Fourier's law that the process of the heat energy transfer in solid, liquid and gaseous media is the subject of probability laws. The process of conductivity is very complicated. It does not occur in a way that the energy input from one end of the sample flows directly linearly to the second end, but the particles which vibrate around the state of equilibrium are the subject to numerous collisions with each other passing the energy to the neighbors. This complicated form of the flow causes the appearance of the temperature gradient in the expression for the heat flux. The law of the heat conduction in the stable conditions says that the density of the heat flux q [W m^{-2}] for the uniform and isotropic medium is proportional to the gradient of its temperature $\partial T/\partial z$ [K m^{-1}], measured along the direction of the heat flow:

$$q = -\lambda \frac{\partial T}{\partial z}. \quad (22)$$

The proportionality coefficient λ is called the coefficient of thermal conductivity and as was shown earlier is characteristic for a given medium from the point of view of its ability to conduct the heat. The minus sign in the above equation results from the fact that the heat flows from a place possessing a higher temperature to the place of lower temperature, so that the segment ∂z determined along the direction of heat flow corresponds to a negative value $-\partial T$ of the temperature increment. There is a relation between the amount of the exchanged heat Q_t [W], and the density of the heat flow in the soil q :

$$Q_t = qS \quad (23)$$

where: S [m^2] is a surface through which the heat is conducted.

It can be stated, as an analogy to the Ohm's law, that the amount of the exchanged heat is proportional to the temperature difference between the opposite surfaces of the system:

$$Q_t = \frac{1}{R_T} (T_1 - T_2) \quad (24)$$

where: the coefficient R_T is called the heat resistance of a given system.

The equation of the heat exchange in the soil can be written as:

$$\Delta T = R_T Q_t. \quad (25)$$

Figure 4 shows the analogy between electrical and heat quantities. Therefore, the temperature difference ΔT [K] = $T_1 - T_2$ corresponds to the voltage U , the amount of the exchanged heat Q_t [W] corresponds to the intensity of current I , whereas the thermal resistance R_T [KW⁻¹] can be assigned to the respective quantity of electric resistance R .

As can be derived from these formulas, the thermal resistance of a system depends on the coefficient of thermal conductivity of the material, which creates a given system, and on its geometry. This resistance for a flat and homogeneous layer equals to:

$$R_T = \frac{d}{\lambda S} \quad (26)$$

where: d [m] – the depth of the layer, λ – the coefficient of the thermal conductivity of a given system, S – surface.

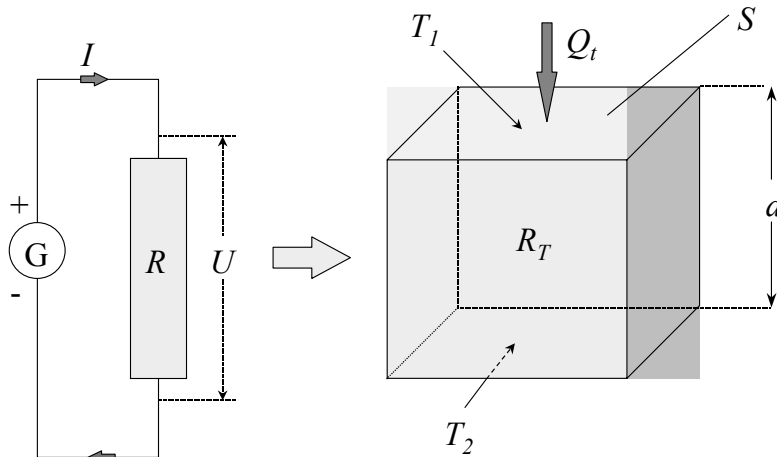


Fig. 4. Schematic comparison of electric and thermal quantities.

The thermal resistance of a system of homogeneous spheres submerged in each other for the radius of the internal sphere – r_k and the external radius – r_z , is calculated from the equation:

$$R_T = \frac{1}{4\pi\lambda} \left(\frac{1}{r_k} - \frac{1}{r_z} \right). \quad (27)$$

If the external radius of the sphere r_z is much higher than the radius of the internal sphere r_k , then the expression $1/r_z$ is very small and can be neglected whereas the resistance of such a sphere is calculated from the equation:

$$R_T = \frac{1}{4\pi\lambda r_k}. \quad (28)$$

Two basic methods of connecting the resistors can be distinguished: parallel and serial (Fig.5). The resistance of a whole parallel system is derived from on the base of the first Kirchhoff's law (which says that the sum of intensities $I_1 + I_2 + \dots + I_k$ of the currents flowing from a nodal point equals to intensity I of the current flowing into this point) and from the Ohm's law (after substituting I_k with U/R_k) with the equation:

$$\frac{1}{R} = \frac{1}{R_1} + \frac{1}{R_2} + \dots + \frac{1}{R_k} \quad (29)$$

while the resistance of the whole serial system is derived on the base of the second Kirchhoff's law (which says that the sum of potential decreases $U_1 + U_2 + \dots + U_k$ in a closed electric circuit is equal to the electromotive force U acting in this circuit) and Ohm's law (after substitution: $U_k = I R_k$) from the formula:

$$R = R_1 + R_2 + \dots + R_k. \quad (30)$$

The second basic term used for the construction of the model is polynomial distribution [43]. This distribution enables us to calculate the probability of occurrence of a given combination of the soil particles:

$$P(x_{1j}, x_{2j}, \dots, x_{kj}) = \frac{u!}{x_{1j}! x_{2j}! \dots x_{kj}!} f_1^{x_{1j}} f_2^{x_{2j}} \dots f_k^{x_{kj}}. \quad (31)$$

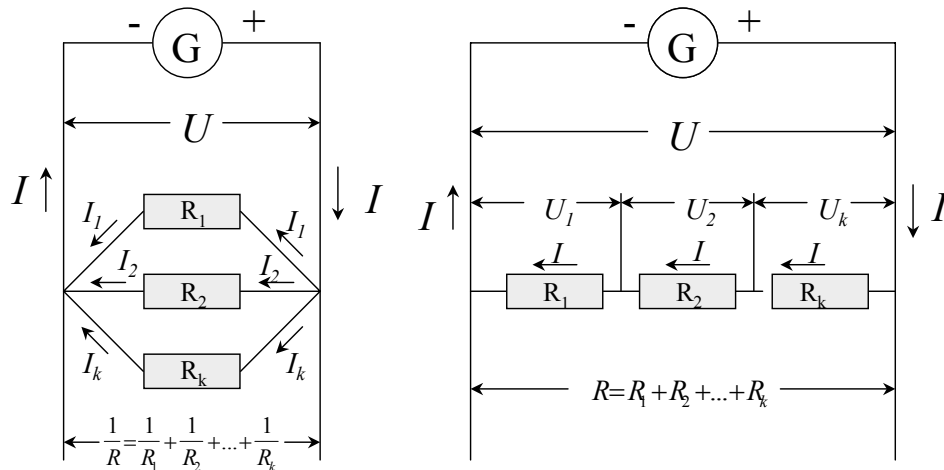


Fig.5. System connection of resistors: parallel and serial.

It expresses the probability that in “ u ” independent tests, precisely x_{ij} results of the type “ j ” will be obtained, if the probability of the result “ i ” in a separate test is f_i , $i = 1, 2, \dots, k$. In our case these are the contents of particular minerals, organic matter, water and air in a volume unit and are treated as probabilities of obtaining the result of type “ i ” in a separate test.

3.4.3. Model construction

The statistical-physical model of the thermal conductivity of soil has been created on the base of the idea of the thermal resistance, two Kirchhoff’s laws and the polynomial distribution [170]. It has been constructed by presenting the unit volume of soil (Fig. 6a), composed of solid particles, water and air, as a system constructed from elementary geometric figures (spheres having specific physical properties), which create overlapping layers (Fig. 6b). It has been assumed that the connections between spheres in a layer and between layers are presented by the parallel connections of thermal resistors, which are presented by the spheres in a layer and serial connections between layers (Fig.6c) [172].

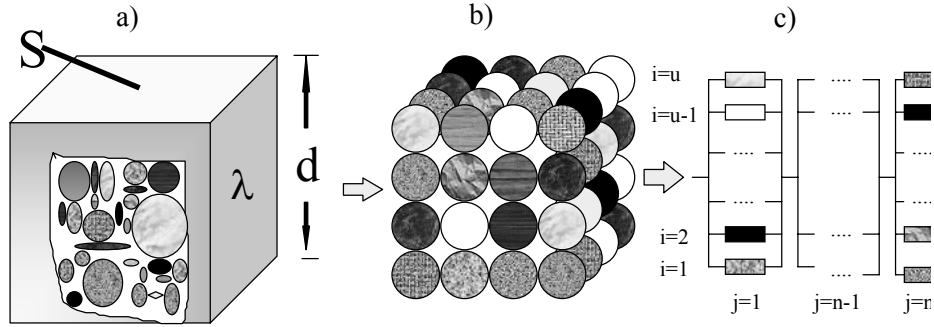


Fig. 6. Schematic diagram of the statistical model construction: a) unit volume of soil, b) the system of spheres that form overlapping layers, c) parallel connection of resistors in the layers and series between layers.

A comparison of the summary resistance of the system of resistors possessing parallel and serial connections, which takes into account all possible configurations of particle connections with mean thermal resistance referring to the unit volume of soil, enables to estimate the thermal conductivity of the soil [166, 168, 170, 172].

Assuming that there are " u " parallel connections in a layer and " n " serial connections between layers, it is possible to calculate the summary thermal resistance for such a system. The thermal resistance for the layer equals:

$$\frac{1}{R_j} = \sum_{i=1}^u \frac{1}{R_{ij}}. \quad (32)$$

The thermal resistance for the whole system is expressed by formula:

$$R = \sum_{j=1}^n R_j = \sum_{j=1}^n \left(\frac{1}{\sum_{i=1}^u \frac{1}{R_{ij}}} \right). \quad (33)$$

On the base of the equation of the thermal resistance for the sphere we can write a general formula:

$$R_{ij} = \frac{1}{4\pi \lambda_{ij} r_{ij}}. \quad (34)$$

Inserting this equation into the formula for a total resistance of the system we obtain:

$$R = \frac{1}{4\pi} \sum_{j=1}^n \left(\frac{1}{\sum_{i=1}^u \lambda_{ij} r_{ij}} \right). \quad (35)$$

The thermal resistance of a rectangular presented in Fig. 6a, under the assumption that the coefficient of thermal conductivity is equal to the mean value – $\bar{\lambda}$ – of all the components creating this system and that the thickness of a studied layer d corresponds to "n" serial connections, whereas the surface S corresponds to "u" parallel connections (Fig. 6b), can be expressed with equation:

$$R = \frac{n}{\bar{\lambda} u}. \quad (36)$$

Comparing the above two equations, after rearranging we obtain a general equation for calculation of the mean value of the thermal conductivity of the investigated system:

$$\bar{\lambda} = \frac{4\pi}{\frac{u}{n} \sum_{j=1}^n \left(\frac{1}{\sum_{i=1}^u \lambda_{ij} r_{ij}} \right)}. \quad (37)$$

The expression given in parentheses is assigned as a_j :

$$a_j = \frac{1}{\sum_{i=1}^u \lambda_{ij} r_{ij}} \quad (38)$$

hence:

$$\bar{a} = \frac{1}{n} \sum_{j=1}^n a_j \quad (39)$$

\bar{a} – denotes the mean value of a_j .

The soil contains various chemical compounds and in a specified unit of soil volume many particles of the same type can be found. Let's assume that in a unit of soil volume there are x_1 particles of the first component with the coefficient of thermal conductivity λ_1 and the radius r_1 , x_2 , particles of the second component which is characterized with λ_2 and r_2 , etc. and that $x_1 + x_2 + \dots + x_k = u$. The coefficients of thermal conductivity of particular components change their values with the change of soil temperature – $\lambda(T)$, therefore calculations should take into account these changes: After inserting the values $\lambda_{ij}(T)$ instead of λ_{ij} , the expression for can be written as follows:

$$a_j = \frac{1}{x_{1j}\lambda_{1j}(T)r_{1j} + x_{2j}\lambda_{2j}(T)r_{2j} + \dots + x_{kj}\lambda_{kj}(T)r_{kj}}. \quad (40)$$

For the soil under constant mineralogical composition, the value of \bar{a} will depend on the content of water in the unit of the soil volume – θ_v [$\text{m}^3 \text{m}^{-3}$], total porosity – ϕ [$\text{m}^3 \text{m}^{-3}$], thermal conductivities of particular soil components – λ_i , soil temperature – T [$^{\circ}\text{C}$], equivalent radii of soil particles treated as spheres – r_i , numbers of particular particles included into a given configuration – x_i and the number of parallel connections between soil particles treated as thermal resistors – " u ", therefore the mean thermal conductivity can be expressed with the formula:

$$\bar{\lambda} = \frac{4\pi}{\bar{a}(\theta_v, \phi, \lambda_i, T, r_i, x_i)u}. \quad (41)$$

Because we are not able to find experimentally the distribution of particles in a studied soil and therefore the mean value – $\bar{a}(\theta_v, \phi, \lambda_i, T, r_i, x_i)$, therefore this value can be changed with the expected theoretical value – $\bar{m}(\theta_v, \phi, \lambda_i, T, r_i, x_i)$, which considers all the possible configurations of particles and probabilities of their occurrence:

$$\bar{\lambda} = \frac{4\pi}{\bar{m}(\theta_v, \phi, \lambda_i, T, r_i, x_i)u}. \quad (42)$$

The expected value \bar{m} can be calculated from a general formula:

$$\bar{m} = \sum_{j=1}^L a_j P_j(a = a_j) \quad (43)$$

where: L is the number of all possible combinations of particles' arrangement, a_j contains x_1, x_2, \dots, x_k – the number of particles of particular components of soil with thermal conductivities $\lambda_1, \lambda_2, \dots, \lambda_k$ and radii of particles r_1, r_2, \dots, r_k , whereas: $\sum_{i=1}^k x_{ij} = u, j=1.2.\dots,L, P(x_{ij})$ – is the probability of occurrence of a given combination of configuration of soil particles. The following condition should be fulfilled:

$$\sum_{j=1}^L P_j(a = a_j) = 1. \quad (44)$$

After substitution of the formula for the mean thermal conductivity with the formula for the expected value, the general equation for calculation of the thermal conductivity of soil (soil conductance – $W m^{-1} K^{-1}$) is obtained:

$$\bar{\lambda} = \frac{4\pi}{u \sum_{j=1}^L \frac{P(x_{1j}, \dots, x_{kj})}{x_{1j}\lambda_1(T)r_1 + \dots + x_{kj}\lambda_k(T)r_k}}. \quad (45)$$

3.4.4. Identification and verification of statistical – physical model

The identification and verification of the proposed model of the thermal conductivity of soil were performed by the analysis of the component elements of the model and comparison of the thermal conductivity values calculated from the model with measured values [170, 172]. The experimental data were taken from literature [84, 89]. It was stated that under changes of the water content and the density of soil in the presented model, the number of parallel and serial connections of thermal resistors is modified. The determination of the summary

resistance of such a system consisted in determination of the parameters of the model, *i.e.* its identification. The studied model was identified, as a model, which modifies the number of parallel connections of thermal resistors along with the change of the ratio of water content in the unit of soil volume to its porosity and modifies the spheres' radii with the change of the organic matter content [166, 172].

The first stage of calculations was to determine the characteristics of the number of parallel connections of thermal resistors " u " as a function of saturation with water, and it was assumed that particles of solid, liquid and gaseous phases will be represented by the spheres of the same radii. Determination of the characteristic of $u(\theta_v/\phi)$ consisted in multiple calculations of thermal conductivity values of soil in a broad range of the water content and the density of soil under various " u " and " r_k ", then comparison of these values with measured ones and in determination of the best agreement between them.

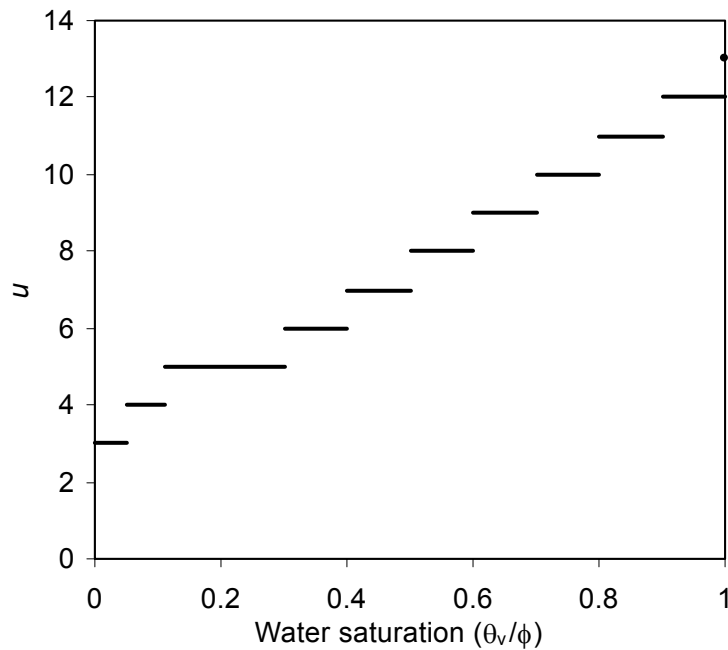


Fig. 7. Number of parallel connections " u " as a function of soil water saturation θ_v/ϕ . [170].

The analysis was made for Fairbanks sand, Healy clay, Fairbanks peat [84], and silt from Felin [89]. It resulted from the performed analyses that values of " u "

determined for particular soils in most cases overlapped each other, therefore a common characteristic was determined of the number of parallel connections of thermal resistors " u " as a function of saturation θ_v/ϕ for all investigated soils [168, 170].

In the second phase of calculations it was looked for, what the radii of spheres depend on. A common radius of spheres for the investigated soils was not found. It occurred that the values of radii of spheres " r_k " contained in the range from 0.044 to 0.08, and the minimum value corresponded to all of the investigated mineral soils whereas the maximum value for the peat soil. On the base of the performed comparison of the calculated values from the model with measured and their analysis the assumption can be made, that for soils that contain both mineral and organic parts, the radius of spheres in first approximation can change according to the formula [166]:

$$r_k = 0.036f_o + 0.044 \quad (46)$$

where: $f_o[\text{m}^3 \text{m}^{-3}]$ – denotes the content of organic matter in the unit of volume.

The leap transition of the value of " u " as a function of soil saturation with water, causes a respective leap increase of calculated values of the thermal conductivity of soil. To avoid such a transition, a procedure of intermediate determination of the thermal conductivity in a given range of soil saturation was proposed. Within this procedure, the thermal conductivity of a medium was determined from the general formula for the thermal conductivity for two succeeding values: u and $u+1$ (Fig. 7) and from corresponding values of the water content of a medium $\theta_v(u)$, $\theta_v(u+1)$, and then from linear equation given below, the value of the thermal conductivity for a needed value of the water content of the medium θ_v :

$$\lambda = \lambda(u) + \frac{\theta_v - \theta_v(u)}{\theta_v(u+1) - \theta_v(u)} (\lambda(u+1) - \lambda(u)). \quad (47)$$

The agreement between modeled and measured data was evaluated with the use of the mean square error (σ_b) and the maximum relative error (η_b):

$$\sigma_b = \sqrt{\frac{\sum_{i=1}^n (f_{mi} - f_{ci})^2}{k}} \quad (48)$$

where: f_{mi} – a measured value, f_{ci} – a calculated value, $k = n - 1$ if $n < 30$ and $k = n$ if $n > 30$. n – number of data. The maximum relative error was calculated from the equation:

$$\eta_b = \max_{i=1,2,\dots,n} \left\{ \left| \frac{f_{mi} - f_{ci}}{f_{mi}} \right| \cdot 100\% \right\}. \quad (49)$$

The practical realization of the theoretical basis of determination of the soil thermal properties can be reduced to the measurement of basic physical quantities referring to soil and calculation according to the algorithm reflecting the statistical-physical model of the thermal conductivity of soil and a mathematical formula for thermal capacity and diffusivity of soil [169].

From among the data referring to a specific kind of soil, five main components have been distinguished: quartz (λ_q), other minerals (λ_m), organic matter (λ_o), water (λ_w) and air (λ_a). These thermal conductivity coefficients are used for calculation of the soil thermal conductivity.

The values of the coefficients of thermal conductivity of the above components of soil and their dependence upon temperature (T), pressure (P) and soil water potential (ψ) is presented in Table 2.

For unsaturated soil, under high temperature gradient in the soil, the coefficient of thermal conductivity of air is replaced with the complex thermal conductivity (λ_{app}) composed of the thermal conductivities of air λ_a and water vapour λ_v [39, 85, 86]. For salt-affected soils, under high gradient salt concentration, the coefficient of thermal conductivity of water λ_w is replaced with the thermal conductivity coefficient of a given solution λ_s [113].

Table 2. Values and expressions for parameters used in calculating the thermal conductivity of soils [T in °C] [172]

Source ^a	Parameters ^b	Expression, value ^b
	λ_q , W m ⁻¹ K ⁻¹	$9.103 - 0.028 T$
2	λ_m , W m ⁻¹ K ⁻¹	2.93
2	λ_o , W m ⁻¹ K ⁻¹	0.251
1	λ_w , W m ⁻¹ K ⁻¹	$0.552 + 2.34 \cdot 10^{-3} T - 1.1 \cdot 10^{-5} T^2$
1	λ_a , W m ⁻¹ K ⁻¹	$0.0237 + 0.000064 T$
2	λ_{app} , W m ⁻¹ K ⁻¹	$\lambda_a + h\lambda_v$
2	h , dimensionless	$exp(\psi M_w / \rho_w R (T + 273.15))$
2	λ_v , W m ⁻¹ K ⁻¹	$LD_a v (d\rho_o/dT)$
1	L , J kg ⁻¹	$2490317 - 2259.4 T$
1	D_{a_s} , m ² s ⁻¹	$0.0000229 * ((T + 273.15) / 273.15)^{1.75}$
2	D_{a_s} , m ² s ⁻¹	$21.7 \cdot 10^{-6} (101.325/P) ((T + 273.15) / 273.15)^{1.88}$
1	v , dimensionless	$P / (P - (h\rho_o R (T + 273.15) / 1000 M_w))$
1	ρ_o , kg m ⁻³	$10^{-3} exp(19.819 - 4975.9 / (T + 273.15))$
1	$d\rho_o/dT$, kg m ⁻³ K ⁻¹	$4975.9 \rho_o / (T + 273.15)^2$

^a 1. Kimball *et al.* [86,85]; 2. de Vries [39]

^b ψ – soil water pressure head, kPa; M_w – molecular weight of water, 0.018 kg mol⁻¹; ρ_w – density of liquid water, 1.0 Mg m⁻³; R – universal gas constant, 8.3143 J mol⁻¹; h – relative humidity; L – latent heat of vaporisation; D_a – diffusion coefficient for water vapour in air; v – mass flow factor; ρ_o – saturated vapour density; P – barometric pressure, kPa, thermal conductivity of: quartz, λ_q , other minerals, λ_m , organic matter, λ_o , water or salt solution, λ_w , and air, λ_a .

3.4.5. Comparison of soil thermal conductivity values obtained from model studies and measurement

In Fig. 8 and in Table 3 the comparison of the results of the soil thermal conductivity results calculated from the model and obtained from the measurement for Fairbanks sand, Healy clay, silt from Felin, Fairbanks peat and loam.

The agreement between calculated and measured results was satisfactory in general. The coefficients of linear regression had values of the slope of straight line close to one, whereas the offset values were close to zero. The values of the coefficient of determination R^2 were high and contained in range from 0.948 to 0.994. The values of the mean square error and maximum relative error contained in the range from 0.057 to 0.123 [$\text{W m}^{-1} \text{K}^{-1}$] and from 12 to 38.3 %, respectively.

The comparison of thermal conductivity values has been conducted, calculated for various soils from the statistical-physical model, from de Vries model and measured ones. The results of this comparison together with the equations of linear regression and coefficients of determination are presented in Fig. 9. Obtained results indicate that these two models evaluate the thermal conductivity of soil with similar accuracy. The model of de Vries requires, however, a special attention during determination of the model's parameters, which significantly influence the accuracy of determination of the thermal conductivity. The statistical-physical model does not possess such limitations as de Vries model.

Table 3. Statistical summary comparison of measured and calculated of soil thermal conductivity [172]

Statistics ^a	silt	loam	clay	sand	peat	together
σ [$\text{W m}^{-1} \text{K}^{-1}$]	0.093	0.057	0.123	0.083	0.022	0.089
η [%]	38.3	12.0	34.1	30.3	33.3	38.3
R^2	0.9527		0.9478	0.9867	0.9937	0.970
Regression equation:	1.0279		0.9722	0.9773	1.1087	0.996
a	0.0338		0.0811	0.0087	-0.0214	0.0449
$(\lambda_c = a \lambda_m + b)$ b						

^a σ [$\text{W m}^{-1} \text{K}^{-1}$] – mean square error, η [%] – maximum relative error.

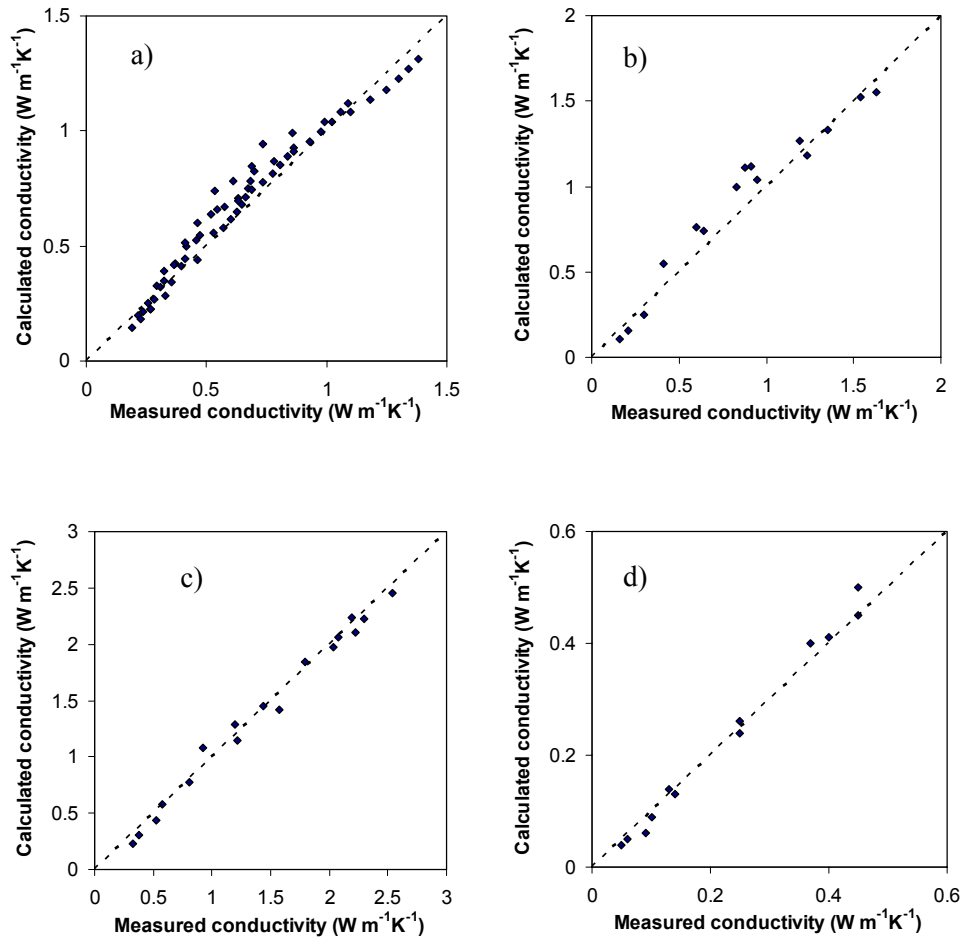


Fig.8. Comparison of calculated λ_c and measured λ_m thermal conductivity for various soils: Felin silt (a); Healy clay (b). Dotted line expresses the relation 1:1. [172]

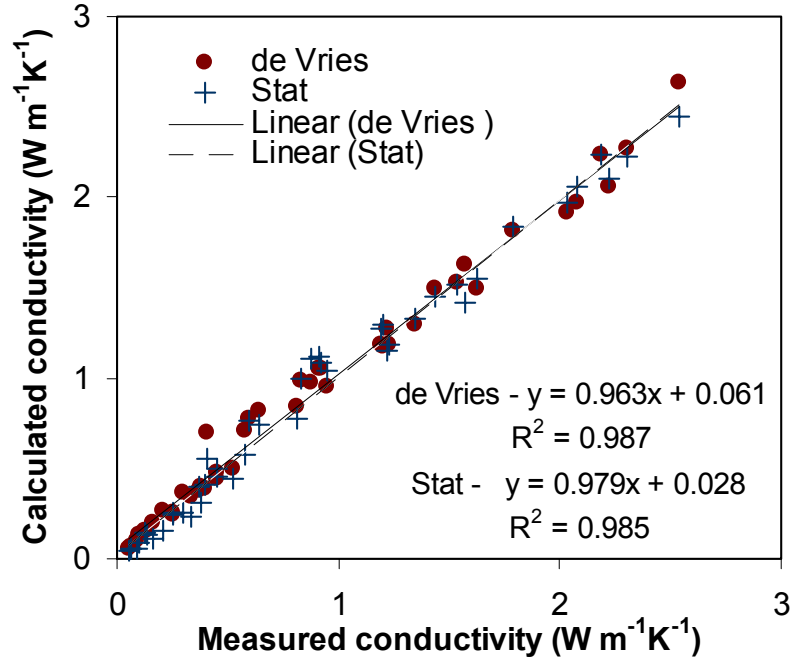


Fig. 9. Comparisons of the thermal conductivity values of various soils measured and calculated from the de Vries and statistical-physical (Stat) models.

3.5. Heat capacity determination

The heat capacity of soil – C , is the amount of heat, which should be delivered to soil or taken away from it to make its increase (or decrease) of 1K. The unit of the heat capacity is [J K⁻¹]. The heat capacity of the soil per unit of volume – C_v [J m⁻³ K⁻¹] depends on the heat capacity per unit of volume of particular components of the solid phase (particles of various minerals and organic matter), liquid phase (free and bound water), gaseous phase (soil air) and shares of these components in the soil. The values of the heat capacity of soil C_v are calculated from the following equation:

$$C_v = \sum_{i=1}^n x_{si} C_{si} + x_w C_w + x_a C_a \quad (50)$$

where: x_{si}, x_w, x_a [$\text{m}^3 \text{m}^{-3}$] – the shares of components in the unit of volume of the solid phase, liquid phase and gaseous phase, C_{si}, C_w, C_a [$\text{J m}^{-3} \text{K}^{-1}$] – the heat capacity values per unit of volume for the respective phases. The following relation exists between the specific heat – c_i [$\text{J kg}^{-1} \text{K}^{-1}$] of particular components of soil and their heat capacity per unit of volume C_{vi} :

$$C_{vi} = c_i \rho_i \quad (51)$$

where: ρ_i [Mg m^{-3}] – the bulk densities of soil components.

It results from the measurements performed by Kersten [84], Czudnowski *et al.* [29], Lang [93], de Vries [37, 39], Feddes [45] Rewuta [133], Molga [106], that the mean bulk density of mineral components of the solid phase is about 2.65 Mg m^{-3} and their heat capacity per unit of volume C_s is $2.0 \text{ MJ m}^{-3} \text{K}^{-1}$. The bulk density of the organic matter contained in the soil is about 1.3 Mg m^{-3} and its C_o is about $2.5 \text{ MJ m}^{-3} \text{K}^{-1}$. The bulk density of water is more than two times smaller than the densities of mineral components, however C_w is two times higher than C_s and it is about $4.2 \text{ MJ m}^{-3} \text{K}^{-1}$. The bulk density of air is about 1/1000 of the water density and its C_a is $1.25 \text{ kJ m}^{-3} \text{K}^{-1}$. It is clear that C_a slightly influences the total C_v and can be neglected in calculation.

It resulted from the studies performed by Czudnowski *et al.* [29, 30], de Vries [39], Feddes [45], Turski and Martyn [164], Hillel [66], Sikora [142], that for typical soils the changeability of the solid phase content ranges between 0.45 and $0.65 \text{ m}^3 \text{m}^{-3}$ while the heat capacity per unit of volume C_v changes from about $1 \text{ MJ m}^{-3} \text{K}^{-1}$ in air-dry state to about $3 \text{ MJ m}^{-3} \text{K}^{-1}$ in the state of complete saturation with water. Under constant contents of mineral and organic components of the soil, the heat capacity depends only on the soil water content and this is a linear dependence nearly in the whole range of water content values. Some non-linearity is observed for the soil under very small water content values. The bulk density and the structure of soil, which can be expressed indirectly by the relation with its bulk [37, 39, 64, 142] density has smaller impact on the heat capacity than the water content. The heat capacity increases with the increase of the bulk density. An overview of the literature indicates a good agreement between the values calculated from the models with the measured ones. To calculate the heat capacity per unit of volume – C_v [$\text{Jm}^{-3} \text{K}^{-1}$], in this study we will use an empirical formula given by de Vries [39]:

$$C_v = (2.0x_s + 2.51x_o + 4.19x_w) \cdot 10^6 \quad (52)$$

where: x_s, x_o, x_w [$\text{m}^3 \text{ m}^{-3}$] – the shares of: mineral, organic and water part in the unit of the soil volume.

3.6. Thermal diffusivity determination

The thermal diffusivity α is the ratio of the thermal conductivity and the heat capacity per unit of volume:

$$\alpha = \frac{\lambda}{C_v}. \quad (53)$$

The thermal diffusivity expresses the ability of a body to equalize its temperature in all points. It is equal to the rate of temperature change $\frac{\partial T}{\partial t}$ in a considered point of the soil, which is caused by a unit change of temperature gradient $\frac{\partial T}{\partial x} \left(\frac{\partial T}{\partial x} \right)$, and is expressed by the equation:

$$\alpha = \frac{\partial T}{\partial t} \left(\frac{\partial T}{\partial x} \left(\frac{\partial T}{\partial x} \right) \right)^{-1}. \quad (54)$$

The unit of the thermal diffusion coefficient is $\text{m}^2 \text{ s}^{-1}$.

The thermal diffusivity (temperature conductance) depends mainly on the soil water content. This dependence is a little bit complicated and a gets nonlinear form. After moistening the dry soil with water, a quick increase of the thermal conductivity takes place and it is more intensive than the increase of the heat capacity. Also, the thermal diffusivity of the soil increases very quickly. Further moistening of the soil causes smaller and smaller increases of the thermal conductivity of the soil and the heat capacity increases all the time with constant intensity. When the rate of increase of the heat capacity with the increase of the water content is higher than the rate of the thermal conductivity increase, the decrease of the thermal diffusivity is observed. The thermal diffusivity reaches its maximum at the water content value, characteristic for each kind of soil. Under this value of the water content, the fastest temperature equalization occurs in the system what is often described as the fastest propagation of the “temperature wave” in the soil.

3.7. Thermal characteristics of the studied soil as a function of water content

In this chapter, a verified model of the thermal conductivity was applied to determine the thermal characteristics as a function of the water content and the density of some garden soils and pure sand. The basic data used for determination of the thermal characteristics are contained in Table 4. The contents presented in the table are expressed in the unit of mass. To apply them in the statistical-physical model of the thermal conductivity, they should be recalculated into the unit of volume. The percentage sum of the components of the solid phase always has to be 100%. The data of the mineralogical composition of these soils have been set with some approximation from the aggregate size distribution. It results from the comparison of the data of the mineralogical composition and the aggregate size distribution of soils of the same type, presented in the papers of Czudnowski *et al.* [29], Uziak *et al.* [174], Wierzchoś [189] and Lipiec *et al.* [95] that a good correlation exists between particular fractions of the aggregate size distribution and the mineralogical composition. Fractions from 0.02 to 1 mm contain mainly quartz, while in fractions smaller than 0.02 mm other minerals are predominant.

The thermal conductivity (Fig. 10a, 11a) increases with the water content and this increase is higher (more intensive) for the soil with higher bulk density. The thermal conductivity is significantly influenced by the mineralogical composition and the content of the organic matter. The more quartz in a given, soil the higher values of its thermal conductivity. The increase of the organic matter content in a given soil causes the decrease of the coefficient of the thermal conductivity. When the soil contains only the organic matter, we can expect on such an object, at the most, the values of the thermal conductivity of water (Fig. 10a – compost soil). The dependence of the thermal conductivity versus the water content is nonlinear. This non-linearity occurs for low and high water content values, whereas between these extreme values of the water content, a relatively linear increase of the thermal conductivity versus the water content is observed. The slope of the characteristics of the thermal conductivity as a function of the water content changes in some areas with the increase of the bulk density. For higher water content values the slope changes slightly, but the values of the coefficient of the thermal conductivity under a given water content value are higher for higher values of the bulk density.

The characteristic of the heat capacity per unit volume as a function of the volumetric water content is linear (Fig. 10b, 11b). It can be stated that the heat capacity increases with the water content and that it increases under a given water

content value with the increase of the bulk density. The change of the heat capacity versus the bulk density is observed until the state of water saturation is reached. After the saturation state is reached, the increase of the solid phase in the unit volume causes the decrease of the water content in the unit volume, thus the decrease of the heat capacity per unit volume. Consequently, if the solid phase content in the compacted soil decreases in the unit volume and it is replaced with water, the heat capacity increases.

The thermal diffusivity of soil is characterized by considerable non-linearity versus the increase of the water content and the bulk density (Fig. 10c, 11c). The thermal diffusivity for given water content value is higher for higher bulk densities. A special interest should be put to the maxima in the characteristic of the thermal diffusivity, which occur in various places of this characteristic. It can be stated unambiguously, that the maxima of the thermal diffusivity of soil move towards lower values of the water content when the bulk density increases.

On the base of the family of characteristics of the thermal diffusivity as a function of the water content and the bulk density it is possible to propose the use of these characteristics for practical purposes. Through the regulation of the water content for various bulk densities, it is possible to obtain specific thermal conditions in the soil. By maximization or minimization of the thermal diffusivity it is possible to change the rate of heating or cooling of particular layers in the soil profile. Exemplary, a characteristic was calculated of the volumetric water content as a function of the bulk density values at which the thermal diffusivity of the grey-brown podzolic soil from Felin gains its maxima.

From the calculated data, the linear regression equation was calculated, which determines the water content versus bulk density dependence for the soil from Felin ($\theta = 0.79 - 0.371\rho$ with correlation coefficient 0.995) at which the thermal diffusivity of this soil gains its maximum. To preserve the maximum thermal diffusivity with the change of the bulk density it is necessary to change the water content according to this equation. Of course, it is possible to determine other sections of the characteristic of the water content as a function of the soil bulk density, under required values of the thermal diffusivity. To maintain a specific rate of heating or cooling for given meteorological conditions and for a specific bulk density value, the remote control of the soil water content will be done to sustain it on a specific level.

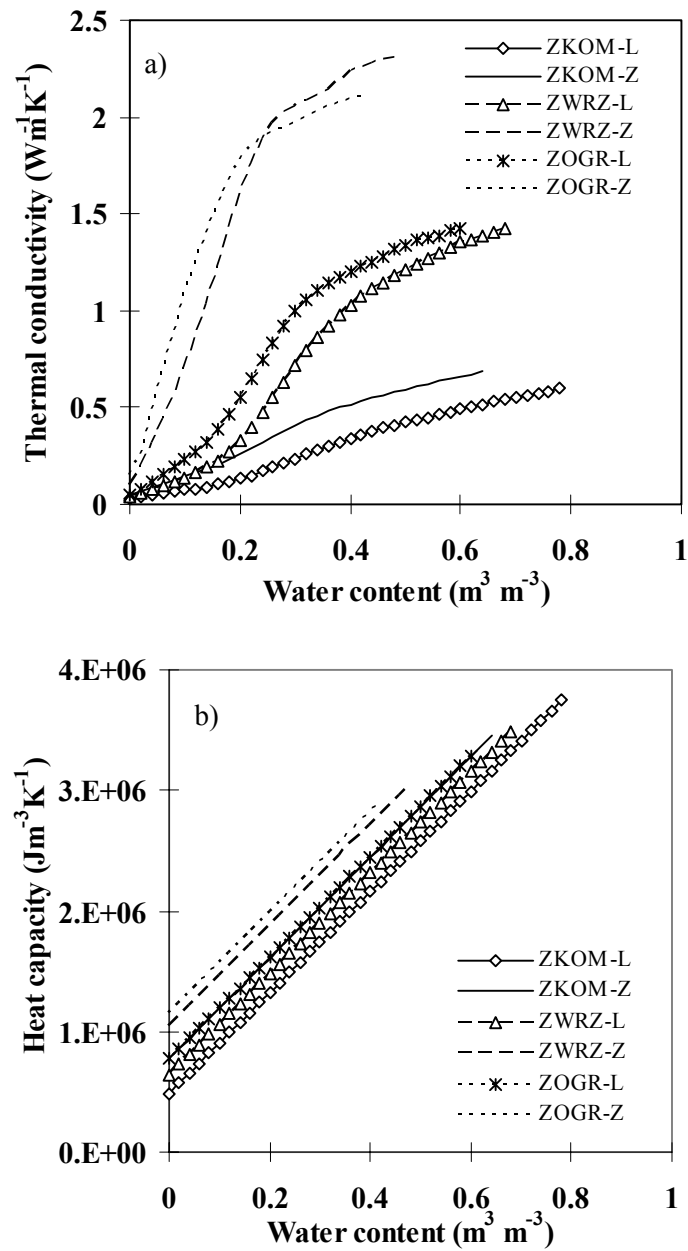


Fig. 10. Thermal properties of soil as a function of water content: a) thermal conductivity, b) heat capacity, c) thermal diffusivity. Explanation: compost – ZKOM, heath soil – ZWRZ, Hortisol – ZOGR. Status of compaction: loose soil – L, compacted soil – Z.

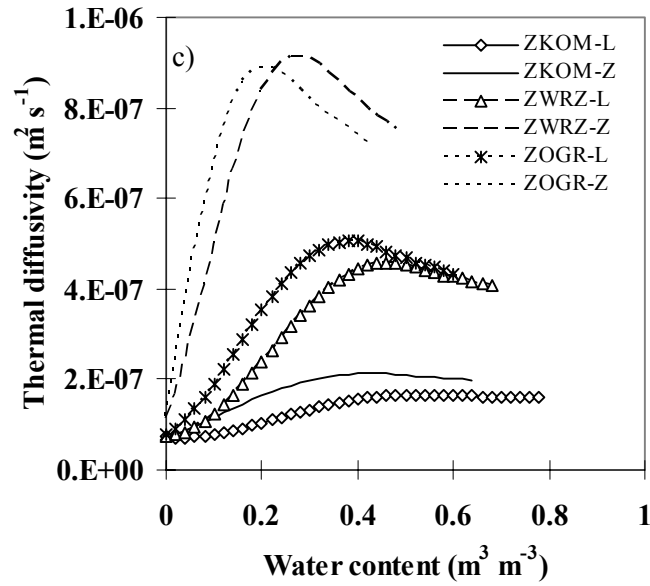


Fig. 10. Soil thermal properties, continuation.

Table 4. Soil physical data used for calculation of thermal conductivity of soils [163]

Kind of material	Comp. state	Bulk density, Mgm^{-3}		Content [%, g g^{-1}]		
		Solid phase	soil	OM	quartz	Other minerals
Compost soil	L	2.10	0.46	28.47	0	100
	Z		0.73			
Heath soil	L	2.57	0.81	2.59	96	4
	Z		1.31			
Hortisol	L	2.63	1.01	3.68	70	30
	Z		1.50			

Comp. state – compaction state, OM – organic matter.

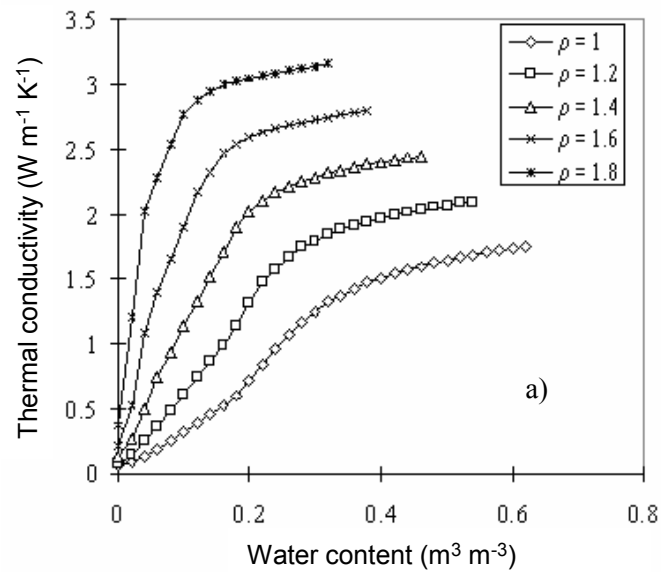


Fig. 11. Thermal properties of sand; a) thermal conductivity, b) heat capacity, c) thermal diffusivity, ρ [Mg m⁻³] – bulk density

The special attention should be paid to the characteristics of the thermal diffusion of the soil because they enable to state unambiguously, that with the increase of the bulk density of the soil, the maxima of the thermal diffusivity move towards the smaller values of the water content.

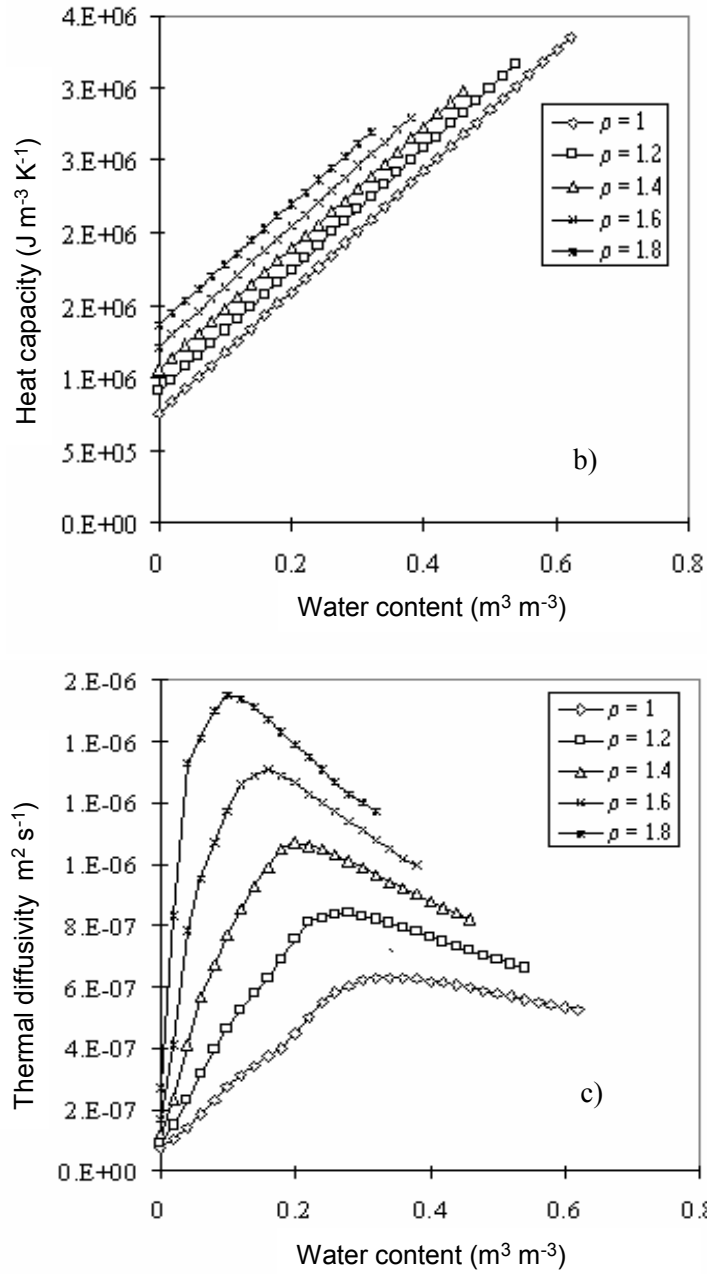


Fig. 11. Soil thermal properties, continuation.

4. RADIATION TEMPERATURE OF PLANTS

4.1. Black body and real bodies radiation

The heat exchange between bodies can take place in three different ways, *i.e.* through conduction, convection and thermal radiation. The thermal radiation of a body in temperature higher than absolute zero relies on the exchange of kinetic energy of chaotic movement of particles into electromagnetic waves. Due to this, it is possible to measure remotely the energy flux of this radiation. It is the fourth power of thermodynamic temperature of the investigated object. For the black body this relation is expressed by Stephan-Boltzmann's law: the total energy W emitted from a unit surface of blackbody in a unit time is expressed by equation:

$$W = \sigma T_t^4 \quad (55)$$

where: σ – Stephan-Boltzmann's constant = $5.6697 \cdot 10^{-8}$ [W m⁻² K⁻⁴], T_t – thermodynamic temperature of a body [K].

Max Planck described the black body radiation as a function of wavelength and temperature:

$$W_{\lambda,b} = \frac{2\pi hc^2}{\lambda^5 (e^{hc/\lambda kT} - 1)} \cdot 10^{-6} \quad (56)$$

where: $W_{\lambda,b}$ – flux density of black body radiation energy for a given wavelength [W m⁻² μm⁻¹], c – light velocity in vacuum $\approx 3 \cdot 10^8$ [m s⁻¹], h – Planck's constant = $6.6256 \cdot 10^{-34}$ [J s], k – temperature of black body = $1.38054 \cdot 10^{-23}$ [J K⁻¹], T – wave length [m].

The ratio of the energy W_{rz} emitted by a real body at a given temperature to the energy W emitted by a black body at the same temperature is called the emissivity coefficient of the real body:

$$\varepsilon = \frac{W_{rz}}{W} \quad (57)$$

Exemplary values of emissivity coefficient of chosen terrestrial bodies according to various authors are contained in Table 5.

It results from equations (55) and (57) that:

$$\sigma T_r^4 = \varepsilon \sigma T_t^4 \quad (58)$$

therefore, the radiation temperature T_r of a real body having the emissivity coefficient ε is equivalent to the thermodynamic temperature T_t multiplied by the 4-th power root of its emissivity coefficient:

$$T_r = \sqrt[4]{\varepsilon} T_t \quad (59)$$

Table 5. Emissivity coefficients for the range 8-13 μm for the chosen objects [9]

Kind of surface	ε	Author
Alfalfa	0.98	Fusch and Tanner (1966)
Shortly cut lawn	0.97	Lorenz (1966)
Grass on wet clayey soil	0.98	Gorodetskij and Filipow (1968)
Snow	0.99	Gorodetskij and Filipow (1968)
Water – Ontario lake	0.97	Davies <i>et al.</i> (1971)
Clean water	0.99	Beuttner and Kern (1965)
Clayey shale	0.98	Taylor (1979)
Gravel	0.97	Taylor (1979)
Dry fine-grained sand	0.95	Gaewskij (1951)
Water saturated fine-grained sand	0.96	Gaewskij (1951)

According to Wien's law the maximum of energy emitted by a body, due to temperature increase, moves towards shorter wavelengths (Fig. 12).

In the range of meteorological temperatures, *i.e.* about 300 K, the maximum of emitted energy corresponds with electromagnetic wave length of about 10 μm . This fact is the base for construction of devices for measuring the radiation temperature. Most of such instruments use the measurement of radiation temperature in the range 8-13 μm . For the radiation in this range the atmosphere is nearly transparent. For the temperature of sun, *i.e.* about 6000 K, this maximum corresponds with optical range of electromagnetic spectrum. The wavelength of electromagnetic spectrum corresponding with the maximum of energy emitted in a given temperature is calculated from the equation:

$$\lambda_{\max} = \frac{C}{T} \tag{60}$$

where: $C = 2898 \mu\text{m K}$.

In the black body the whole incident energy is absorbed by its surface (absorptance $a = 1$). In the real bodies a fraction of incident energy is reflected (reflectance r), a fraction is transmitted (transmittance p) and the rest is absorbed. Therefore:

$$r + p + a = 1. \tag{61}$$

Among real bodies we can select: white bodies ($r=1$), transparent bodies ($p=1$), opaque bodies ($p=0$) and grey bodies ($a<1$).

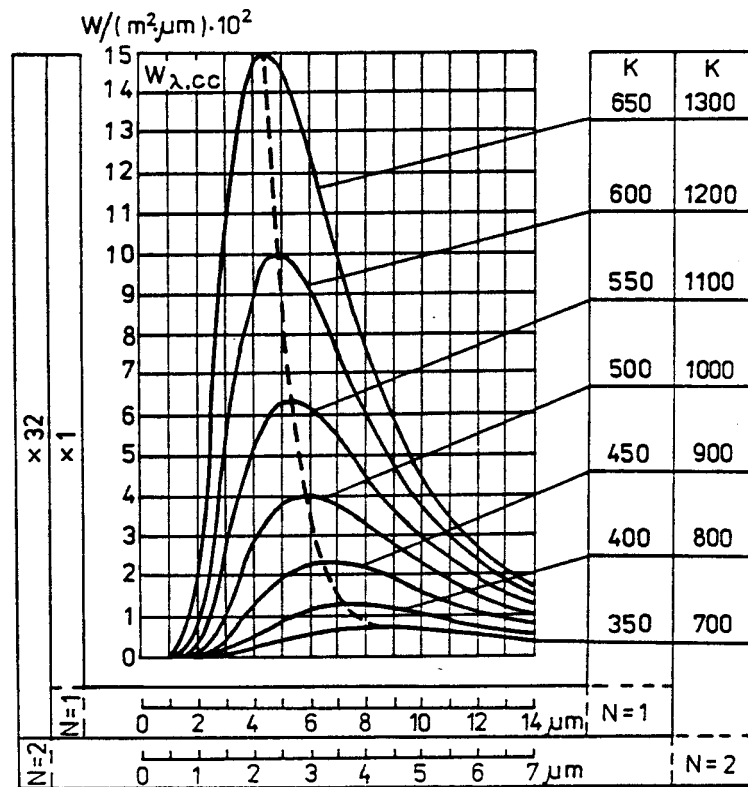


Fig. 12. Radiation flux density (emittance) of back body as a function of wavelength for different temperature values [137]

The amount of energy of infrared radiation incoming to the detector is influenced not only by its spectral but also by geometrical distribution. The Lambert's law says that the intensity of radiation from a flat surface (the density of an emitted flux into the unit spherical angle) changes with the angle of deflection (β) from the perpendicular to the emitted surface according to the equation:

$$I_{\beta} = I_n \cos \beta \quad (62)$$

where: I_{β} – radiation intensity for the angle β [$\text{W m}^{-2}\text{sr}^{-1}$], I_n – radiation intensity in the direction normal to the emitting surface [$\text{W m}^{-2}\text{sr}^{-1}$]. Therefore, for the angle $\beta=0$ between the axis of thermographic device and the emitted surface, the signal registered by the detector is the strongest.

Only in the case of radiant emission from a perfect body the vector of field intensity for all directions creates a sphere. For real bodies these spheres are deformed and the highest deviation from the Lambert's law usually occur for the angles 60° - 90° (Fig. 13).

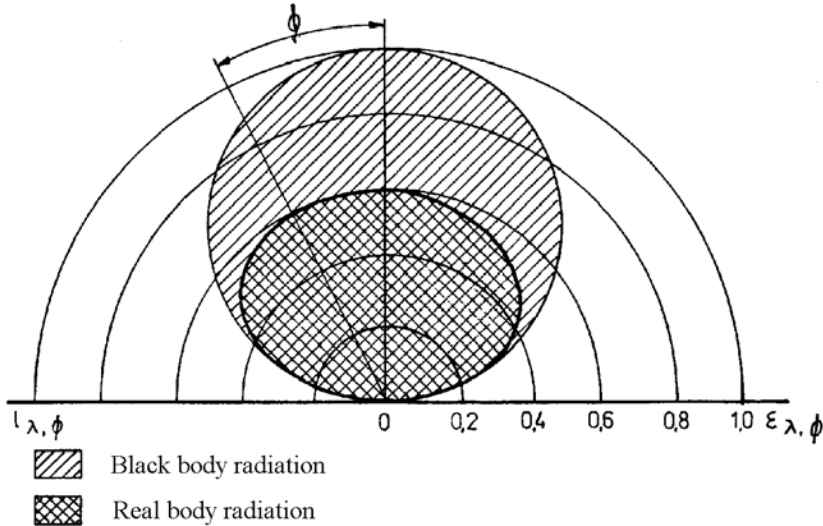


Fig. 13. Directional emissivity distribution $\varepsilon_{\lambda, \phi}$ and surface radiation density $l_{\lambda, \phi}$ of black body and a real body in hemisphere, ϕ – angle between radiation intensity vector and normal to the emitting surface [137]

4.2. Factors influencing the measurement of plant cover radiation temperature

Plant temperature is nearly always different from the temperature of surrounding air and it is influenced by a set of external factors and physiological processes within plants determined by these factors. All these factors have impact on the transpiration rate, which apart from the air temperature and the solar radiation determines the actual value of the plant cover temperature. During the transpiration process, *i.e.* water evaporation from plants, large amounts of heat are consumed (about 2.5 MJ per one kilogram of water). The higher is transpiration rate, the more intensive is plant cooling.

Numerous factors influence radiation temperature of plant surface. They can be divided into three groups:

- properties of plant surface and canopy (emissivity ε , albedo α_s , *i.e.* fraction of global radiation reflected by the surface, aerodynamic roughness z_0 , soil cover expressed by the leaf area index (LAI), position of the canopy surface in relation to the incident solar radiation);
- physical status of the boundary layer of atmosphere and the processes taking place in it (shortwave R_s and longwave R_l solar radiation fluxes, air temperature T_a , air pressure p_a , water vapour pressure in the air e_a , wind speed u) and in the soil (soil water potential Ψ_g , soil water content Θ , temperature in the soil profile T_g , soil water characteristics $K(\Theta)$ and $\Psi_g(\Theta)$, soil heat properties, *i.e.* thermal conductivity λ , thermal diffusivity α , heat capacity c_v , content of chemical substances, soil pollution);
- physical status and physiological processes in plant, (variety, phase of physiological development, depth of the rooting system, diseases, *etc.*).

All these factors (Fig. 14) influence the transport of water and energy in plants, expressed by the heat balance equation, in which the conditions of the stability of the atmosphere just above the crop should be included [14,15].

The actual value of plant temperature depends mainly on the intensity of transpiration, which is determined by availability of soil water for the rooting system [94] and on meteorological factors. Heat conditions in the soil and on its surface are less important. Soil water loses as a result of evaporation limit water availability for plants. The intensity of evaporation depends besides meteorological factors on the soil structure in the subsurface layer, including its compaction and aggregation.

The inner factors include the intensity of metabolic processes, plant construction, leaf size, its anatomic structure (number of stomas, thickness of cuticle) and rooting system status. In the experimental station ENSA in Rennes, France, Duschene [42] conducted measurement of radiation temperature of wheat canopy, growing in homogeneous, in respect to soil conditions, field. Some parts of the canopy showed in the morning hours, when the airborne thermal imaging was conducted, the increased temperature. It was stated that plants in this plots suffered a considerable damage of the rooting system by Nematoda pests, which caused ceasing of water uptake from the soil and decrease of transpiration intensity.

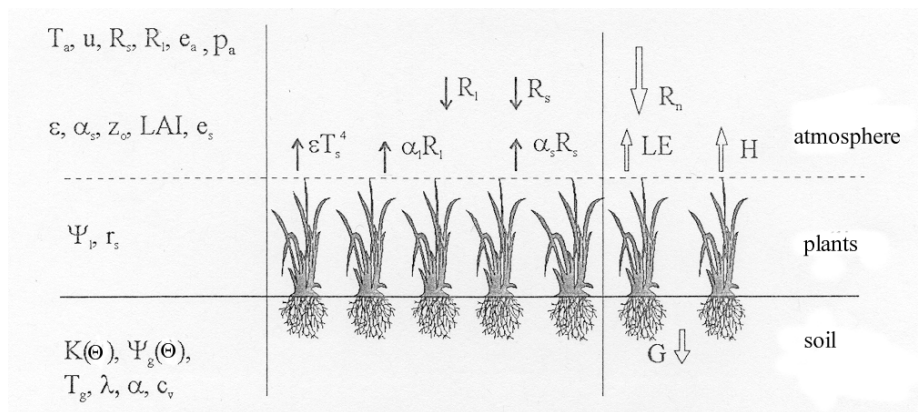


Fig. 14. Physical parameters determining actual value of radiation temperature of plant cover

Meteorological parameters, *i.e.* external conditions (air temperature, air humidity, wind speed, solar radiation intensity) have high impact on plant temperature. Solar radiation is also a factor increasing the rate of physiological processes in plants and transpiration intensity [4, 6, 28, 29].

The actual value of radiation temperature of plants reflects a state of energetic equilibrium expressed by the balance equation for fluxes coming from the atmosphere, investigated surface and soil. On the base of studies performed by Thofelt [159] in laboratory conditions it was stated that, the increase of radiation from 300 to 2000 W m^{-2} can cause the increase temperature of healthy leaf and the temperature of the surrounding even by several degrees.

The influence of light on plant temperature is discussed by Łukomska and Rudowski [97]. Rapid increase of lighting intensity after moving a plant from the

darkness into the daily light causes the increase of plant temperature by some degrees. However, a violent, forced in laboratory conditions decrease of the relative air humidity by about 30% does not cause the disappearance of differences between the leaf temperature and the temperature of surrounding air.

During the measurements in the open space, the influence of the wind speed onto the measured value of the radiation temperature should be considered. According to the instruction contained in the training materials of AGEMA firm [3] it is not recommended to perform measurements of radiation temperature under the wind speed values exceeding 8 m s^{-1} . This firm recommends also the use of a correlation coefficient, which enables to recalculate the values of the radiation temperature measured under various values of the wind speed into the values corresponding to the wind speed of 1 m s^{-1} . In Fig. 15, the correlation coefficient values for various wind speeds are presented.

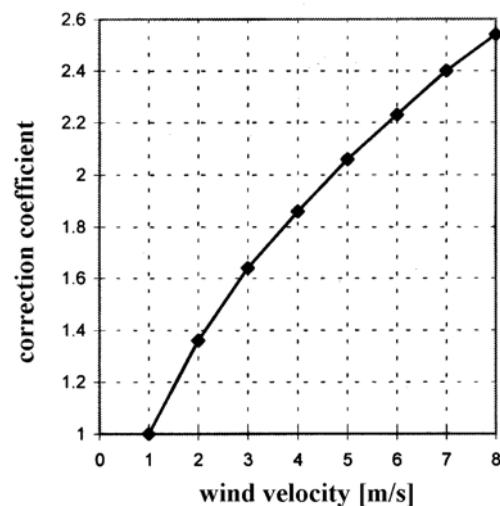


Fig. 15. Correction coefficient for radiation temperature measurements under different wind speed values [3]

It was stated by the analysis of a several day distribution of radiation temperature on the wheat canopy covering the soil with favourable water conditions during the hours with the highest solar radiation intensity, that the increase of the wind speed influences the decrease of radiation temperature and the increase of evapotranspiration [7].

An essential factor, which modifies the radiation temperature of plant cover, is the relative humidity of air. It results from the studies of Fusch [48] that the relative air humidity above 70% causes the decrease of the radiation temperature differences between plants, being in varying conditions of soil water availability for the rooting system.

The measurement with a thermographic device covers the surface, which cannot be easily defined because it creates a complicated dynamic system, including various parts of plants with a complex geometry and, in case of incomplete soil cover, also gaps of bare soil. Each plant possesses some physiological mechanisms, which enable to modify the surface characteristics under the impact of external factors (*e.g.* heliotropism). Therefore, the measured value of the radiation temperature depends significantly on the angle between the camera and the studied surface and on the position in relation to the direction of solar radiation (Fig. 16).

The studies of the influence of the angle of inclination of the radiation thermometer (8-14 μm) towards the surface of wheat canopy were performed by Hatfield [62]. Making measurements from the height of 1m he put the radiation thermometer in the direction perpendicular to the surface and at the angle of 45° from main directions (N, S, E, W). It was stated by the author, that in case of incomplete cover of the soil surface with plants, lower values of radiation temperature of the surface were obtained for the angle of 45° than for 90° , due to the fact that in the former case less energy incoming to the detector comes from the bare soil.

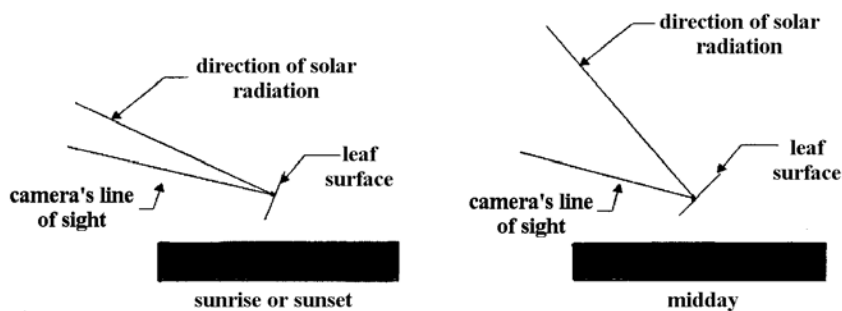


Fig. 16. Change of leaf surface direction towards thermographic device with change of solar radiation angle [62]

The occurrence of differences in canopy radiation temperature in respect to the angle between direction of measurement and direction of solar radiation was stated by Nielsen *et al.* [111]. They conducted the measurement of the radiation temperature of a field with soybean from the angle of 30° to the horizontal level simultaneously from four main directions (N, S, W, E).

In case of incomplete soil cover with plants, the total temperature of the surface T_{sf} , measured remotely, is a function of soil temperature and plants temperature multiplied by respective fractions of their surfaces in relation to the total surface. The energy balance equation of the surface is as follows (Heilman *et al.* 1981 and Kustas *et al.* 1990):

$$[\varepsilon_c f_c + \varepsilon_s (1 - f_c)] \sigma T_{sf}^4 = f_c \varepsilon_c \sigma T_c^4 + (1 - f_c) \varepsilon_s \sigma T_s^4 + f_c (1 - \varepsilon_c) R_l + (1 - f_c) (1 - \varepsilon_s) R_l \quad (63)$$

where: f_c – the ratio of the surface covered with plants to the total surface; T_{sf} – the total temperature of the surface [K]; T_s – soil temperature [K]; T_c – plant temperature [K]; ε_c – emissivity of plants; ε_s – emissivity of soil; σ – Stefan-Boltzman's constant [$\text{W m}^{-2} \text{K}^{-4}$]; R_l – flux density of longwave surrounding radiation reaching the studied surface [W m^{-2}].

The quantity of R_l is determined on the base of the measurement of air temperature T_a and the knowledge of air emissivity ε_a :

$$R_l = \varepsilon_a \sigma T_a^4 \quad (64)$$

Under some simplifications resulting from the assumptions of the conditions of measurement, the terms of the longwave reflected radiation could be omitted in equation (63). Thus:

$$T_{sf}^4 = f_c T_c^4 + (1 - f_c) T_s^4 \quad (65)$$

The values of T_{sf} obtained by Kustas *et al.*, [90] from this simple model for the cotton canopy differed from the values obtained from ground measurements by 2°C, on average. These authors stated that in case of incomplete soil cover with plants, the differentiation of soil temperature, resulting from its non-uniform illumination, should be considered.

5. STUDY OF ACTUAL EVAPOTRANSPIRATION ON THE BASE OF PLANT TEMPERATURE MEASUREMENT

The modelling of actual evapotranspiration is a complex research problem due to majority of physiological and physical processes, which influence the rate of water transported from the soil, through the rooting system and plant tissue into the atmosphere.

The theoretical bases of evapotranspiration determination were given by Penman, who analysed the processes of water vapour and energy transport from evaporating surface on the base of semiempirical equations [119-122]. The author states that the transport of water vapour from the evaporating surface is determined by the gradient of water vapour pressure between the surface and the air above it, and is strongly modified by the wind speed. On the other hand, the transport of energy from the evaporating surface, which analysis requires taking into account the heat balance on the surface, includes the process of energy supply for the water transition from the liquid phase into gaseous phase in the form of the latent heat. The equations, formulated by Penman, describing both kinds of transport contained the parameter of surface temperature or/and the water vapour pressure on the evaporating surface, which according to the author could not be measured during the routine measurements in agro-meteorological stations at that time. Therefore, the author made a modification of the heat balance equation, including an aerodynamic component to eliminate the necessity of measurements of these parameters.

Penman equations for calculation of the evapotranspiration rate, which revealed the importance of the temperature of evaporating surface, made many researchers look for possibilities of measuring this quantity. First measurements of plant cover temperature were conducted with the use of contact thermometers [105]. However, the accuracy of this method was very small. In nineteen fifties Stoll and Hardy [152] elaborated a radiometer working in the infrared range for the temperature measurement of the natural environment. Gates [49] successfully used this device for the measurement of the plant cover temperature.

A rapid development of the infrared sensors in nineteen sixties and seventies, caused increased production of hand-held thermal radiometers and first thermographic systems, which enabled to measure the surface temperature with accuracy of 0.5-0.1°C. Monteith and Szeicz [107], Tanner [158], Wiegand and Namken [188] were among the first who used the infrared thermometry in the

studies of plant temperature in the context of its relation to the soil water conditions. Further studies of plant temperature under different soil water content values made it possible to state that plant temperature increase occurs for limited availability of water for plants, therefore it can be an indicator of plant water stress [8, 10, 44, 47, 70, 74, 100, 101, 103, 104, 117, 125, 145, 185, 187].

The intensive studies of radiation temperature of the bare soil and plant cover for determination of actual evapotranspiration were initiated in nineteen seventies. Airborne and satellite thermal images became available from multispectral scanners containing thermal channels and temperature distribution of large agricultural areas were analysed to create new models of actual evapotranspiration.

Remote sensing methods of soil and plant cover temperature measurements of large areas replaced point measurements and a new perspective was created to determine actual evapotranspiration in regional scale. It was a milestone in the analysis of the water balance of large areas. Fundamental studies on this topic were performed by Bartholic *et al.* [16], Brown [20], Stone and Horton [153] as well as Heilman *et al.* [65]. They analysed the physical relations between radiation temperature of plant cover measured from different levels and intensity of evapotranspiration.

In the nineteen eighties and nineties the studies were continued to apply thermal images of plant cover from different levels for calculation of actual evapotranspiration [10, 32, 34, 101, 102, 103, 124, 125, 126, 140, 145, 181, 185].

These studies were the foundation for further modeling of the actual evapotranspiration with the use of the measured crop cover radiation temperature. The main assumptions of these models were:

- radiation temperature of plant cover is determined by the processes of water and heat transport in the soil-plant-atmosphere system;
- energy exchange on the plant surface is expressed by the heat balance equation;
- plant temperature can be used for determination of actual evapotranspiration by connecting the heat balance equation of the active surface with the equations of vertical transport of latent and sensible heat fluxes.

4.3. Methods of evapotranspiration determination

All methods of evapotranspiration determination can be divided into direct and indirect. Within direct methods the loss of water from water or soil evaporimeters or lysimeters is measured in a given period of time. Indirect

methods enable to determine the flux of water vapour by indirect measurements, physical and statistical equations and models which simulate the process of evaporation.

From the point of view of the measurement methods, considered processes and mathematical methods used for evapotranspiration determination, the following groups of methods can be distinguished:

- methods which are based on turbulence transport of energy, mass and momentum in the surface layer of the atmosphere;
- methods which are based on measurement of mean profiles of meteorological elements;
- methods which are based on the heat balance equation;
- combined methods;
- methods which use the mass balance equation (hydrological equation);
- empirical methods.

– from among the methods of actual evapotranspiration determination, the methods which are based on turbulence transport of energy, mass and momentum in the surface layer of the atmosphere are considered as the most precise; These methods are based on measurements of fluctuations in wind speed, water vapour pressure and temperature. These methods comprise the eddy-correlation and dissipation methods. They do not require determination of the atmosphere stability functions and not contain any empirical equations. Although these methods are treated as standard ones, they are used quite rarely because they need very precise and expensive instrumentation, which enables to register the measured quantities with very short time step. In the eddy-correlation method the turbulent fluxes of water vapor, momentum or sensible flux are determined from covariances. Not only fast response time of the measuring instruments but also necessity of averaging measured data coming from a sufficiently long period, the precision in placement and orientation of the velocity sensors, limit the applicability of this method to strictly research purposes. The dissipation method is based on the budget equations for covariances and it requires not only the measurement of turbulent variables but also uses some similarity assumptions. The main advantage of this method is that, unlike the eddy-correlation method, it does not contain so strict requirements for sensors' orientation.

By obtaining the mean vertical profiles of wind speed, air temperature and water vapor pressure, it is possible to determine evapotranspiration with the use of semiempirical equations of the turbulence theory. When applying these methods the equilibrium state in atmosphere should be considered. Methods of mean

profiles belong to the most precise methods. A disadvantage of these methods is that they need consideration of the equilibrium state in atmosphere, *i.e.* determination of the equilibrium function, which includes empirical equations [23]. Another problem is connected with limited number of meteorological stations which register mean values from 30 minutes and averaging data coming from larger periods incorporates big error of determined evapotranspiration values.

In the studies described in this book, the method was used, which is based on the heat balance equation and combined methods, therefore it is justified to present more extensively their basic assumptions.

The heat balance of radiation usually refers to a layer of the medium the border with the atmosphere (water, soil, plant cover). It can be infinitely thin or it can have a specific thickness, *e.g.* corresponding to the thickness of plant cover. To express the basic processes of energy exchange in the system, the following form of the heat balance equation is used [21]:

$$R_n - L \cdot E - H + L_p \cdot F_p - G + A_h = \frac{\partial W}{\partial t} \quad (66)$$

where: R_n – the net radiative flux density at the upper surface of the layer [W m^{-2}], H – the sensible heat flux density [W m^{-2}], G – the density of the heat flux in the soil [W m^{-2}], L – the latent heat of vaporization ($2448000 \text{ J kg}^{-1}$), E – the water vapor flux density [$\text{kg m}^{-2} \text{ s}^{-1}$], L_p – the thermal conversion factor for fixation of CO_2 [J kg^{-1}], F_p – the specific flux of CO_2 [$\text{kg m}^{-2} \text{ s}^{-1}$], A_h – the energy advection into the layer expressed as specific flux [W m^{-2}], $\delta W/\delta t$ – the rate of energy storage per unit area in the layer [W m^{-2}].

Depending on kind of application, some components of this equation occur less important and can be omitted. The most frequently used form of the heat balance equation takes into account four quantities: $L \cdot E$, H , R_n , G .

The methods, which are based on the heat balance equation, consist of assuming one component of this equation as the unknown (usually it is $L \cdot E$ or H) and determination of other components by indirect methods.

A qualitatively new attitude towards the problem of the evapotranspiration determination with the use of the heat balance method occurred, when a possibility appeared to measure remotely the evaporating surface temperature. The radiation temperature measured by remote sensing instruments with high accuracy and for large areas, gives a chance to modify the heat balance method to

apply it for regional scale. The sensible heat flux, expressing the transport of heat energy from the evaporating surface into the atmosphere is proportional to the difference of the air temperature at some level and the temperature of the studied surface. Till today, several efforts have been undertaken to use the heat balance equation for evaluation of the evapotranspiration from large areas.

The group of combined methods consists of the methods, which consist of two or more methods of evapotranspiration determination. This group contains the methods that are based on Penman's equation. In 1948 he developed jointly the equations of heat and water balance to eliminate from them a quantity, which was difficult to be measured that days – the temperature of the evaporating surface [121-122]. The Penman's derivation combines the heat balance method with the aerodynamic method. The original purpose of Penman's equation was to enable evaluation of mean monthly evaporation from an open-water surface by using standard meteorological data of solar radiation, wind speed, air temperature and humidity. Further on, this equation was applied for evaporation from the bare soil and the soil covered with plants.

The Penman's equation from 1948 has the following form:

$$LE = \frac{\Delta \cdot (R_n - G) + \gamma \cdot f(v) \cdot [e_a^* - e_a]}{\Delta + \gamma} \quad (67)$$

where: LE – the latent heat flux density [W m^{-2}], R_n – the net radiation flux [W m^{-2}], G – the heat flux in the soil [W m^{-2}], γ – the psychrometric constant [kPa K^{-1}], $f(v)$ – the function of wind speed v , which takes into account the turbulent movement of air between the studied surface and a reference level z [m s^{-1}], e_a – the water vapor pressure at the reference level [kPa], e_a^* – the saturated water vapor pressure under the air temperature T_a [kPa], Δ – the slope of the saturation water vapor pressure curve in relation to the temperature axis [kPa K^{-1}].

The function $f(v)$ which occurs in equation (67) can be presented as an empirical expression:

$$f(v) = a_w + b_w v_{2m} \quad (68)$$

where: a_w, b_w – the empirical coefficients, v_{2m} – the wind velocity measured at the height of 2 meters over the soil surface.

The analysis of the coefficients for the whole vegetation period for clover and grass was performed by Wright [192], who expressed them as a function of the day of year and latitude. Because the data, which were the base for determination of the coefficients came from the lysimetric station in Kimberly, Idaho, this method of evapotranspiration determination was called Kimberly Penman.

The modification of equation (67) known as “Penman 1963” [122] enables to calculate evapotranspiration through a larger number of measurable quantities, which create three segments of the equation: the shortwave radiation segment, the longwave radiation segment and the aerodynamic segment:

$$LE = \frac{\Delta}{\Delta + \gamma} R_s (1 - \alpha) - \frac{\Delta}{\Delta + \gamma} R_{lb} + \frac{\gamma}{\Delta + \gamma} f(v) [e_a^* - e_a] \quad (69)$$

where: R_s – the density of incoming shortwave radiation flux [W m^{-2}], α – the albedo of the evaporating surface. R_{lb} – the density of the longwave radiation flux balance [W m^{-2}].

Some authors [35, 150] tried to calculate evapotranspiration in a similar way using the equation:

$$LE = a \frac{\Delta \cdot R_n}{\Delta + \gamma} \quad (70)$$

where: a is an empirical coefficient (equal to about 1.3).

The original Penman equation was refined by incorporating the stomata resistance r_c as influencing the transport of the water vapour, and the roughness of the surface that influences the intensity of the momentum transfer towards the plant surface.

The Penman-Monteith equation [107], derived in 1965 combines a logarithmic function of rotational diffusion with the resistance of the stomata and has a form:

$$LE = \frac{\Delta \cdot (R_n - G) + \rho \cdot c_p \cdot [e_a^* - e_a] / r_a}{\Delta + \gamma \cdot (1 + r_c / r_a)} \quad (71)$$

where: ρ – the bulk density of air [kg m^{-3}], c_p –the specific heat of air [$\text{MJ kg}^{-1} \text{ }^\circ\text{C}^{-1}$]. The units of other quantities are: LE , R_n and G [$\text{MJ m}^{-2} \text{ s}^{-1}$], e_a^* and e_a [kPa], r_c and r_a [s m^{-1}].

In 1981 Monteith [109] gave a modification of his formula from 1965:

$$LE = \frac{\Delta R_n (1 - \tau) + D c_p / r_H}{\Delta + \gamma [(r_a + r_c) / r_H]} \quad (72)$$

where: D – the water pressure deficit [kPa], r_H – an effective aerodynamic resistance for heat and longwave radiation transfer [s m^{-1}], defined by the equation:

$$r_H^{-1} = r_a^{-1} + (c_p / 4 \varepsilon_c \sigma T_a^3)^{-1} \quad (73)$$

where: ε_c – the emissivity coefficient of canopy, σ – Stefan-Boltzmann's constant [$\text{W m}^{-2} \text{ K}^{-4}$], T_a – air temperature [K], other quantities as previously.

In the last years, some semiempirical formulas for potential evapotranspiration calculation, called FAO-24 [41,64] have gained an increasing popularity. It refers to: FAO-24 Penman's method, FAO-24 Blaney-Criddle's method, FAO-24 radiation method and FAO-24 method which is based on the measurement with water evaporimeters. These methods enable to calculate reference potential evapotranspiration for grass and alfalfa, taking into account some empirical correction coefficients, which were obtained in precisely controlled field experiments conducted under various meteorological conditions with the use of the multiple regression method with climatic parameters as independent variables.

Methods, which are based on the mass balance, use the law of mass conservation with reference to a part of the hydrological cycle. The main assumption in this approach is, that the intensity of influx lessened by the intensity of outflow gives the intensity of the change of stored water.

One of the ways of determination of evapotranspiration, using the mass balance, is application of lysimeters and soil evaporimeters, which enable to measure the amount of water evaporating from the soil monolith. The principle of lysimeters consists of regulation the level of the soil water, maintained artificially, whereas evaporimeters measure the change of soil monolith weight. Both

lysimeters and evaporimeters are containers filled with soil, and their sidewalls and bottoms are water-resistant.

Empirical methods use the relations between the evapotranspiration and fundamental meteorological elements, such as: solar radiation, water vapour deficit the air, air temperature and others. These relations are obtained for a specific site using statistical methods of analysis for a representative data set. It results in limitation of application of the obtained evapotranspiration formulas only for similar topographic conditions. Because only some chosen meteorological elements are considered in calculations in empirical methods, they are burdened with high error.

4.4. Heat balance equation of active surface. Water and heat transport in soil-plant-atmosphere system

The heat balance equation (66) describes the process of energy exchange of the studied evaporating surface (e.g. plant cover surface). Depending on the aimed application, particular terms of this equation are less important and can be omitted. The most frequently used form of the heat balance equation is:

$$L \cdot E + H + R_n + G = 0 \quad (74)$$

where: $L \cdot E$ – the density of the latent heat flux (an energetic equivalent of the evapotranspiration flux) [W m^{-2}]; L – the latent heat of vaporization ($L=2.45 \cdot 10^6 \text{ J kg}^{-1}$); E – the flux of evapotranspiration [$\text{kg m}^{-2} \text{ s}^{-1}$]; H – the sensible heat flux density [W m^{-2}]; R_n – the net radiation flux density of the upper surface of the considered layer [W m^{-2}]; G – the density of the heat flux in the soil [W m^{-2}];

The fluxes in this equation, which are directed towards the surface, are assumed to be positive and the fluxes directed in the opposite direction are negative. The components of the heat balance equation are graphically presented in Fig. 14.

The net radiation flux R_n is the result of combination of all the fluxes absorbed and emitted by the active surface. The sun emits mainly shortwave radiation ($<4 \mu\text{m}$), whereas clouds, air, soil and plants emit the longwave radiation ($>4 \mu\text{m}$). The net radiation R_n is a difference between the incoming short- and long-wave radiation and the reflected shortwave and emitted longwave radiation.

$$R_n = (1 - \alpha_s)R_s + (1 - \alpha_l)R_l - \varepsilon\sigma T_c^4 \quad (75)$$

where: α_s , α_l – the reflection coefficients of the surface for shortwave and longwave radiation, respectively; R_s , R_l – the densities of shortwave and longwave radiation [W m^{-2}]; T_c – the surface temperature [K]; ε – the emissivity of the surface; σ – the Stefana-Boltzman's constant ($5.67 \cdot 10^{-8} \text{ W m}^{-2}\text{K}^{-4}$); because $\varepsilon + \alpha_l = 1$ so equation (75) can be written in the form:

$$R_n = (1 - \alpha_s)R_s + \varepsilon(R_l - \sigma T_c^4) \quad (76)$$

In the evapotranspiration models, which use the remote-sensing data, the net radiation R_n occurs as a quantity measured directly or calculated on the base of the measurement of other quantities, also these measured with remote-sensing methods [33, 75, 119]:

Jackson at al. [85] elaborated a method of determination of the net radiation, which uses the point ground measurements of incoming short- and longwave radiation and remote-sensing multi-scanner measurement of the reflected short-wave radiation and emitted longwave radiation from the surface. The data coming from the point measurement could be extrapolated onto the areas of the surface of several kilometres in case they were obtained under the conditions of cloudless sky and stable atmosphere.

In this method the longwave radiation emitted by soil with plant cover was derived on the base of the measurement of surface temperature (thermal channel of multispectral radiometer). It enabled to estimate the influence of temperature difference between canopy and air caused by differentiated soil moistening on the intensity of the emitted longwave radiation. According to the authors, the range of the temperature difference between plant cover and air corresponds to the conditions from the active transpiration under unlimited availability of the soil water (-10°C) to a complete inhibition of transpiration as a result of unavailability of the soil water ($+5^\circ\text{C}$). For this range of the temperature difference between the plant cover and the air, the values of the density of long-wave radiation change by about 90 W m^{-2} under the air temperature of 30°C .

Because the plant surface temperature depends on the soil water potential, also R_n changes with the change of the soil potential. It was stated experimentally that change of T_c for various levels of the soil water potential, the net radiation flux R_n changes up to 20% of its maximum value [119].

The heat flux in the soil is according to the Fourier's law proportional to the gradient of the soil temperature and the soil thermal conductivity.

$$G = -\lambda \frac{\partial T_g}{\partial z} \quad (77)$$

where: G – the density of the heat flux in the soil [W m^{-2}]; λ – the soil thermal conductivity [$\text{W m}^{-1} \text{K}^{-1}$]; z – the depth in the soil profile [m]; T_g – the soil temperature [K].

The soil thermal conductivity depends on its water content, bulk density, porosity, mineralogical composition and the content of the organic matter. The most popular models of determination of the soil thermal conductivity are: the dispersion model of de Vries and the statistical-physical model of Usowicz [171]. Both models are presented more detailly in Chapter 3.

Some models of actual evapotranspiration omit the term of the heat flux in the soil, assuming that this flux constitutes a negligible percent of the net radiation flux [18,128]. Some studies showed, that under a complete soil cover, the heat flux in the soil G constitutes about 0.1 of the net radiation flux R_n , whereas for the bare soil its values reach $0.3 R_n$. [85,121].

In Poland, the studies on empirical relation between the heat flux in the soil G , the air temperature T_a and the net radiation flux R_n , for the meadow plant cover were conducted in Agrometeorology Department of Agricultural University in Poznań and in the Institute of Geodesy and Cartography in Warsaw. Additionally, these studies took into account the density of plant cover, expressed as LAI (Leaf Area Index) [33]. The obtained relation is presented by the formula:

$$G = -4.27 + 0.063 \cdot R_n + 0.355 \cdot T_a + 0.87 \cdot LAI . \quad (78)$$

This relation was used to evaluate the evapotranspiration from meadows on the base of NOAA satellite images.

Heat and water transport in the soil-plant-atmosphere system can be described with the use of the resistance model, constructed as an analogue of the electric circuit. The scheme of this model is presented in Fig. 17.

The transport equations for the sensible heat flux H and the latent heat flux $L \cdot E$ are as follows;

$$H = \rho \cdot c_p \frac{T_c - T_a}{r_{ah}} \quad (79)$$

$$L \cdot E = \frac{\rho \cdot c_p}{\gamma} \frac{e_c^* - e_a}{r_{av} + r_s} \quad (80)$$

where T_c – the temperature of the plant cover [K]; T_a – the air temperature [K] measured at the reference height z_a ; e_c^* – the saturated water vapour pressure [Pa] in temperature T_c ; e_a – the water vapour pressure in the air [Pa] measured at the reference height z_a [m]; r_{ah} , r_{av} – the aerodynamic resistance of atmosphere for transport of heat and water vapour, respectively [$s \text{ m}^{-1}$]; r_s – the diffusion resistance of plants for the transport of water vapour [$s \text{ m}^{-1}$]; ρ – the air bulk density [kg m^{-3}]; γ – the psychrometric constant [Pa K^{-1}].

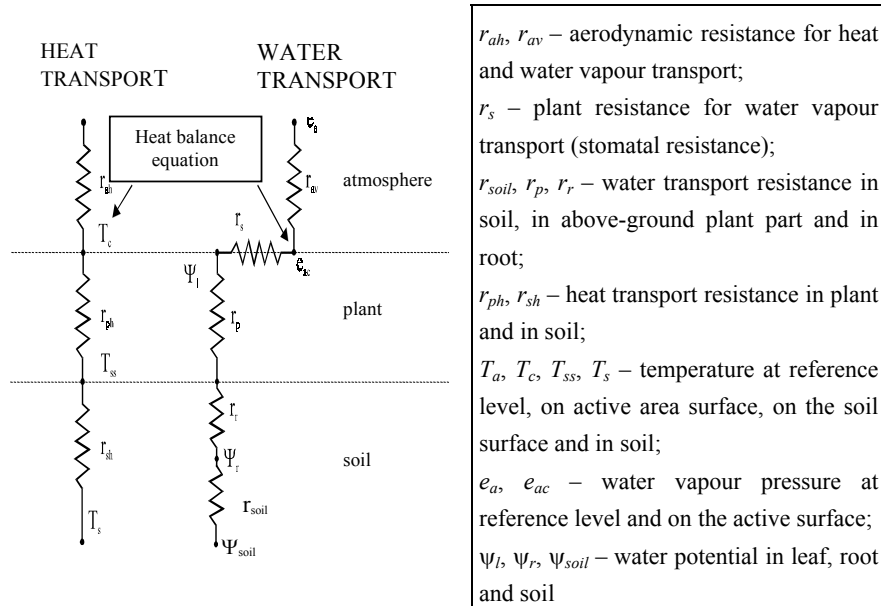


Fig. 17. Simplified resistance model of water and heat transport in the soil-plant-atmosphere system

The aerodynamic resistance of the atmosphere for the transport of heat r_{ah} is a function of wind velocity, stability of atmosphere over the plant cover and the nature of the surface (height and type of plants).

The state of thermodynamic equilibrium expresses the relation between the aerodynamic effusion forces, connected with the vertical temperature gradient in the air and the outer forces caused by the horizontal movement of the air masses.

The conditions of the atmospheric stability can be determined through the relation between the plant cover temperature and the temperature of the atmosphere above canopy. In the neutral conditions ($T_c \approx T_a$) the resistance r_{ah} is expressed as a function of the wind velocity and the roughness of the surface:

$$r_{ah} = \frac{\ln\left(\frac{z_a - d}{z_{om}}\right) \cdot \ln\left(\frac{z_a - d}{z_{oh}}\right)}{k^2 u} \quad (81)$$

where: z_a – is the reference level, at which the measurement of the wind velocity and the air temperature is conducted [m]; d – the zero plane displacement height [m]; z_{om} , z_{oh} – the roughness parameters of the surface for momentum and sensible heat, respectively [m]; k – von Karman's constant determined experimentally as equal to 0.41 and independent on the type of the surface; u – the wind velocity [m s^{-1}];

The unstable conditions occur when the limited evapotranspiration causes the increase of the plant temperature ($T_c > T_a$). In such conditions the increase of the vertical transport of mass and heat takes place. The semiempirical equation for the aerodynamic resistance according to Paulson [118] is:

$$r_{ah} = \frac{\left[\ln\left(\frac{z_a - d}{z_{om}}\right) - P_1 \right] \cdot \left[\ln\left(\frac{z_a - d}{z_{oh}}\right) - P_2 \right]}{k^2 u} \quad (82)$$

where: P_1 , P_2 – the function of atmosphere stability and other quantities as in equation (81).

The functions P_1 , P_2 are expressed by equations:

$$P_1 = 2 \cdot \ln\left(\frac{1+x}{2}\right) + \ln\left(\frac{1+x^2}{2}\right) - 2 \cdot \arctan(x) + \frac{\pi}{2} \quad (83)$$

$$P_2 = 2 \cdot \ln\left(\frac{1+x^2}{2}\right) \quad (84)$$

where:

$$x = \left(1 - 16 \cdot \frac{z_a - d}{L} \right)^{0.25} \quad (85)$$

The quantity L [m] occurring in this equation is called the Monin-Obuchov's length and expresses the height from which the main mechanism in vertical processes of mass and energy exchange is free convection:

$$L = \frac{u_*^3 \cdot \rho \cdot c_p \cdot T_a}{k \cdot g \cdot H} \quad (86)$$

where u_* – the friction velocity expressing the effectiveness of the momentum transfer from the air flowing over the active surface towards this surface [m s^{-1}]; ρ – the air bulk density [kg m^{-3}]; c_p – the specific heat of the air [$\text{J kg}^{-1} \text{K}^{-1}$]; g – the acceleration due to gravity (9.813 m s^{-2}); T_a – air temperature [K]; k – von Karman's constant.

In case of stable conditions of the atmosphere ($T_c < T_a$) the aerodynamic resistance of the atmosphere for the heat transport is expressed by the following semiempirical equations [22]:

$$r_{ah} = \frac{\left[\ln \left(\frac{z_a - d}{z_{om}} \right) + 4.7 \cdot \frac{z_a - d}{L} \right] \cdot \left[\ln \left(\frac{z_a - d}{z_{oh}} \right) + 4.7 \cdot \frac{z_a - d}{L} \right]}{k^2 u} \quad \text{for } L > z_a - d \quad (87)$$

$$r_{ah} = \frac{\left[\ln \left(\frac{z_a - d}{z_{om}} \right) + 4.7 \right] \cdot \left[\ln \left(\frac{z_a - d}{z_{oh}} \right) + 4.7 \right]}{k^2 u} \quad \text{for } 0 < L \leq z_a - d. \quad (88)$$

In TERGRA model [146] it was assumed that the roughness parameters for the momentum and the sensible heat z_{om} , z_{oh} are equal ($z_{om} = z_{oh} = 0.13 h_c$, where h_c – the mean height of the plant cover). The value of the roughness parameter for the heat transport z_{oh} is about 0.1 of that for the momentum z_{om} . According to the same author the quantities z_{om} i z_{oh} are connected with the plant height through the following formulas:

$$z_{om} = 0.123 \cdot h_c \quad (89)$$

$$z_{oh} = 0.0123 \cdot h_c . \quad (90)$$

However, a recommended value of the zero plane displacement height d is given by formula:

$$d = 0.67 \cdot h_c . \quad (91)$$

Another method for determination of the aerodynamic resistance r_{ah} was proposed by Jackson [71]. It determines the conditions of the stability in the atmosphere on the base of Richardson number R_i , which expresses the relation between the forces of vertical and horizontal transport of mass and energy:

$$R_i = \frac{g(T_a - T_s)(z_a - d)}{T_a u^2} \quad (92)$$

where: g – the acceleration due to gravity [m s^{-2}], and the other symbols as in earlier equations.

This depiction gives the following formulas for the aerodynamic transport of heat:

$$r_{ah} = \frac{\left\{ \ln \left[(z_a - d + z_0) / z_0 \right] / k \right\}^2 (1 + 15R_i)(1 + 5R_i)^{1/2}}{u} \quad \text{for } (T_s - T_a) < 0 \quad (93)$$

$$r_{ah} = \frac{\left\{ \ln \left[(z_a - d + z_0) / z_0 \right] / k \right\}^2}{\left\{ 1 - 15R_i / \left[1 + C(-R_i)^{1/2} \right] \right\}} \cdot u \quad \text{for } (T_s - T_a) > 0 \quad (94)$$

where: the parameter C is expressed as:

$$C = \frac{75k^2 \left[(z_a - d + z_0) / z_0 \right]^{1/2}}{\left\{ \ln \left[(z_a - d + z_0) / z_0 \right] \right\}^2} . \quad (95)$$

The method of the heat balance with aerodynamic resistance expressed by the above equations (92-95) was compared with the Bowen ratio method for

fields with cotton and wheat and a high agreement was obtained (within 10%) of the instantaneous values of the evapotranspiration calculated with both methods.

4.5. Use of radiation temperature of plant cover for determination of actual and potential evapotranspiration as well as plant water stress

The actual evapotranspiration rate gives the information about the availability and usefulness of the soil water for plants. However, a considerable differentiation of the evapotranspiration intensity exists during the day, due to changes of meteorological conditions.

The tendency exists in agricultural practice to obtain simple for interpretation indices of transpiration intensity or availability of soil water for plants from singular measurements of *e.g.* radiation temperature of canopy which could be indispensable for fast intervention to optimise water conditions in the living environment of plants. Hence, many indices of plant water stress, which are based on the canopy radiation temperature measurement appeared in literature [27, 28, 44, 68, 76, 85, 96, 100, 110]. When individual measurements of the radiation temperature of the plant cover are in disposal such indices should combine the value of the actual evapotranspiration with reference evapotranspiration for a given evaporating surface. Technical possibility of radiation temperature measurements was used in the investigation of physical state of plant cover as early as in the sixties. Tanner [158], using Barnes radiation thermometer noticed that the radiation temperature of plant growing in inconvenient water conditions is different then the temperature of plants in irrigated fields, despite the lack of visual symptoms of water deficit. Fusch and Tanner [47] were among the first who accepted radiation temperature of plant cover in irrigated fields as a reference, to be compared with radiation temperature of plant growing in different water conditions. Meanwhile, Aston and van Bavel proposed [6] the water deficit indicator of plants expressed by radiation temperature variability of plant cover in several measuring points of the field. These authors concluded that the case of observed high differentiation of crop radiation temperature in the field indicated the occurring of plant water stress. Further investigations focused on analysing the differences between plant radiation temperature and air temperature [10, 12, 14, 140]. Ground and airborne measurements of plant radiation temperature for the areas with different crops, *i.e.* wheat, corn, clover were the base for creation of Stress Degree Day (SDD) water stress index, defined as a daily sum of the differences between temperature of

plant cover and air temperature [6, 62, 74]. Gardner *et al.* introduced the daily index of temperature stress TSD (Temperature Stress Day), defined as a daily sum of differences between the temperature of plants under water stress and the temperature of reference plants growing on well irrigated fields. It was assumed in the beginning that this index did not depend on environmental parameters and therefore it was commonly used due to its simplicity. More detailed analysis of the usefulness of this index for determination of water stress of different crops showed some shortages of its applicability mainly because it did not consider the impact of meteorological parameters on measured temperature differences. The indices SDD and TSD proved to be useful in arid areas. According to Nieuwenhuis [112], the applicability of Jackson's method in the areas with big variability of meteorological conditions, *e.g.* the Netherlands is limited because this index is not sensitive to the changes of the important meteorological parameters, like wind speed, air humidity and solar radiation. The linear dependence between the difference of crop – air temperatures and water pressure deficit in the air was observed by Ehrler [44], while O'Toole and Hathfield [116] showed the impact of wind speed on the difference $T_c - T_a$. This was the base for creation of Crop Water Stress Index (CWSI). This index assumes the existence of theoretical upper and lower limits of the $T_c - T_a$ differences under any values of water pressure deficit in the air. The upper limit refers to the plants with completely stopped transpiration, whereas the lower limit refers to the conditions of water comfort for plants.

By combining the equations (74), (79) and (80) the formula is obtained for the relation between the actual value of the radiation temperature of canopy and agro-meteorological parameters in the active layer of the atmosphere:

$$T_c = T_a + \frac{r_a(R_n - G)}{\rho c_p} \cdot \frac{\gamma \left(1 + \frac{r_c}{r_a}\right)}{\Delta + \gamma \left(1 + \frac{r_c}{r_a}\right)} \cdot \frac{e_a^* - e_a}{\Delta + \gamma \left(1 + \frac{r_c}{r_a}\right)}. \quad (96)$$

It results from this equation that the difference between the crop surface temperature and the air temperature is linearly dependent on the water vapour pressure deficit in the air $VPD (e_a^* - e_a)$, assuming that r_a , R_n and G are constant. This relation was used by Jackson *et al.* [70] to create the Crop Water Stress

Index (*CWSI*). This index is based on the relation of the actual evapotranspiration to the potential evapotranspiration and is expressed as:

$$CWSI = 1 - \frac{E_a}{E_p} \quad (97)$$

where: E_a – the actual evapotranspiration flux [$\text{kg m}^{-2} \text{s}^{-1}$]; E_p – the potential evapotranspiration flux [$\text{kg m}^{-2} \text{s}^{-1}$].

If the actual evapotranspiration ceases completely as a result of unavailability of soil water for the rooting system, the stomatal resistance approaches infinity ($r_c \rightarrow \infty$). In this case the equation (96) takes the form:

$$(T_c - T_a)_{ul} = \frac{r_a(R_n - G)}{\rho c_p} \quad (98)$$

where: $(T_c - T_a)_{ul}$ – the upper limit of the difference between crop and air temperatures, appointing the total limitation of transpiration.

Under unlimited availability of soil water, when plants transpire with potential intensity, the stomatal resistance receives a potential value and in this case we deal with a lower limit of the difference of crop temperature and air temperature $(T_c - T_a)_l$:

$$(T_c - T_a)_l = \frac{r_a(R_n - G)\gamma^*}{\rho c_p(\Delta + \gamma^*)} - \frac{(e_a^* - e_a)}{\Delta + \gamma^*} \quad (99)$$

where:

$$\gamma^* = \gamma \left(1 + \frac{r_{cp}}{r_a} \right). \quad (100)$$

The lower limit $(T_c - T_a)_l$ creates a set of straight lines for various values of the air temperature, under the assumption that R_n , G_a and r_a are constant.

The Crop Water Stress index (*CWSI*) can be written with the use of equations (98-100) as:

$$CWSI = \frac{\gamma \left(1 + \frac{r_c}{r_a}\right) - \gamma^*}{\Delta + \gamma \left(1 + \frac{r_c}{r_a}\right)} \quad (101)$$

or

$$CWSI = \frac{(T_c - T_a)_a - (T_c - T_a)_{ll}}{(T_c - T_a)_{ul} - (T_c - T_a)_{ll}} \quad (102)$$

The crop water stress index *CWSI* was used for determination of the water stress of various plants [25, 44, 57, 74, 75, 91, 92, 104, 108, 132, 151, 153, 138] and some modifications of this index were created, which took into account some empirical relations between the physical quantities being included into the heat balance equation [76, 96]. It was stated that this index strongly depends on many meteorological parameters such as net radiation, wind velocity, soil temperature and that it is sensitive to even small changes of the soil water potential [76, 100, 108].

5. EXPERIMENTAL STUDY ON PLANT WATER STRESS DETECTION AND ACTUAL EVAPOTRANSPIRATION DETERMINATION

5.1. Aim of the study

In the Institute of Agrophysics, Polish Academy of Sciences, the studies were conducted concerning the application and interpretation of the thermal imaging for agricultural purposes. First experiences in this topic were gained in the period 1987-88 during participation in the project CPBP No. 01.20: "Development and application of space studies" sub-programme No. 4: "Remote-sensing" by realization of the task: "Determination of the relation between the soil water content and radiation temperature of the plant cover on the base of laboratory pot experiments". The Polish coordinator of this task, the Institute of Geodesy and Cartography in Warsaw delivered the measuring system AGA 680 SWB (Short Wave Band). Experiments and measurements were conducted in a plant house belonging to Agricultural University in Lublin in cooperation with the Laboratory of Grassland Farming of Agricultural Department. In frame of these studies the first stage of the work was done.

The studies were continued in the lysimetric station in Sosnowica belonging to the Local Research Branch of the Institute of Land Reclamation and Grassland Farming in Falenty, Poland (second stage).

The studies, that have been conducted so far, concerning the application of measurement of the radiation temperature showed a wide range of factors influencing its actual value: different kinds of stress, diseases, genotypes as well as combined action of these factors in various agroclimatical conditions (the changes of the air temperature, the water vapour pressure, the wind speed, etc.). The sensitivity of radiation temperature for various factors in various conditions testifies for a very broad range of its possible agricultural application. However, at the same time, it is extremely difficult or sometimes even impossible to interpret and especially compare any results obtained in varied dynamical natural conditions.

The aim of the study was to:

- investigate the influence of the energetic status of water (soil water content and soil water potential) on distribution of radiation temperature of the natural plant cover in laboratory and lysimetric (field) experiments.

- compare and verify some models for calculation of the actual and potential evapotranspiration with the use of measurement of the radiation temperature of plants; it was decided to realize this purpose in two stages, *i.e.* firstly, through evaluation and preliminary selection of the methods of evapotranspiration determination on the base of literature study, and secondly, through the verification of some chosen methods on the base of the lysimetric study of the plant cover.
- derive the energetic status of water in plants using the Crop Water Stress Index (*CWSI*) with the use of measurement of the water potential in soil and plant.

It was assumed in experiments that the soil water conditions in lysimeters should be controlled and regulated, whereas other measured parameters could be identical for all the variants of humidity conditions in pots and lysimeters. A special attention was paid to perform the measurements with the use of objective techniques and measuring procedures in agreement with the rules of metrology. The studies were performed in the aspect of evaluation the possibility of application of airborne and satellite thermal images for the evaluation of soil water conditions of the agriculturally used areas.

5.2. Object of the study

The object of the study was meadows of the Grassland Experimental Station in Sosnowica belonging to the Laboratory of Grassland Farming of Agricultural University in Lublin (Fig. 18). These meadows are a part of bigger complex of low moorsh in the central part of the Wieprz-Krzna Channel in the Piwonia river. These areas belong to the subregion of Łęczyńsko-Włodawski Lake District being the part of Lublin Polesie Region. Open drainage ditches ameliorated this grassland area in 1964-65. At the lysimetric station organic soils cover 74% of the area and mineral soils – 24%. It comes from 10 soil pits and additional probing that the organic soil in the area of the station is characterized with the described in Table 6.

The selection of the soil types was performed to obtain the highest possible differentiation from the point of view of physical, biological and economic importance of the soils. Therefore, one of the chosen meadows was on a typical peat-muck soil being in a medium stage of mucking created from the sedge peat

of medium decomposition, bedded with reed peat. This site belongs to moorshy meadows using mainly capillary rise water.

Table 6. Exemplary organic soil profile in Sosnowica [138]

Layer in cm	Symbol	Soil horizon and its characteristic
0-5	M ₁	Humus-reed muck outgrown with roots
5-20	M ₁	Strongly decomposed muck, at the bottom nests of unrecompensed peat with morhic structure of remaining plant tissues
20-64	T ₁	Reed-sedge peat, R2
64-150	T ₂	Reed peat, R1. silted up with layers
>150	D	coarse sand

The second meadow represented mineral, hydrogenic black soil with shallow humus layer and low level of ground water. This soil is numbered among sandy soils, which use mainly rainfall water (Table 7).

Table 7. Exemplary mineral soil profile in Sosnowica [138]

Layer in cm	Symbol	Soil horizon and its characteristic
5-8	Ad	Humus-reed horizon strongly outgrown with roots
8-23	A ₁	Humus, light-brown loose sand
23-55	A ₃	Elution with dripstone, smooth boundary, loose sand
55-88	B	Illuviation, red-faded colour, coarse sand
>88	C	Matric rock, coarse sand

The studies were conducted in the lysimetric station in Sosnowica belonging to Lublin Research Branch of the Institute of Land Reclamation and Grassland

Farming in Falenty, Poland. The station is situated in the central part of the Wieprz-Krzna Channel district, 164 m above sea level, (51°31'30"N, 23°04'48"E).

The lysimeters of the area 1600 cm² and the height 120 cm were filled with soil monoliths taken in undisturbed form together with natural plant cover. For both soils the water retention characteristics (pF) were completed. The soil samples were taken from three genetic levels: 0-5 cm, 10-15 cm and 25-30 cm, *i.e.* from the soil layer in which the rooting system of the meadow plants develops. Fig. 19 presents the values of the volumetric water content for the drying curve, for chosen pF values of both soils.

In lysimeters and in surrounding meadows, the three-harvesting system was applied with a respective fertilization system [103, 145].

Both meadows possess typical characteristics of majority of grasslands situated in Lublin macroregion.

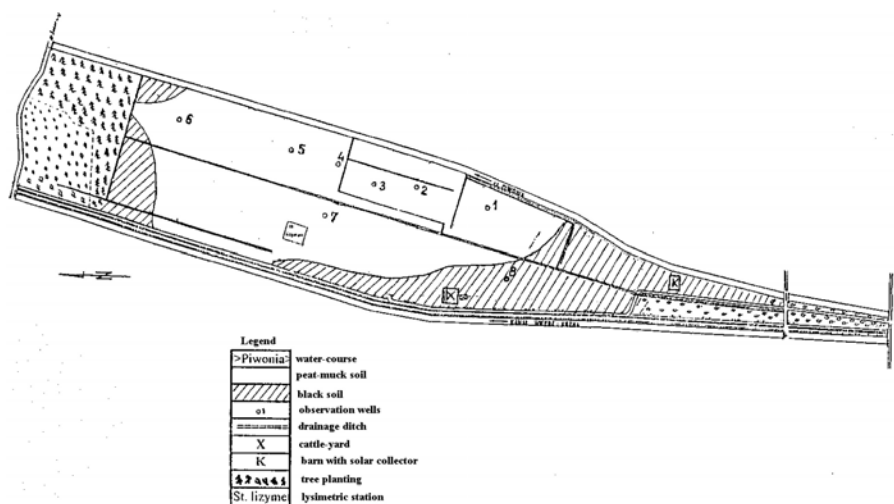


Fig. 18. Scheme of grassland belonging to Experimental Grassland Farming Station in Sosnowica of Agricultural University in Lublin [13]

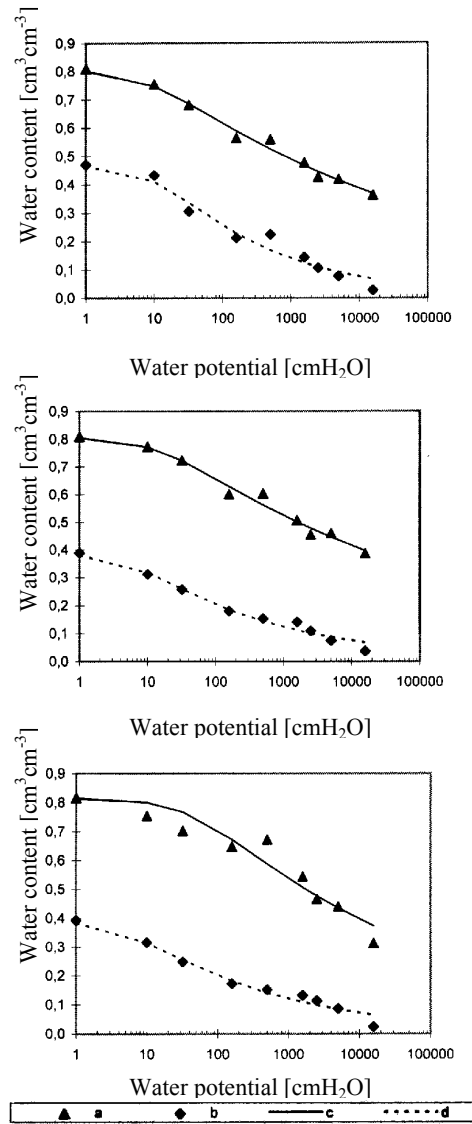


Fig. 19. Values of pF (for drying curve) for three soil levels. Measured values: organic soil (a), mineral soil (b), and pF curves obtained with Mualem method [182]: organic soil (c), mineral soil (d).

5.3. Description of measuring system

5.3.1. Description of thermographic system AGA 680 SWB

In laboratory experiment the radiation temperature of the plant cover was measured using the thermographic system AGA 680 SWB (Short Wave Band), working in the range 3-5.5 μm . This system is composed of the scanner, the display unit and additional colour monitor. The monitors were equipped with attachments, which enabled to register the obtained thermograms on a photographic film for further densitometric analysis.

The radiation temperature measurement was initially conducted with the use of the isotherm directly on the display unit. Because this kind of measurement occurred to be imprecise and bearing an error connected with subjective sense of the measuring person it was decided to modify it. After it was stated that the isotherm couldn't be applied for the measurement of the temperature differences, an additional electronic system was used, which made it possible to measure directly the differences in temperature of the objects being simultaneously in the field of view of the camera. The designed and constructed system was able to change the output signal from the camera into the electric voltage measured with the digital voltmeter. This system was used to perform precise measurement of the radiation temperature in any selected points of the screen, if only the image was stable during the measurement (5-7 seconds) and the object's temperature did not change considerably during this period (the limit value was $0.01^\circ\text{C s}^{-1}$).

5.3.2. AGEMA 880 LWB thermographic system

In AGEMA 880 LWB thermographic camera (Fig. 20), the radiation coming from the observed object gets through the system of germanium lenses into the mechanical system of the image analysis.

Firstly, the infrared radiation is focused on an oscillating mirror decomposing the image vertically, then, it comes through the system of three mounted mirrors and is focussed on a polygon prism, which rotates with the speed 16000 rotations/min.

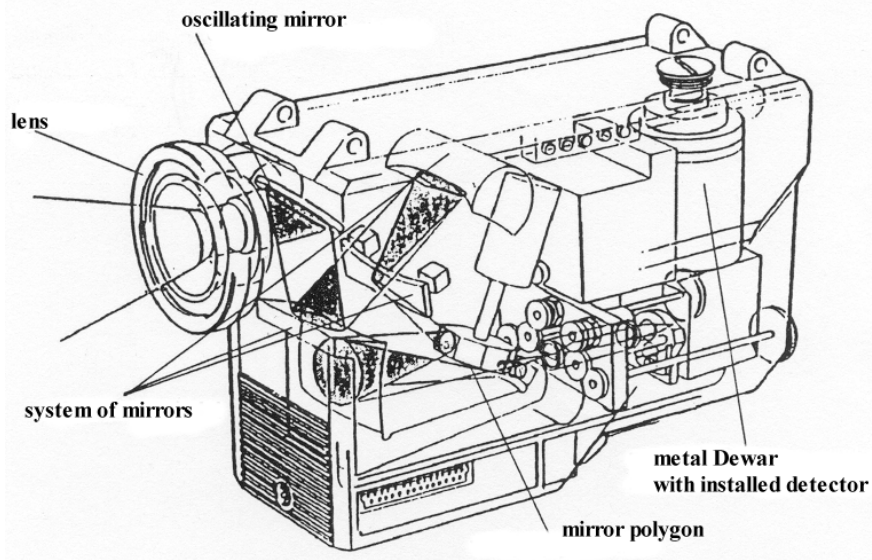


Fig. 20. Cutaway view of AGEMA 880 LWB thermovision scanner [3]

Both mobile mirrors are controlled by a microprocessor. The movement of the horizontal and the vertical mirrors is synchronized to obtain an image composed of 70 active horizontal lines in four vertical frames (together 280 active lines per image). Six complete images are obtained every second. The radiation flux, reflected from the horizontal rotating mirror, after it goes through the system composed of an aperture and a filter is focused on a point detector (diameter of $150\ \mu\text{m}$) mounted at the side wall of the Dewar container with liquid nitrogen. The electrical signal from the photoelectric detector is sent to the display unit and properly processed. The sensitivity range of the thermographic camera is the sum of the spectral sensitivities of the germanium optics and the detector (Fig. 21).

Thermographic devices are used for measurement of the radiation temperature distribution of the studied surfaces. However, this measurement is not direct. The detector registers the infrared radiation coming from the investigated object. The density of the flux of this radiation is connected with the temperature of the emitter, but it is also influenced by the radiation absorbed by the atmosphere, the background infrared radiation reflected from the object of study and the radiation of the optical and scanning systems. Therefore, to

determine the radiation temperature some special correction procedures should be applied, which take into account the impact of these factors.

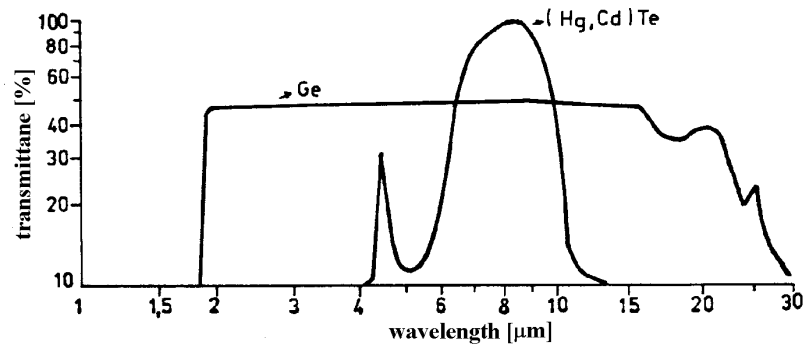


Fig. 21. Optics transmittance and spectral sensitivity of the detector of AGEMA 880 LWB thermovision scanner [3]

The measure of the infrared radiation, registered by the thermographic camera's detector is the Thermal Value expressed in the units of the isotherm (IU – Isothermal Units). The relation between the thermal unit and the registered flux of the infrared radiation is linear. However, the relation between the thermal value and the temperature of the object is expressed by the calibration function:

$$I = \frac{R}{\exp\left(\frac{B}{T}\right) - F} \quad (103)$$

where: I – the thermal value corresponding to the temperature $T[IU]$, T – the absolute temperature of the object [K], R , B , F – the reaction, spectral and shape coefficients, respectively.

The calibration function for each scanner is derived by registering the radiation of the blackbody radiator for different temperatures and calculating the R , B , F coefficients in the model with the least square method. Under simplified assumptions ($\varepsilon=1$ and $a=1$), the calibration chart can be directly used to change the thermal values into temperature. It is useful in field conditions to evaluate temperatures of the examined objects, when the measuring system consists only of the display unit and the camera.

The configuration of components of the thermographic system AGEMA is presented in a diagram (Fig. 22).

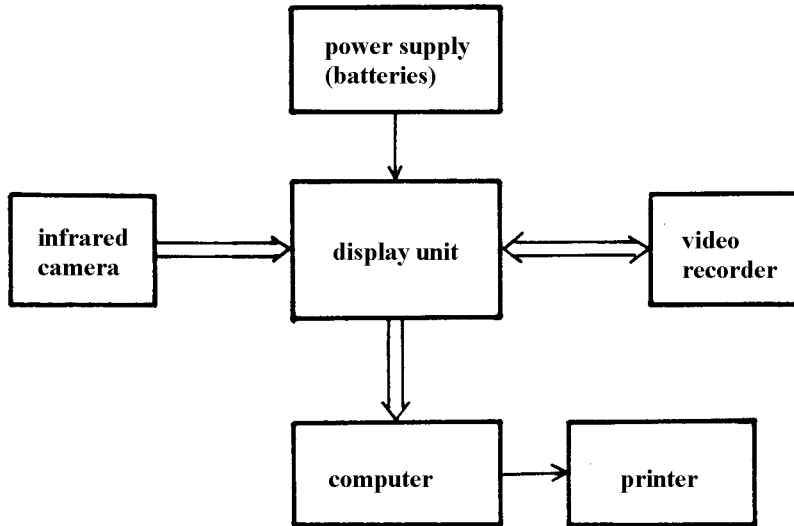


Fig. 22. Schematic presentation of AGEMA 880 LWB system configuration

5.3.3. Reflectometric water content measuring device (TDR)

Apart from the radiation temperature, the water content was measured in the experiment. Both in laboratory and lysimetric experiments, the reflectometric measurement of the soil water content was preferred. The principle of operation of the reflectometric TDR measuring device is based on the measurement of the propagation of the electromagnetic wave in a studied medium (*e.g.* soil) under established parameters of the transmission line. This velocity is expressed by the ratio of the light velocity in vacuum to the square root of the dielectric constant of the studied object. The dielectric constant of a given soil depends mainly on the water content in the unit volume of the soil and can be described with good accuracy by a polynomial of the third order. In practice, the measurement of the soil water content by the TDR method is reduced to the measurement of the time needed to transmit the electromagnetic wave from the moment of its entering the medium (first reflection occurs there) along the needle probe up to its end (for second time the pulse reflection occurs). By using specific equations, the

measured time of wave propagation is recalculated into the water content value per unit of the soil volume.

The TDR device, produced according to the licence of the Institute of Agrophysics PAN in Lublin consists of a battery powered measuring unit, controlled by a microprocessor with a matrix graphical display and of a probe connected to the measuring unit. The probes of various lengths of the core made of PCW (outer diameter of 2 cm) are ended with iron needles 10 cm long and with spacing of 1.6 cm. The instrument can measure the water content in the range 0-100% with accuracy of $\pm 2\%$ and resolution of 0.1%. The time of individual measurement is about 10 s [99].

5.3.4. Total water potential measuring system

The water potential in soil and in plants was measured with Wescor Inc. instrument, USA. The method of this measurement is based on determination of the relative water vapour pressure within the sample. This parameter in the range from zero to fifty bars is a linear function of the potential. In the equilibrium state between solid and gaseous phases, the water potential in the sample is equal to the water vapour potential. Therefore, by measuring the relative humidity of the air surrounding the thermocouple, it is possible to determine the potential of the water vapour in the sample. Because any internal properties of the sample do not influence the accuracy of measurement, this method can be applied for measurement of the water potential both in the soil and in the tissue of plants.

The relation between the potential and the relative water vapour pressure in the system is expressed by the equation:

$$\Psi = RT \ln \frac{e_a}{e_a^*} \quad (104)$$

where: Ψ – the water potential [J kg^{-1}] expressed as a negative value; T – the temperature of the water vapour [K]; R – the gas constant [$\text{J kg}^{-1} \text{K}^{-1}$]; e_a – the actual pressure of the water vapour [Pa]; e_a^* – the saturated water vapour pressure [Pa] in a given temperature.

The measuring set is composed of a sampling chamber, type Wescor C-52 with chromel-constantan thermocouple, of a microvoltmeter type Wescor Hr-33 with electronic control circuit, which automatically maintains the temperature of the junction in the dew-point temperature and of a power supply adapter of direct

current +18 V, -18 V. The thermocouple is contained in a tightly closed chamber Wescor C-52, directly above the soil or leaf sample, placed in a special cylindrical dish. Under isothermal conditions, after about 15 minutes, the equilibrium state between the water vapour pressure in the air and in the sample is gained. At that moment, a current of a few milliamperes is passed in a short time through the junction in such a direction that to make it cooling as a result of Peltier's effect. The cooling time depends on the kind of the sample, but in the performed experiment for all samples it was five seconds. The rate of temperature decrease of the junction depends on the relative air humidity and temperature in the chamber. The electromotive force released in the junction is a function of the relative humidity and, respectively, of the water potential in the measured sample.

5.3.5. Automatic system of agrometeorological data acquisition

One of the assumptions of the experiment was to conduct a twenty-four-hour registration of courses of meteorological elements to possess these data in case of possible necessity of physical interpretation of unexpected, surprising results. To complete this task, the automatic measuring system, designed and constructed in the Institute of Agrophysics PAN was used [185].

In the experiment, the automatic registration of measured quantities was conducted. Therefore, all the measuring sensors had electric signals as the output. The block scheme of the system is presented in Fig. 23.

The following elements can be distinguished in the measuring system: the set of sensors, the commutator, the measuring circuit and the IBM PC computer. The analogue signals obtained directly from the sensors or through the processing circuit of non-electric quantities were sent to the output of the commutator. After selection by the commutator according to the computer program, the signals were processed in the measuring system into the digital form. From the output of the measuring system the digital signals were sent to the computer, to be initially processed and written into the memory disk.

The measuring system was composed of two measuring lines. The first of them had four measuring nodes (the distance between nodes was 10 m). The measuring nodes possessed 16 analogue inputs for measurement of temperature in the range from -30 to 50°C with resolution of 0.1°C and accuracy ± 0.5 . In every node, 16 thermocouples of copper-constantan were installed. Temperatures from particular thermoelectric sensors were measured in relation to the reference thermocouple, placed with a model semiconductor thermometer. The correction

for reference temperature was realized during the data processing by a computer programme.

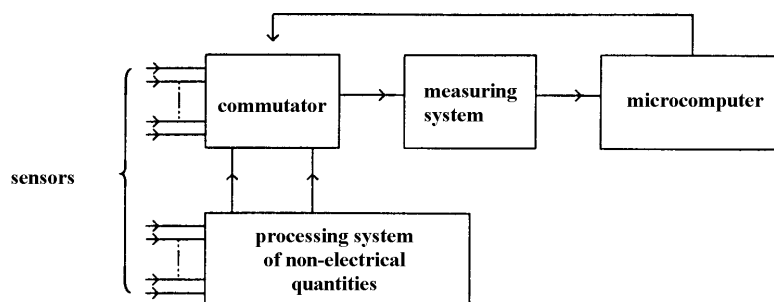


Fig. 23. Block scheme of measurements system [185]

The second measuring line had 16 analogue inputs with output voltage from -1 V to $+1$ V. The anemometers and solar radiation sensors were connected to these inputs or directly to the computer integrator of the solar radiation.

The control of the system work was done according to the programme assigned by user through the central IBM PC unit.

The primary control program supported the following options:

- installation used to fix measuring parameters for all the analogue-digital channels of the converter in the measuring system;
- registration enabled to perform periodical measurement of all the channels, the results were registered into the computer disk memory;
- reviewing and data selection enabled to view the files with the results of measurement according to assigned parameters.
- joining the files from diskettes used to create one file from a number of measuring data files.

The measuring system was composed of two subsystems referring to the soil and atmosphere, respectively. The soil subsystem contained thermoelectric thermometers elaborated and constructed according to Malicki and Mazurek's procedure. Multisensor thermoelectric thermometers and the semiconductor temperature converter (Usovicz [168]) with electric measuring circuit were installed into the soil permanently. The copper-constantan thermocouple and a semiconductor diode composing the point of temperature reference were placed into the lowest measuring level to assure thermal stability of the measuring

system. The sensors were placed at the following levels: 1, 1.5, 2, 3, 4, 6, 8, 10, 12, 16, 20, 24, 32, 48, 64, 96 cm.

The subsystem referring to the atmosphere was composed of air thermometers, anemometers, an albedometer, a solarimeter and a net radiation sensor.

The thermocouple air thermometers were used to measure the vertical stratification of air temperature and to derive the relative humidity of the air (measurement of dry- and wet-bulb temperatures). The vertical distribution of the air thermometers followed the scheme of geometric series: $H_{n+1} = 2 \cdot H_n$, $n=0, 1, 2, \dots$. Sensors containing copper-constantan junctions (diameter of 0.6 mm) were placed in casings, which enabled free air convection and protected sensors from solar radiation.

The temperature sensors, which measured temperatures of dry and wet thermometers, were placed together with their casings in the measuring nests of Assman's psychrometers produced by WSZ in Cracow, Poland. The accuracy of temperature measurement for the whole system was $\pm 0.5^\circ\text{C}$.

The wind velocity was measured with N 188 anemometers, produced by Meratronik firm from Szczecin, Poland. They worked in the range from 1.5 to 30 m s^{-1} with error of measurement not higher than $\pm 0.5 \text{ m s}^{-1}$. These instruments measure the frequency of voltage of constant amplitude pulses, transmitted through the cable from the transmitter to the receiver. The pulse frequency was proportional to the wind velocity. The series of pulses in the receiver were converted with the help of a diode pump into the constant voltage sent to the meter situated in the front panel of the anemometer.

The solar radiation in the range from 300 to 2800 nm was measured with thermocouple pyranometers with Moll pile, produced by Kipp & Zonen. The albedometer was composed of two solarimeters looking in opposite directions. First of them measured the incoming radiation and the second the reflected radiation from the studied surface. The piles of pyranometers were composed of 14 thermocouples. The sensitivity of the piles was $11.5 \mu\text{V W}^{-1} \text{ m}^2$ the internal resistance was 10 ohms, linearity was better than $\pm 1.5 \%$ in the whole measuring range, *i.e.* 0-1000 W m^{-2} .

The net radiation flux (the difference between direct incoming and reflected short- and longwave radiation) was measured with net radiometer of Middleton. The device consisted of a thermopile composed of 45 thermocouples. The sensitivity of this thermopile was $35 \mu\text{V W}^{-1} \text{ m}^2$ and the internal resistance 78

ohms. Two polyethylene semispheres with measuring elements were filled with gaseous nitrogen.

5.4. Description of laboratory experiment

The measurement of the impact of the water stress on plants with the use of an infrared camera is a difficult meteorological problem because of the required high accuracy and strong need to consider many intercorrelated parameters.

Two soils were chosen for the experiment: organic and mineral with natural meadow plant cover. The experimental pots 23×29×29 cm in size, were filled with natural meadow turf taken to the depth of 29 cm. Four sets containing eight pots were created (two sets for each soil). The cultivation in pots was conducted in such a way, that to differentiate the identical sets from the point of view of frequency and dates of harvesting (two- and three-harvesting systems). Thus, the obtained sets differed with the phases of physiological development of grass, and from the point of remote-sensing measurements, they possessed different coefficients of soil cover. To maintain all the pots of a set in identical outer conditions, they were placed on carts – eight pots on each cart. The central position on the cart's surface was left unoccupied with pots to maintain for all the pots in each set the same angle of view of the infrared camera. The position of the pots on carts was fixed to let them cover the whole field of view of the camera and enable a good separation of particular pots within the thermal images, what was important because of the possibility of grass lodging, especially these, cultivated within two-harvesting cycle.

Another important factor decided about the position of pots on the carts. It was the necessity of applying the measuring method, which would enable to compare simultaneously the temperatures of all the pots being in the angle of view of the camera. This requirement resulted from instability of the air temperature during the measurement. The method of measurement of individual pots at a time would lead to inappropriate results due to the impact of changeable trend, which had nothing to do with the soil water content but only with changes of air temperature in the plant house and with the drift of the measuring system.

The idea of differentiation of soil water content in pots is presented in Fig. 24. Exemplary course of real changes of the water content during the period of succeeding few days for consecutive four pots is presented in Fig. 25. Initially, the pots were watered up to the mass corresponding to 6% of the air porosity. In

this case the soil dried to the level specific for evapotranspiration conditions during eight days.

The measurements showed small and irregular differentiation of the radiation temperature of plant cover between particular pots of the sets. It was decided to deepen drying by watering the pots to the mass corresponding to 50% of air porosity.

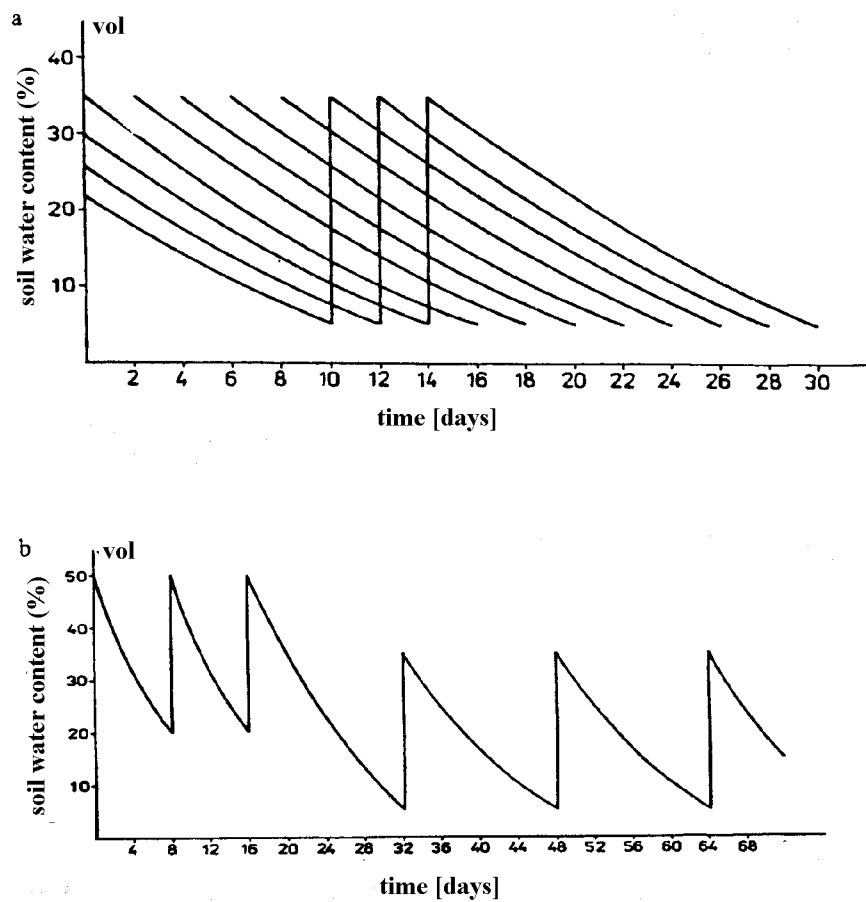


Fig. 24. Procedure of soil drying cycle in pots representing the course of soil water content changes in time: a) soil water content changes for eight pots in watering cycle every two days for succeeding pot, b) one pot course of soil drying cycle for every eight and sixteen days

From that moment considerable differentiation of radiation temperature between particular pots of each set was observed. When excessive drying in any pots occurred, the immediate watering with the dose of 0.5 dm^3 of water was applied.

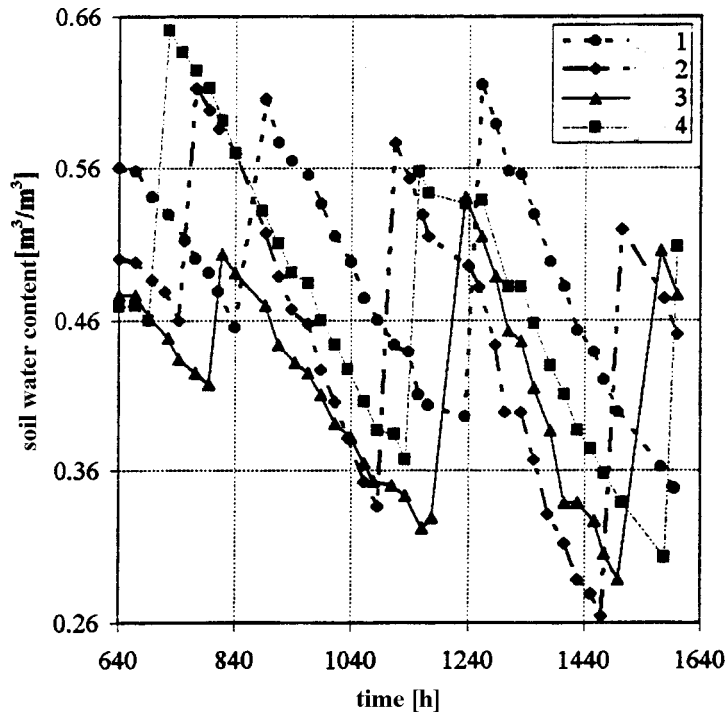


Fig. 25. Real course of soil water content changes in for four chosen pots of one set

It was stated in the initial stage of the measurements, that the influence of the ambient infrared radiation of the surrounding objects couldn't be omitted.

The radiation of the walls of the plant house, which was changing in time, after being reflected from the studied plant cover, considerably disturbed the measurement and made it impossible to interpret properly obtained readings. To diminish this impact, the isolating box was constructed of chipboards and polystyrene with installed additional curtains made of thick cloth. The only hole in this box was a rectangular skylight in the roof, which enabled the infrared camera, mounted over it, to observe from the height of 3.5 meters the studied objects. This isolation reduced most of inconvenient effects, making the radiation

temperature measurement more precise. Before the measurement, an individual cart was put inside the box and after several minutes of waiting for temperature stability, the measurement was performed.

5.5. Description of field experiment

The experiment was conducted at the lysimetric station in Sosnowica, belonging to the Institute of Land Reclamation and Grassland Farming in Lublin in the period 1991-1994. The object of the study was natural grass cover in lysimeters of area 1600 cm² and height 120 cm. The lysimeters contained mineral sandy soil and organic peat-muck soil at the medium stage of decomposition, which were taken from the meadows in the neighbourhood of the station, the same as taken for the laboratory experiment. Each autumn, preceding the measuring season, the turf in all the lysimeters was supplemented together with the soil blocks.

In the initial phase of the experiment the groundwater level of 60 cm was maintained in all the lysimeters. A month before starting the whole day measurement, the differentiation of the water content in lysimeters was initiated and pairs of lysimeters were created. On the base of several years of studies of grassland farming researchers, the levels of groundwater corresponding to comfort soil water conditions were established for mineral soil as 40 cm and for organic soil as 60 cm. These levels were maintained during the experiment in lysimeters, in which it was expected to obtain evapotranspiration values close to potential ones. Each pair consisted of such a lysimeter and a lysimeter with gravitation water carried away. After three weeks from the moment of water content differentiation in lysimeters the water stress situation occurred for the plant cover. The water level in lysimeters was regulated every day.

The measurement of radiation temperature of plant cover in lysimeters was carried out with the use of AGEMA 880 LWB system working in the range 8-13 μm. Particular sequences of thermal images were registered each day to the video-recorder in three periods, *i.e.* between 10-13, 13-17, 17-20. The measurements of radiation temperature of each pair of lysimeters were done at the selected points, situated 2.3 m from the lysimeters at the height of 1.5 m above the grass surface and from the distance 7.3 m and the camera height 2.5 m. The angle between the optical axis of the camera and the perpendicular was 60°.

The measurements in lysimetric station in Sosnowica were conducted during three seasons in July and August. The registration of radiation temperature of plant surface and the analysis of obtained thermal images were performed by AGEMA 880 LWB system (measuring range 8-13 μm). Thermal images of particular pairs of lysimeters were taken every hour during the day and every two hours at night. The whole day registration of meteorological elements was conducted with the automatic measuring system. Applied sensors and measuring devices made it possible to study the distribution of particular physical quantities in the boundary layer of atmosphere and in soil profiles.

The wind velocity and air temperature was registered for the levels: 0.25 m, 0.5 m, 1 m, 2 m and 4 m. The relative air humidity was measured at the height of 2 m. The sensors of solar radiation (albedometer, net radiation meter) were placed 1m over the active surface. Daily loses of water in lysimeters were measured by weighing method in the morning before starting other measurements. After each series of radiation temperature registration, the water content of the soil in lysimeters was measured in two layers: 0-10 cm and 30-40 cm with TDR equipment.

Before starting the experiment, to protect the lysimeters from uncontrolled changes of the soil water content as result of rainfall, special canopies were built of plastic foil and placed about 1m over the lysimeters at night and when during the day rainfall occurred.

To measure the water potential in soil and plants, a measuring set was used, composed of a sampling chamber Wescor C-52 and a micro-voltmeter Hr-33 (described in Chapter 6.3.4). This device uses the hygrometric method of soil water potential measurement in the investigated sample. Soil samples for water potential measurements were taken from the depths of 0-10 cm and 30-40 cm.

5.6. Chosen methods of evapotranspiration determination in field study

The analysis of the methods of actual and potential evapotranspiration determination conducted in Chapter 5 enabled to select methods, which were verified during the experiment.

For determination of actual evapotranspiration the method was selected, based on the heat balance method, in which the radiation temperature of crop surface is used to derive the sensible heat flux. Two modifications of this method were verified. They use different ways of determination the aerodynamic resistance for the heat transport. The chosen method of calculation of the actual

evapotranspiration requires a relatively small number of input data, available in standard meteorological stations, except for the temperature of evaporating surface. This parameter, even for large areas, can be obtained in form of remote-sensing data from various levels. The availability and quality of such materials is still being improved.

To determine potential evapotranspiration, the combined methods were chosen, which are based on Penman's equation. The advantage of these methods is that the correlation coefficients appearing in the equations were estimated in precisely controlled conditions. Furthermore, these methods enable to decrease the number of input data by incorporating into the equations, experimentally verified relations between the physical quantities included into the models.

Methods based on the measurement of turbulent transport of mass and energy in the boundary layer of the atmosphere and methods of mean profiles of meteorological elements were not used in this study. Although these methods are characterized with best precision, they require very expensive measuring sensors and conducting the measurements in very short time intervals, what is the source of some problems with data acquisition and averaging the data for longer time periods.

For calculation of hourly and daily values of actual evapotranspiration the model was used, based on the heat balance equation (74). In this equation the latent heat flux was treated as unknown and other terms were calculated from measuring data. The net radiation flux density was directly measured with Middleton net radiation meter. Temporary values of the heat flux in the soil were derived indirectly by calculation on the base of measurements of net radiation, air temperature and height of plants from equation (78).

Two methods of determination of the turbulent diffusion aerodynamic resistance were applied in the study. The first one used semiempirical equations of mass and energy transport. The turbulent aerodynamic resistance for the heat transport r_{ah} was derived from equations (81) – (88). The equilibrium state of the boundary layer of the atmosphere was considered in calculations, by measuring the temporary values of air and plant temperatures difference and by applying appropriate equations (81), (82) or (87) – (88), depending on the sign of this difference. In case of unstable conditions the iteration method of solving the equation for the aerodynamic resistance was used.

The second applied method proposed by Jackson used Richardson's number (92) for determination of the atmospheric stability conditions. Even though this method uses some empirical coefficients, it gave good results for the USA

conditions and good correlation with Bowen's method. For Polish conditions an attempt at applying this method to evaluate evapotranspiration from NOAA satellite images was undertaken by Dąbrowska-Zielińska [33]. She notified that by considering the stability conditions of the atmosphere with this method, the error of the sensible heat flux estimation decreased by 30%, improving the accuracy of the evapotranspiration evaluation.

In both applied modifications of the heat balance method of the actual evapotranspiration determination, the input data included the measurement of the radiation temperature of plant cover and standard agroclimatical data measured inside the lysimetric station.

Temporary values of the potential evapotranspiration were derived using Penman's equation from 1963 (69) and generally applied modifications of this equation, such as: "Penman – Monteith" with aerodynamic resistance (71), "1982 Kimberly Penman" (67 and 68).

The intensity of the water stress in particular lysimeters was derived on the base of calculated values of actual and potential evapotranspiration, by using the Crop Water Stress Index (CWSI) according to equation (97).

6. RESULTS AND THEIR INTERPRETATION

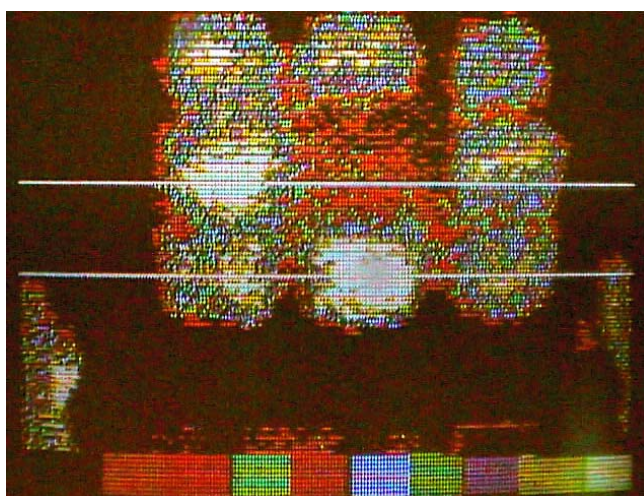
6.1. Analysis of thermal images

In the laboratory pot experiment, the AGA 680 SWB system was used for measurement of the radiation temperature of plant cover. Even first measurements showed that it is impossible to conduct measurements by traditional method of isotherms because of too small accuracy caused by high level of noise and a very large sensitivity of the image for setting the handwheel of the reference voltage. Furthermore, the visual reading of the placement of the isothermal points on the screen was burdened with an error, caused by a subjective evaluation of the degree of filling various areas on the screen by isothermal points. To enable measurement of radiation temperature, at the same time resigning from its evaluation by the isotherm, a system was designed and constructed in the Institute of Agrophysics PAN, which changed the output signal from the camera into electric voltage (description in Chapter 5.3.1).

The measuring system enabled to make a precise measurement of radiation temperature in a chosen point of the screen, if only the image was static during the measurement and the temperature of a studied object did not change rapidly at that moment. The used measuring system made it possible to read immediately the differences of radiation temperature of any two selected pots. For each set of the studied pots, the measurement was conducted in such a way that one measuring line was placed on the reference pot, which was in comfort water conditions, the second line was placed in turn on other pots. The measurements of the radiation temperature for each pair of pots was performed three times by choosing consecutive pairs of measuring lines. Then, the averaged value of the temperature differences was derived. Seven averaged values of the differences of radiation temperature between the studied pots were obtained that way. Every time after finishing the electronic measurement, the photos from the black-and-white and colour monitors were taken. An exemplary thermal image of a set of pots with chosen lines for differential measurement of radiation temperature is presented in Photo 1.

In the lysimetric field experiment, the thermographic system AGEMA 880 LWB, working in the range 8-13 μm , was used for the measurement of the radiation temperature. This system was supplied with a package of software CATSE 2.0 for the computer analysis of thermal images. This software enables

also to control the accuracy of the system work (*e.g.* error reports of communication between camera and computer) and to adjust the initial parameters of the work (type of camera, focus, apertures, temperature unit, encoding of grey scale and colours, number of averaged images in a sequence, *etc.*).



Phot. 1. Thermal image of set of pots with chosen electronic lines of temperature measurement

Thermal images from the lysimetric experiment, recorded at the videotape, each year, after the measuring season were analysed and elaborated by a computer system. Firstly, particular images were reproduced. The time of an individual registration was about one minute. An averaged image of the radiation temperature distribution for all the registered images in a sequence was created and all such averaged images were saved in the computer's memory, considering the parameters of the image during the registration, *i.e.* the emissivity, the ambient temperature, the distance of object from camera. It was assumed for all the recorded images, that the emissivity of meadow plant cover is 0.98. This way about 1000 images of particular pairs of lysimeters were gathered in the period 1991-94.

The next step of the image analysis was to distinguish in the image areas representing the plant cover in lysimeters. For this purpose, the programme's function was used, enabling to create areas covering any surfaces and to save the shape of each area in computer's memory. Other functions of CATSE programme

helped to calculate extreme values of radiation temperature in selected areas as well as mean values and standard deviations of radiation temperature and numbers of pixels in particular areas.

To obtain the whole-day courses of radiation temperature changes, it was decided to conduct the measurement from 20:00 till 8:00 every two hours, and for the rest of the day every one hour. Every measurement included the recording of one-minute sequences of images for created pairs of lysimeters. Obtained recordings, saved on the videocassettes, were the subjects of a quantitative computer analysis. The original AGEMA system of image analysis was used to perform it, together with CATSE 2.0 E calculation software. From registered sequences, averaged images were created, which considered the conditions of registration, *i.e.* the distance between the camera and the studied object, the range and level of each image, the ambient temperature and the emissivity (assumed as 0.98 for meadow plant cover in the whole period of the experiment).

To obtain mean values of radiation temperature of plant cover in lysimeters, two areas were distinguished in each thermal image, encircling the areas of lysimeters. Thermal images were compared with images obtained in visible range of the spectrum with video camera, to precisely determine the geometry of each set and to select in thermal images pixels, which did not belong to the studied objects. By analysing thermal images in particular dates, it was stated that there was high differentiation of radiation temperature distribution within the area of the studied lysimeters. Table 8 presents the statistics of radiation temperature distribution of plants in all pairs of lysimeters with set levels of ground water, corresponding to comfort and stress water conditions, for eighteen hours of day and night. The base for this analysis consisted of 888 thermal images from the studies.

Table 8 contains mean and extreme values as well as standard deviation values of the radiation temperature, calculated for all pixels within studied areas. Differences of the mean values of radiation temperature during evening and night hours (*i.e.* from 19:00 till 4:00) for lysimeters with varied availability of the soil water did not exceed 0.2°C. Also small values of mean standard deviations in this evening-night period (from 0.18 to 0.28 for lysimeters with unlimited availability of soil water and from 0.20 to 0.31 for lysimeters with gravitational water carried away) indicate small differentiation of temperature within the studied areas.

During the daily hours, the mean and extreme values of radiation temperature as well as standard deviation values showed large differences for both kinds of lysimeters and within studied areas.

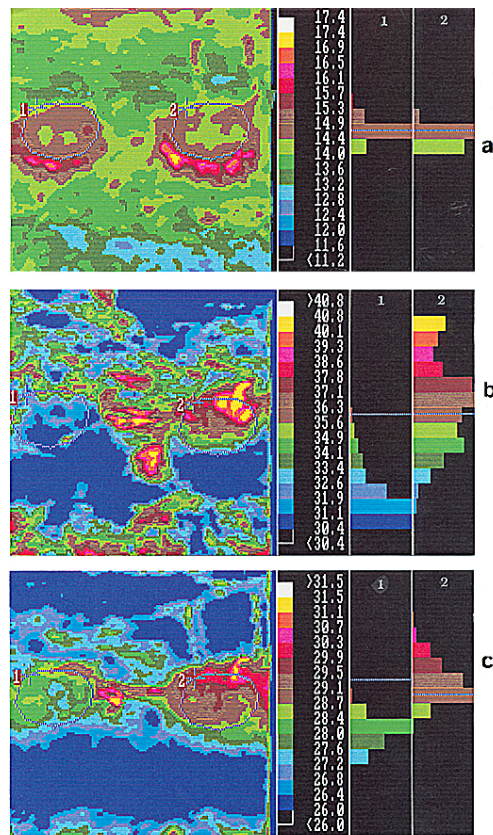
The mean and extreme values and standard deviation values of radiation temperature were higher for lysimeters with removed gravitational water. For instance, at 13:00 the difference of mean values of radiation temperature of plant cover in lysimeters with comfort and stress water conditions was 1.8°C, respective minimum temperatures varied by 0.4°C, maximum temperatures by 2.3°C, and standard deviations by 0.28.

Table 8. Analysis of radiation temperature differentiation plants surface in particular measuring times under different soil water levels

Hour	Number of images	Lysimeters with comfort soil water condition				Lysimeters with stress soil water condition			
		Mean Temp.	Min. Temp.	Max. Temp.	Std. deviation	Mean Temp.	Min. Temp.	Max. Temp.	Std. deviation
0	32	15.9	13.6	19.1	0.18	15.9	14.0	19.0	0.22
2	36	14.9	12.5	18.5	0.19	14.8	12.0	17.9	0.21
4	36	14.3	11.0	17.9	0.18	14.3	11.1	18.0	0.20
6	35	18.1	15.9	21.7	0.42	18.1	15.8	22.0	0.46
8	32	25.3	21.4	31.4	0.80	25.9	20.4	32.6	0.89
9	35	27.5	23.1	35.7	0.76	28.8	23.3	35.6	0.89
10	63	26.2	16.8	35.9	0.71	27.8	17.2	38.7	0.93
11	65	26.2	15.1	37.6	0.62	28.1	17.2	39.5	0.93
12	60	26.6	17.9	36.1	0.66	28.4	18.3	39.8	1.00
13	63	26.7	17.3	39.6	0.65	28.5	17.7	41.9	0.93
14	61	27.2	16.9	35.7	0.58	28.7	17.1	40.6	0.87
15	61	26.8	16.4	38.6	0.50	28.2	18.0	38.9	0.77
16	63	25.9	15.3	33.8	0.52	27.2	16.6	38.0	0.66
17	64	25.3	16.8	34.4	0.45	26.3	17.7	35.5	0.59
18	60	24.3	15.4	31.4	0.38	24.9	16.0	32.3	0.43
19	43	23.4	18.5	26.5	0.28	23.6	18.4	27.5	0.31
20	43	20.0	15.0	24.0	0.24	20.1	14.8	24.4	0.26
22	36	16.8	13.7	18.7	0.19	16.7	13.7	19.1	0.23

Put together colour photographs (Phot. 2 a, b, c), containing thermal images of one pair of lysimeters coming from three time limits of measurement, present

differentiation of distribution in radiation temperature and temperature histograms for all the pixels within studied areas. The area in the right side of the image represents a lysimeter with limited availability of soil water. It can be noticed that both for particular time limits and for two analysed lysimeters, histograms are significantly different.



Phot 2. Thermal images of pair of lysimeters with histograms of radiation temperature in selected areas: a – 2¹¹ a.m., b – 13¹⁶ p.m., 18⁰⁹ p.m.

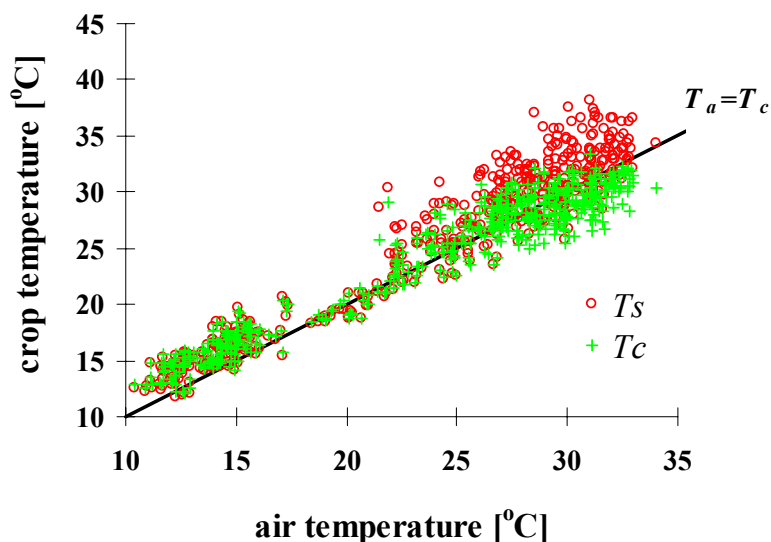


Fig. 26. Relation between average radiation temperature of plant cover in lysimeters with limited soil water availability T_s and with comfort water conditions T_c and air temperature

It results from Table 8 and from Photographs 2 a, b and c that in the evening and night hours, *i.e.* when the air temperature reaches minimum values, the radiation temperature differences between the studied objects were small. Figure 26, presenting radiation temperature data from day and night measurements, confirms it. In the range of radiation temperatures from 10°C to 20°C, their differences for plant cover in comfort and stress water conditions were small. The straight line in the plot represents the case when the temperature of the plant cover was equal to the air temperature.

For air temperatures below 20°C in majority of cases the plant temperature was higher than the air temperature. It referred mainly to night measurements. The thermal inertia of soil, heated during daily hours, causes then, the increase of the radiation temperature of the plant cover. Only for air temperatures higher than 20°C, considerable differences of radiation temperature occurred between plant cover in lysimeters with extremely different conditions of soil water availability, reaching up to seven-Celsius degrees.

6.2. Results of water stress study

The laboratory experiment was conducted during two succeeding years. Each year there were about 100 days of measurement. Mean radiation temperature measurements between electronically chosen areas of the size 1.5×15 cm were done. The averaged radiation temperature in pots was measured for various shares of soil and plants depending on phonological development of plants. The measurements were performed under varying ambient conditions. After combining all the results of the radiation temperature differences as a function of the soil water content and the soil water potential it was impossible to find out any correlation.

The interpretation of the averaged temperature, even if the degree of the plant cover is known, is very difficult because water conditions influence the radiation temperature of plants and soil in different ways, and this influence depends on actual ambient conditions, such as temperature, water content and on the course of changes of these parameters (thermal inertia). As a consequence of this, it was decided to analyse only the results measurements performed in conditions of plant cover degree close to 100%.

The analysis of the results coming from particular days characterized by varying relative humidity and temperature of the air in the greenhouse enabled to state that considerable differences of radiation temperature were observed only for the days, for which the relative humidity of the air was relatively low, *i.e.* below 75% and the air temperature was high. Due to this, further analysis included only the results coming from these days.

It was noticed that for the mineral soil under the soil water content values higher than 10% and in organic soil 40% the differences of the radiation temperature in majority of measuring points contained in the range from 0 to -0.3°C . For the soil water content below 10% in mineral soil and below 40% in organic soil a considerable increase of the differences of radiation temperature of plants is observed.

The relations between the difference of radiation temperature of meadow plants in lysimeters and the volumetric soil water content in mineral and organic soils are presented in Fig. 27.

It results from this figure that boundary values of the volumetric soil water content exist, below which the increase of the temperature differences occurs. For the mineral soil the occurrence of high differences of radiation temperature, reaching up to 7°C is observed for the volumetric soil water content below 10%

and for the organic soil below 40%. Under higher values of soil water content of these soils, the temperature differences do not exceed 2°C. It should be mentioned that this figure contains measurement values coming from different dates of observation under varying meteorological conditions.

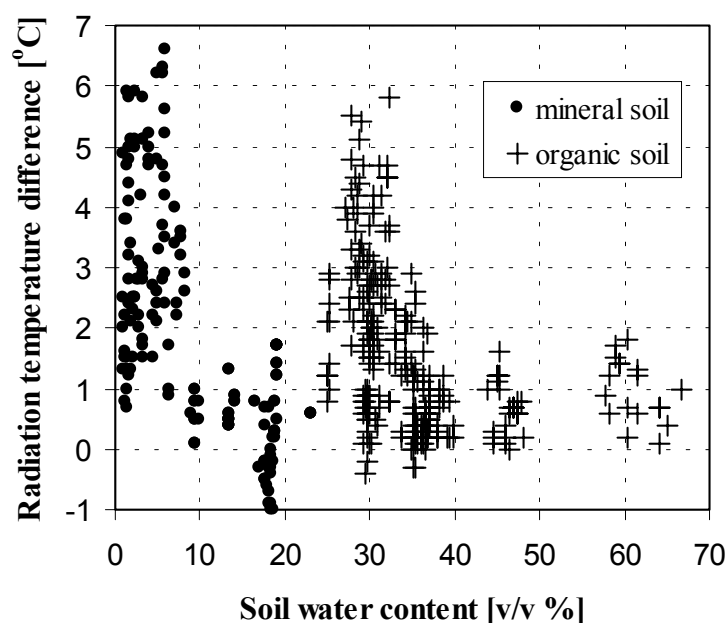


Fig. 27. Relation between radiation temperature of natural meadow plant cover and volumetric soil water content

In both pot (greenhouse) and lysimetric (field) experiments, the differences of radiation temperature, as compared to the control object, occurred for both soils under various values of the soil water content. These characteristic values were 10% for mineral soil and 40% for organic soil. Therefore, the water content is not a parameter that could universally explain the occurrence of differences of radiation temperature. Plant as a sensor can indicate through the radiation temperature change the disturbance in the course of physiological functions.

In this case, the dysfunction is caused by insufficient amount of water taken by the rooting system to ensure, in given conditions, a required evapotranspiration rate. The limited water uptake can be caused, or by to high absolute values of the

soil water potential, or by too low values of water diffusivity in given conditions of soil, or by these two factors acting at the same time.

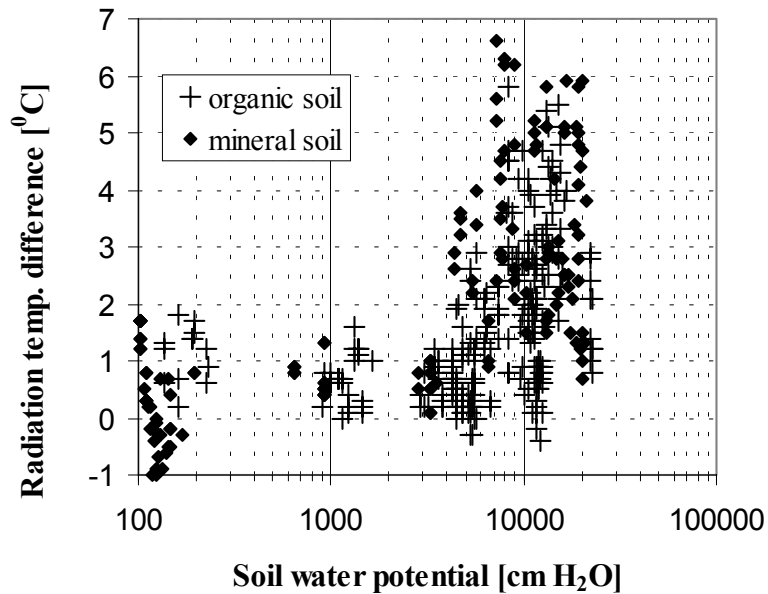


Fig. 28. Relation between radiation temperature of natural meadow plant cover and soil water potential for mineral and organic soils

To explain this problem, the plots the relation: soil water potential – the difference of radiation temperature for pot and lysimetric experiments were made. This relation was derived from measured soil retention curves, *i.e.* from the relation between the soil water potential and the soil water content for both kinds of soil: mineral and organic.

The values of the soil water content for mineral and organic soils were recalculated according to the retention curves of these soils for the level 25-30 cm (Fig. 19) into the respective values of the soil water potential. It can be noticed in Fig. 28 that differences of the radiation temperature occur for two studied soils under the soil water potential of about 5000 cm H₂O (pF 3.7). This value, as results from Fig. 1 corresponds to the point of complete inhibition of plant growth. Starting from this value of potential up to about 15000 cm H₂O (pF ~

4.2), the difference of radiation temperature in lysimetric study reaches the value of about 7°C.

Both in pot and lysimetric experiments and for two soils: mineral and organic, the highest differences of radiation temperature occur under the same value of the soil water potential, *i.e.* 15 000 cm H₂O (pF 4.2 or 15 bars). Collective plots in Fig. 29 present the dependence between the differences of radiation temperature of plant cover and the soil water potential obtained during the pot (laboratory) experiment and the lysimetric (field) experiment for mineral and organic soils. The value of the soil water potential equal to 15 bars or pF 4.2 refers to the potential at which water becomes unavailable for plant, called the permanent wilting point (Fig. 1). The results of this study show that the main factor, connected with soil water status, influencing the radiation temperature of plant cover is the soil water potential.

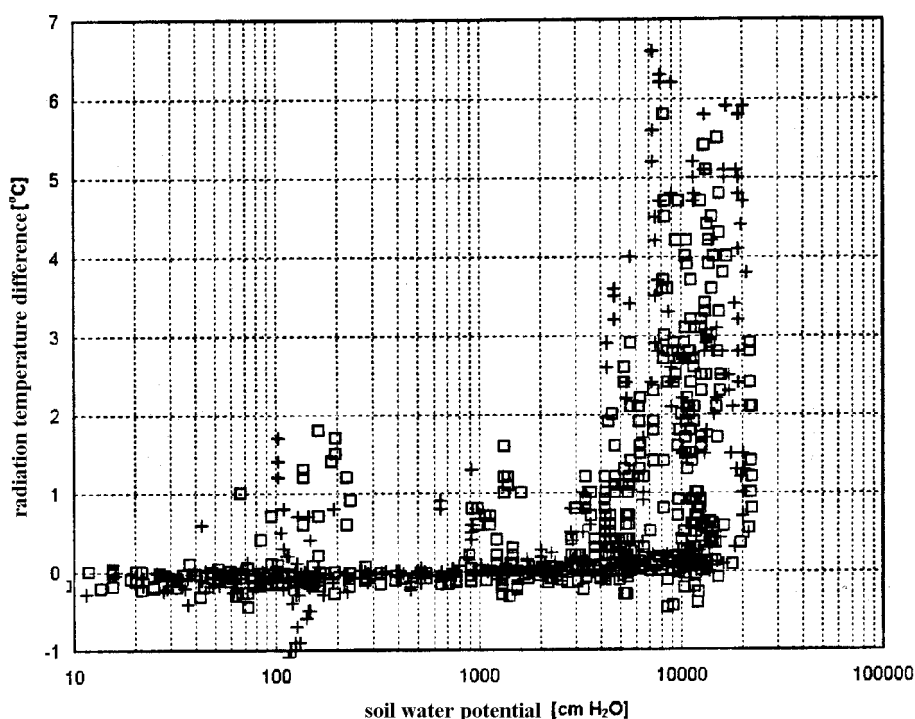


Fig. 29. Combination of relations between plant cover radiation temperature differences and soil water potential obtained in laboratory and field investigations: mineral soil (+), organic soil (□)

To evaluate the impact of the soil water diffusion on limitation of its flux incoming to the rooting zone, the measurement of the potential in soil and plant samples was done. If water diffusion dominated as a factor limiting water availability, the increase of radiation temperature should be stated under the water potential corresponding to the water easily available and in the nearest surrounding of roots, the water potential would be higher, and in this area the resistance would occur, limiting water flow to the roots. Detailed studies of the diffusion resistance as a limiting factor are very difficult because they require the knowledge of local changes of the soil water content and the soil water potential around plant roots as well as determination of the total root surface taking water, because the product of the diffusion flux and the root surface is a parameter notifying about a total water flux into plants. The measurement was done with Wescor instrument, described in Chapter 5.2.4 for soil samples taken with a mini soil sampler and for grass leaves taken at the same time.

Within the error of the method, a situation was not stated, when the increase of the radiation temperature of plant cover occurred under absolute values of the thermodynamic soil water potential, lower than these corresponding to points of limitation or complete inhibition of plant growth. It indicates that other factors, *e.g.* diffusivity, do not cause the limitation of water supply for plants in a situation when the thermodynamic potential of water does not limit its availability.

Obtained results let us state, that thermal images of plant cover of airborne or satellite origin cannot be used for the evaluation of water resources retained in the soil. However, they can be used for stating the incoming or existing plant water stress, and this evaluation can be precise only in case when a reference points exist within the area of thermal imaging, representing areas with comfort water conditions. In case of large areas of grasslands, these points can be easily defined as being in the neighbourhood of water-courses and water reservoirs, what does not require any ground observations.

It results from field (lysimetric) studies (Fig. 27 as well as a collective Fig. 29), that the occurrence of radiation temperature differences higher than 2°C between the reference point and chosen areas projected in the thermal airborne or satellite image, can be treated as a result confirming the danger of approaching or existing plant water stress.

The airborne and satellite observations which lead to evaluation of a danger of plant water stress occurrence, can, in practice of large agricultural areas, be used to evaluate irrigation needs and control of irrigation systems, *e.g.* by regulation of water level in drainage ditches.

6.3. Influence of meteorological conditions on measured values of radiation temperature of plants

The measurements were performed in lysimetric conditions, which were closely related with natural ones. The agrometeorological conditions in the period of the conducted studies showed high differentiation. Therefore, it was purposeful to determine the influence these conditions on measured values of radiation temperature of plants.

The analysis of distribution of radiation temperature of plant cover in lysimeters under varying soil humidity conditions revealed high differentiation of temperature for particular hours of measurement, what could be connected with changing meteorological conditions between measurements.

To study quantitative relation between the radiation temperature of the studied surfaces and a set of meteorological parameters, the statistical multiple regression method was used. The following independent variables X_p were put into the models of multiple regression: the air temperature at the height of 2 m above the active surface T_a , the relative air humidity W_a , the net radiation R_n and the wind velocity at the height of 2 m v_{2m} . The dependent variables Y in particular models were: the radiation temperature of plant cover in lysimeters with limited availability of soil water T_s , the radiation temperature of plant cover in lysimeters with comfort soil water conditions T_c and the difference of radiation temperatures $T_s - T_c$. On the base of measurements carried out during the whole day and night, several files were created containing data from early morning measurements, *i.e.* 6⁰⁰-10⁰⁰ from intensive evapotranspiration hours 11⁰⁰-19⁰⁰ and night hours 20⁰⁰-5⁰⁰. The analysis was performed separately for plants growing in mineral and organic soils and jointly for all lysimeters.

The model of multiple regression was used, in which for a declared dependent variable Y and independent variables X_1, \dots, X_p the coefficients of multiple regression are calculated from the equation:

$$Y = B_0 + B_1 \cdot X_1 + \dots + B_p \cdot X_p + u \quad (68)$$

where: B_0, B_1, \dots, B_p – coefficients of multiple regression, u – the experimental error.

To obtain models with limited number of the most important independent variables, the step method of analysis was applied in which independent variables

were separately added or removed from the model in succeeding steps of regression, until the best model was gained.

The total standard deviation of calculated values of dependent variable Y was calculated from the model:

$$sc = \sqrt{\frac{ZC}{n-1}} \quad (69)$$

where: n is the number of samples, ZC – the total variation expressed as a sum of deviation squares of particular observed values of variable Y from its mean value \bar{Y} . The residual variation is given by the equation:

$$ZR = \sum_{i=1}^n \left(Y_i - \hat{B}_0 - \hat{B}_1 \cdot \hat{X}_{i1} - \dots - \hat{B}_p \cdot X_{ip} \right)^2 \quad (70)$$

where: $\hat{B}, \hat{B}_1 \dots \hat{B}_p$ – solutions of a set of normal equations:

$$\mathbf{S}\hat{\mathbf{B}} = \mathbf{X}'\mathbf{Y} \quad (71)$$

in which \mathbf{S} is the covariance matrix of variables X_1, X_2, \dots, X_p , whereas $\mathbf{X}'\mathbf{Y}$ is a vector of covariance of variable Y with variables X_1, X_2, \dots, X_p . As a measure of regression fitting, the differences was assumed between total variation ZC of the observed value of variable Y and residual variation ZR obtained by elimination from variable Y its best estimation with the use of a linear function of variables X_1, X_2, \dots, X_p .

Table 9. Multiple regression models of temperature T_s for two kinds of soil

Time of measurement	Dependent variable T_s													
	Mineral soil							Organic soil						
	Independent variables of the model	Regression coefficients	t Student	Correlation coefficients	Summary of the regression model	Independent variables of the model	Regression coefficients	t Student	Correlation coefficients	Summary of the regression model				
6-10	T_a	0.7915	10.970	0.836	N=56 R=0.99 F=844.61 SBE=1.626	T_a	0.9022	13.277	0.777	N=121				
	W_a	-0.6044	-2.709	-0.352		W_a	-0.0503	-3.052	-0.273	R=0.95				
	R_n	-	-	-		R_n	-0.0053	-3.086	-0.275	F=260.04				
	V_{2m}	0.1490 Bo 1.9223	2.306 4.113	0.305		V_{2m}	0.2766 Bo 8.3626	2.089 3.626	0.190	SBE=1.634				
11-19	T_a	0.8348	21.614	0.8122	N=245 R=0.92 F=466.22 SBE=1.809	T_a	0.8253	31.757	0.824	N=480				
	W_a	-0.0334	-2.646	-0.168		W_a	-0.0441	-5.579	-0.248	R=0.93				
	R_n	0.0075	10.593	0.564		R_n	0.0037	8.259	0.354	F=1024.6				
	V_{2m}	- Bo 5.6837	- 3.840	-		V_{2m}	- Bo 6.0346	- 6.213	-	SBE=1.668				
20-5	T_a	0.7700	21.337	0.939	N=64 R=0.94 F=228.10 SBE=0.927	T_a	0.7566	30.718	0.929	N=153				
	W_a	-	-	-		W_a	-	-	-	R=0.93				
	R_n	0.0409	2.990	0.358		R_n	0.0224	2.768	0.220	F=472.14				
	V_{2m}	- Bo 5.4351	- 9.028	-		V_{2m}	- Bo 5.2803	- 13.242	-	SBE=0.933				
Whole day and night	T_a	0.8552	40.753	0.906	N=364 R=0.95 F=1846.2 SBE=1.783	T_a	0.8022	35.853	0.795	N=754				
	W_a	-	-	-		W_a	-0.0198	-3.154	-0.114	R=0.96				
	R_n	0.0072	11.785	0.527		R_n	0.0033	8.254	0.289	F=2706.6				
	V_{2m}	- Bo 3.6741	- 8.523	-		V_{2m}	- Bo 5.7818	- 6.928	-	SBE=1.672				

Table 10. Multiple regression models of temperature T_c for two kinds of soil

Time measurement	Mineral soil					Organic soil				
	Independent variables of the model	Regression coefficients	t Student	Correlation coefficients	Summary of the regression model	Independent variables of the model	Regression coefficients	t Student	Correlation coefficients	Summary of the regression model
6-10	T_a	0.8522	16.189	0.913	N=56 R=0.99	T_a	0.8578	20.813	0.887	N=121
	W_a	-	-	-	R=815.65	W_a	-	-	-	R=0.95
	R_a	-0.0041	-2.328	-0.307	SBE=1.633	R_a	-0.0040	-2.855	-0.255	F=337.14
	v_{2m}	0.0963 Bo 5.5156	2.122 5.840	0.282		v_{2m}	0.2990 Bo 4.6317	2.759 6.286	0.247	SBE=1.356
11-19	T_a	0.7547	22.738	0.826	N=245 R=0.92	T_a	0.7897	33.922	0.841	N=480
	W_a	-0.0427	-3.933	-0.246	F=446.33	W_a	-0.0199	-2.907	-0.132	R=0.93
	R_a	0.0021	3.485	0.219	SBE=1.555	R_a	0.0010	2.300	0.105	F=719.56
	v_{2m}	- Bo 7.2057	- 5.664	-		v_{2m}	0.2410 Bo 4.9744	5.036 5.763	0.225	SBE=1.447
20-5	T_a	0.7388	21.000	0.937	N=64 R=0.94	T_a	0.7552	31.917	0.934	N=153
	W_a	-	-	-	F=221.31	W_a	-	-	-	R=0.93
	R_a	0.0435	3.264	0.386	SBE=0.904	R_a	0.0207	2.663	0.212	F=509.95
	v_{2m}	- Bo 6.0837	- 10.366	-		v_{2m}	- Bo 5.5154	- 14.398	-	SBE=0.897
Whole day and night	T_a	0.7783	41.228	0.908	N=364 R=0.94	T_a	0.7723	67.094	0.926	N=754
	W_a	-	-	-	F=1444.2	W_a	-	-	-	R=0.96
	R_a	0.0016	3.005	0.156	SBE 1.604	R_a	0.0010	2.594	0.094	F=2807.6
	v_{2m}	- Bo 4.7231	- 12.181	-		v_{2m}	0.1469 Bo 4.7752	3.768 19.916	0.136	SBE=1.406

Dependent variable T_c

Table 11. Multiple regression models of temperature difference $T_a - T_c$ for two kinds of soil

Time of measurement	Mineral soil					Organic soil				
	Independent variables of the model	Regression coefficients	t Student	Correlation coefficients	Summary of the regression model	Independent variables of the model	Regression coefficients	t Student	Correlation coefficients	Summary of the regression model
6-10	T_a	0.2595	6.371	0.659	N=56 R=0.99	T_a	0.0553	2.138	0.193	N=121
	W_a	-	-	-	F=1795.3	W_a	-0.0371	-4.997	-0.418	R=0.78
	R_n	0.7802	22.021	0.949	SBE=1.617	R_n	-	-	-	F=91.322
	v_{2m}	Bo -4.7125	-5.183	-	-	v_{2m}	-	-	-	SBE=0.746
11-19	T_a	0.0615	2.912	0.184	N=245	T_a	Bo 2.2545	2.174	-	N=480
	W_a	-	-	-	R=0.62	W_a	0.0476	3.291	0.149	R=0.66
	R_n	0.0054	10.585	0.563	F=76.862	R_n	-0.0248	-5.824	-0.258	F=92.993
	v_{2m}	Bo -0.5707	-1.102	-	SBE=1.308	v_{2m}	0.0025	9.641	0.405	F=92.993
20-5	T_a	0.0319	4.204	0.471	N=64	T_a	-	-	-	N=754
	W_a	-	-	-	R=0.47	W_a	-	-	-	R=0.73
	R_n	-	-	-	F=17.676	R_n	-	-	-	F=210.97
	v_{2m}	Bo -0.6133	-5.074	-	SBE=0.195	v_{2m}	-	-	-	SBE=0.821
Whole day and night	T_a	0.0769	5.551	0.280	N=364	T_a	0.0355	3.195	0.116	N=754
	W_a	-	-	-	R=0.76	W_a	-0.0172	-5.574	-0.200	R=0.73
	R_n	0.0055	13.750	0.586	F=241.98	R_n	0.0025	11.760	0.395	F=210.97
	v_{2m}	Bo -1.0490	-3.684	-	SBE=1.178	v_{2m}	-0.1892	-8.284	-0.290	SBE=0.821
						Bo 0.7574	1.823			

Table 12. Multiple regression models of temperature T_s jointly for two kinds of soil

Dependent variable T_s					
Time of measurement	Mineral and organic soil Independent variables of the model	Regression coefficients	t Student	Correlation coefficients	Summary of the regression model
6-10	T_a	0.8459	14.411	0.740	N=176
	W_a	-0.0469	-3.218	-0.238	R =0.94
	R_n	-0.0022	-1.623	-0.123	F=413.41
	v_{2m}	-	-	-	SBE=1.810
		Bo 9.503	4.648		
11-19	T_a	0.8350	34.908	0.793	N=725
	W_a	-0.0385	-5.165	-0.189	R =0.91
	R_n	0.0047	11.892	0.405	F=1218.0
	v_{2m}	-	-	-	SBE=1.878
		Bo 5.8922	6.622		
20-5	T_a	0.7619	48.679	0.948	N=269
	W_a	-	-	-	R =0.96
	R_n	-	-	-	F=1409.6
	v_{2m}	0.3213	3.354	0.201	SBE=1.052
		Bo 4.6100	18.049		
Whole day and night	T_a	0.8067	40.603	0.773	N=1118
	W_a	-0.0167	-2.967	-0.089	R =0.95
	R_n	0.0046	12.915	0.361	F=3431.4
	v_{2m}	-	-	-	SBE 1.826
		Bo 5.5864	7.502		

The error of approximation was calculated as a standard estimation error SEE , expressed as:

$$SEE = \sqrt{\frac{ZR}{n-p-1}} \quad (72)$$

The square of multiple correlation coefficients was calculated according to the formula:

$$R^2 Y(1, \dots, p) = \frac{ZC - ZR}{ZC} \quad (73)$$

The significance of multiple correlation coefficient was checked by F-Snedecor test. The significance of coefficients B_0, B_1, \dots, B_p of multiple regression was determined by t-Student test.

In all models of multiple step regression, it was assumed that the boundary value of F for adding an individual independent variable into the model was

0.0001 and the value of F that eliminated an independent variable from the model was 0.0.

Table 13. Multiple regression models of temperature T_s jointly for two kinds of soil

Dependent variable T_c					
Mineral and organic soil					
Time of measurement	Independent variables of the model	Regression coefficients	t Student	Correlation coefficients	Summary of the regression model
6-10	T_a	0.8480	23.898	0.877	N=176
	W_a	–	–	–	R =0.94
	R_n	–0.0038	–3.132	–0.232	F=420.02
	v_{2m}	0.1804	1.951	0.147	SBE=1.459
		Bo 5.0989	7.949		
11-19	T_a	0.7808	40.388	0.833	N=725
	W_a	–0.0267	–4.583	–0.168	R =0.92
	R_n	0.0013	3.597	0.133	F=1043.3
	v_{2m}	0.1855	4.634	0.170	SBE=1.490
		Bo 5.5832	7.729		
20-5	T_a	0.7323	49.958	0.951	N=269
	W_a	–	–	–	R =0.96
	R_n	–	–	–	F=1500.6
	v_{2m}	0.3695	4.118	0.245	SBE=0.985
		Bo 5.3235	21.828		
Whole day and night	T_a	0.7734	77.697	0.919	N=1118
	W_a	–	–	–	R =0.95
	R_n	0.0012	3.942	0.117	F=3679.7
	v_{2m}	0.0816	2.453	0.073	SBE=1.476
		Bo 4.7944	23.011		

Results of the analysis with use of multiple step regression are presented in Tables 9-14. The independent variables, which were included in particular models were written with bolt font. The independent variables were selected into to models on the base of the t-Student test. In the created models all the values of the t-Student test for the regression coefficients have values higher than the critical ones for the confidence level $\alpha = 0.05$. At the same time the models were created only in case when the value of F Snedecor test of the model was higher than the critical value $F_{0.05}$, what was the base for rejection of the zero hypothesis and confirming that the regression coefficients and the multiple correlation coefficients were significant. In Tables 9-14 the critical values of F-Snedecor and t-Student tests were not presented, but they can be read for particular models from the number of degrees of freedom and the number of independent variables included in the studied models.

The coefficients of multiple correlation for majority of models built for dependent variables T_s and T_c were relatively high (0.92). However, the models of the difference T_s-T_c achieved in majority of cases low values of the multiple correlation coefficients R. In two cases, for night hours, it was not possible to create the models of multiple regression for the dependent variables T_s-T_c , because the regression coefficients and the multiple correlation coefficient occurred to be insignificant. It confirms the hypothesis, that a set of meteorological parameters does not decide of a temperature difference T_s-T_c , but it is influenced by soil conditions, which limit transpiration, *i.e.* the availability of soil water for plants or physiological processes within plants.

Table 14. Multiple regression models of temperature difference T_a-T_c jointly for two kinds of soil

Dependent variable T_s-T_c					
Mineral and organic soil					
Time of measurement	Independent variables of the model	Regression coefficients	t Student	Correlation coefficients	Summary of the regression model
6-10	T_a	–	–	–	N=176 R =0.65 F=129.38 SBE=1.086
	W_a	–0.053	–11.375	–0.653	
	R_n	–	–	–	
	v_{2m}	–	–	–	
	Bo	4.8927	15.658	–	
11-19	T_a	0.0543	3.198	0.118	N=725 R =0.52 F=67.493 SBE=1.308
	W_a	–0.0118	–2.298	–0.085	
	R_n	0.0035	11.210	0.385	
	v_{2m}	–0.0975	–2.774	–0.103	
	Bo	–0.0266	–0.042	–	
20-5	T_a	–	–	–	N=269
	W_a	–	–	–	
	R_n	–	–	–	
	v_{2m}	–	–	–	
	Bo	–	–	–	
Whole day and night	T_a	0.0463	3.664	0.109	N=1118 R =0.66 F=211.26 SBE=1.151
	W_a	–0.0115	–3.217	–0.096	
	R_n	0.0035	14.414	0.397	
	v_{2m}	–0.1190	–4.572	–0.136	
	Bo	0.2025	0.426	–	

The analysis of significance of four studied parameters in multiple regression equations leads to the statement that the air temperature T_a plays the prevailing role in them. This parameter is included in all the obtained models and in majority of cases it has the highest values of the correlation coefficient, exceeding several times correlation coefficients of other parameters included into

the regression equations. When the models of radiation temperature of plant cover are analyzed separately for mineral and organic soils it can be stated that the wind velocity occurs in the models only for morning hours, *i.e.* 6-10 a.m. However, the analysis of the models, which consider data for both soils jointly, shows that especially in case of plant cover temperature in favorable soil water conditions T_c , the independent variable v_{2m} is included into all created models.

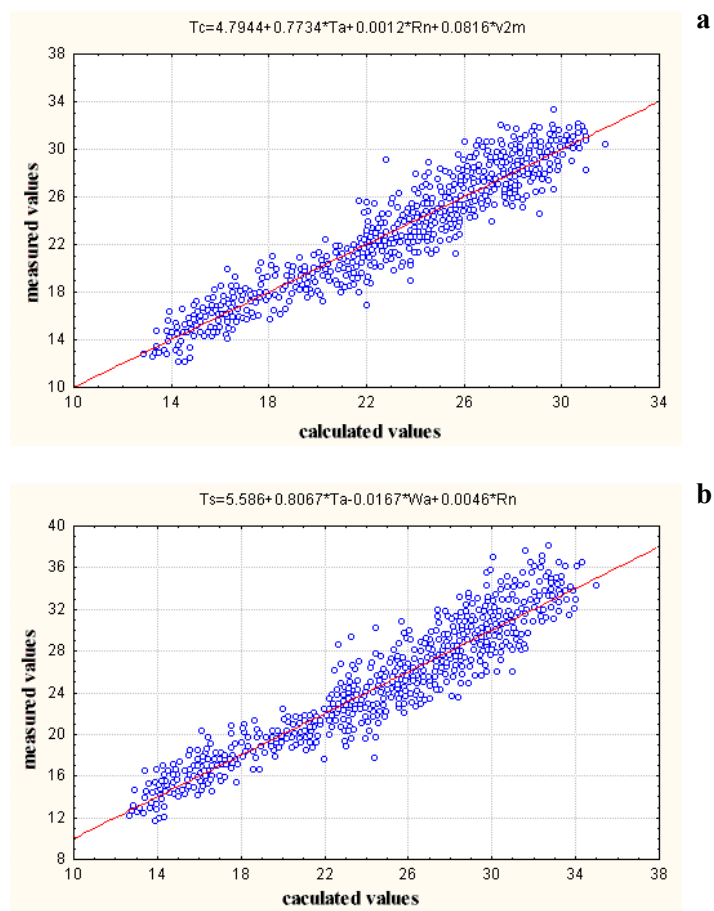


Fig 30. Measured and calculated from multiple regression models values: a – temperature T_a and b – T_c

Also the frequencies of occurrence of the relative air humidity W_a and the net radiation R_n in the models created for both soils separately and jointly are diverse.

For instance, the models of T_s and T_c created separately for mineral and organic soils, in case of night hours contain two parameters (air temperature and net radiation). However, the models of T_s and T_c for night hours, joined for both soils, contain parameters of air temperature and wind velocity.

It should be noticed that in case of the models of T_s and T_c for the hours from 11 a.m. till 7 p.m. they contain three parameters (T_a , W_a and R_n) with one exception of four-parameter model.

Figures 30a and b present an interrelation between the measured day and night values of T_s and T_c and the values calculated from the multiple regression models. The analysed data came from the period 1992-1994.

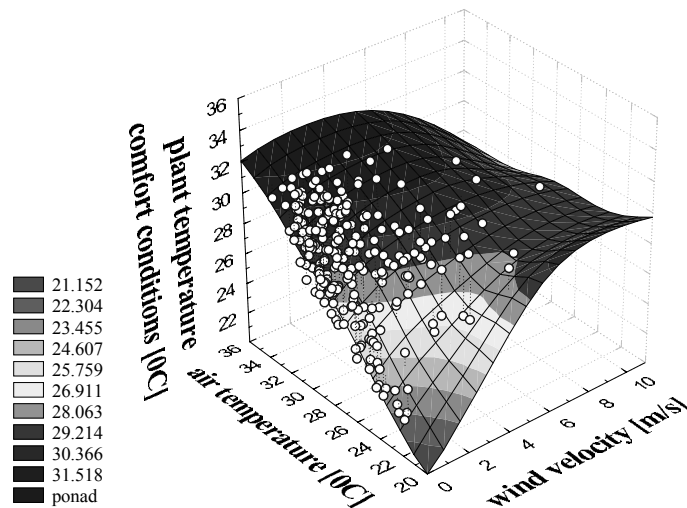


Fig. 31. A scatter plot of plant temperature under comfort water conditions as a function of air temperature and wind speed

To analyse the influence of various factors on values of the radiation temperature, three-dimensional plots were created, presenting the scatter of measured values and the surface fitted with the least square method. It results from Fig. 31 that plant temperature in conditions of water comfort is strongly correlated with the air temperature and the wind velocity. Generally, the increase of the air temperature causes the increase of the plant cover temperature, however in case of high wind speed values this effect of plant heating is diminished.

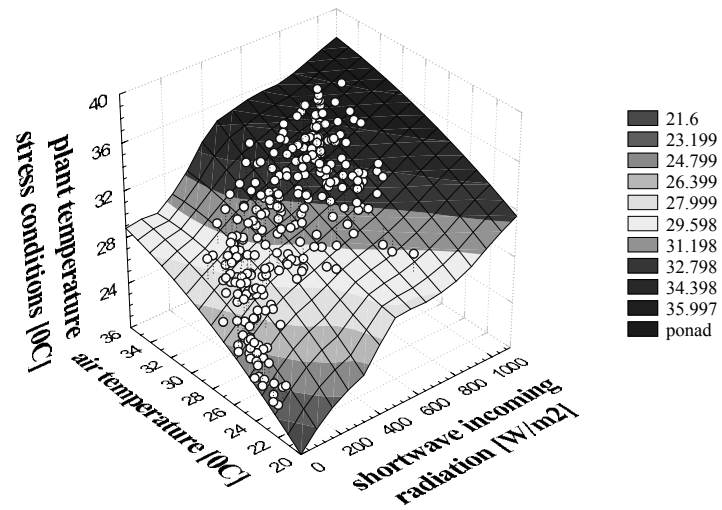


Fig. 32. A scatter plot of plant temperature under comfort water conditions as a function of air temperature and shortwave radiation

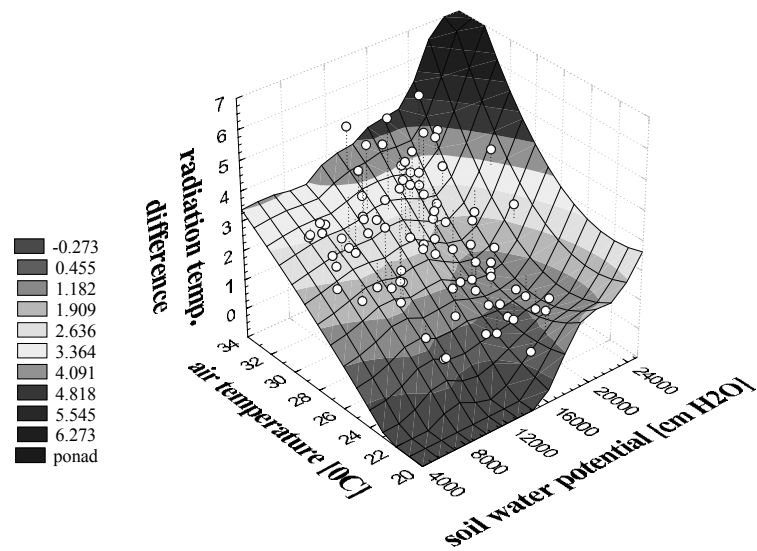


Fig. 33. A scatter plot of temperature differences $T_s - T_c$ as a function of air temperature and soil water potential

In the model of plant temperature in the conditions of water stress, the air temperature and the incoming shortwave solar radiation occurred to be statistically important independent variables. Changes of measured temperature of plant cover in water stress conditions versus air temperature and the shortwave incoming solar radiation are presented in Fig.32.

It can be noticed from Fig. 33, which shows the relation between the difference of radiation temperature of plant cover in stress and comfort water conditions, air temperature and soil water potential, that the highest values of this difference occur for the air temperatures exceeding 25°C and the soil water potentials higher than 15000 cm H₂O.

6.4. Determination of hourly and daily values of actual evapotranspiration on the base of heat balance equation of active surface under varying soil water content

Day and night courses of plant temperature under the conditions of unlimited soil water T_c , soil water stress (pF over 2.7) T_s , air temperature T_a and relative air humidity W_a for two chosen days of measurement are presented in Fig. 34. The first of presented in Fig. 34 series of courses concerns a pair of lysimeters with organic soil and the second with mineral soil.

The analysis of the obtained courses showed that for hours with high intensity of solar radiation and low relative air humidity, the differences of plant cover temperature in both lysimeters of each pair reached some degrees. In such conditions, the radiation temperature of plant cover maintained in stress soil water conditions was higher than the air temperature.

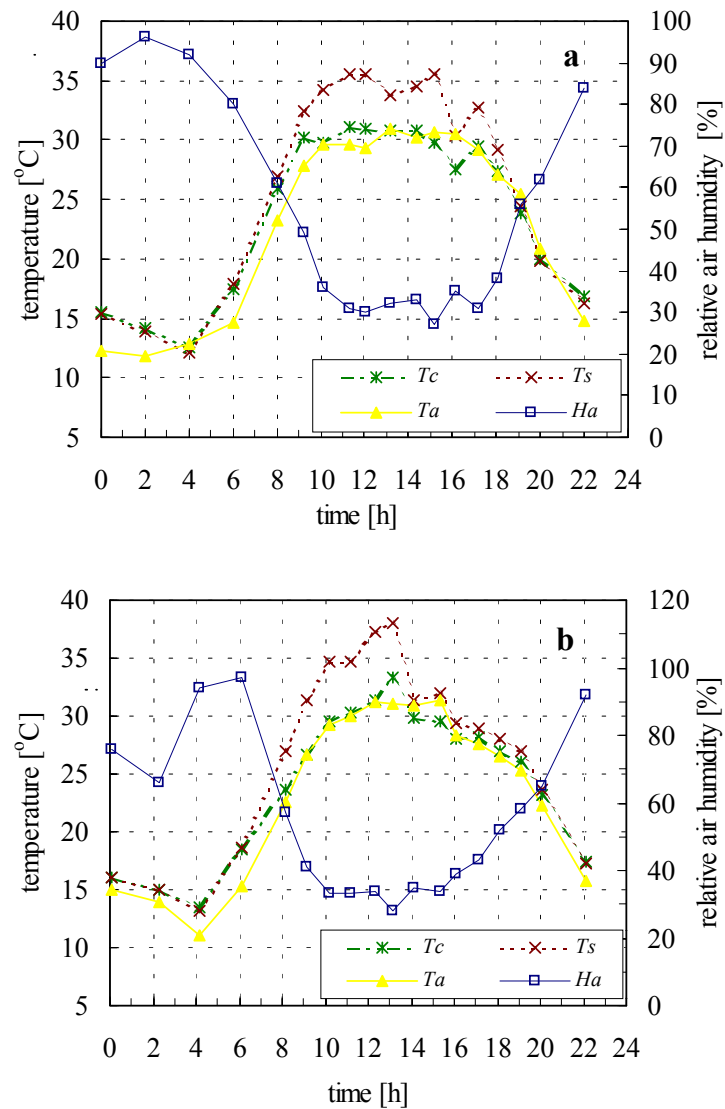


Fig. 34. Daily courses of air temperature – T_a , relative air humidity – H_a and radiation temperature of plant cover: T_s – in lysimeters with stress water condition, T_c – in lysimeters with comfort water condition (*a* – 28.07.94 organic soil, *b* – 02.08.94 mineral soil)

Plant cover growing in lysimeters with comfort conditions of soil water availability, had radiation temperature close to or lower than the air temperature.

It was connected with the effect of cooling plant surface as a result of unrestricted transpiration.

At night, when the relative air humidity was high and solar radiation was not present, the differences between temperatures T_s and T_c of plant cover disappeared.

The preformed study enabled to state a considerable similarity of day and night courses of plant cover radiation temperature for pairs of lysimeters with organic and mineral soil.

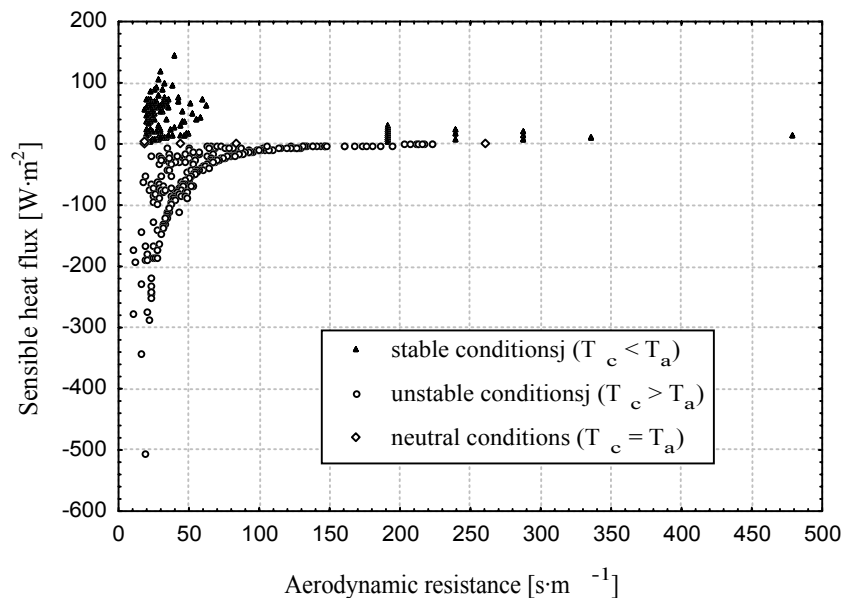


Fig. 35. Dependence of sensible heat flux and aerodynamic resistance under different air stability conditions

Taking into consideration the stability conditions in the atmosphere has a considerable impact on calculated values of the sensible heat flux. In Fig. 35 the experimentally obtained relation between the sensible heat flux and the aerodynamic resistance under various stability conditions in the atmosphere is shown. For the aerodynamic resistance higher than 70 s m^{-1} the stability conditions in the atmosphere do not influence the sensible heat flux, which is in this case close to zero. However, for the aerodynamic resistance values smaller than 70 s m^{-1} the sensible heat flux under stable conditions ($T_c < T_a$) takes positive values up to 150 W m^{-2} under unstable conditions ($T_c > T_a$) it changes from 0 to –

500 W m⁻² and for neutral conditions ($T_c=T_a$) its values lower than 50 W m⁻² were observed. The situation at which the aerodynamic resistance exceeds 70 s m⁻¹ corresponds to the weather conditions characterized by the lack of wind or its very small speed. Such conditions in the performed experiment were observed mainly during night hours.

Twenty-four hour courses of the heat balance components for two pairs of lysimeters for chosen two days are presented in Fig. 37. High differences in courses of the sensible heat flux and the latent heat flux for both lysimeters of particular pairs were noticed. The stability conditions of the atmosphere and the turbulent aerodynamic resistance were calculated in this case from equations (81-88).

The structure of the solar radiation balance for the same chosen two days of measurement is presented in Fig. 36. These two days are characterized by high values of shortwave radiation fluxes and net radiation fluxes. Instantaneous decreases of the solar radiation intensity, observed in the figures, were caused by the transitory cloudiness. Densities of the emitted longwave radiation fluxes R_{lps} and R_{lpc} (the last term in equation 75) were calculated for plant surfaces being in temperatures T_s and T_c , respectively.

During the hours with intensive solar radiation, the sensible heat flux for lysimeters with comfort water conditions revealed high stability. Its values oscillated around zero W m⁻² and its sign underwent changes. However, in case of lysimeters with stress water conditions, the sensible heat flux achieved negative values as result of the thermal energy transfer from the evaporating surface to the atmosphere. Values of this heat flux changed considerably during the twenty-four hours.

Courses of the soil heat flux calculated from equation (78) and presented in Fig. 37 achieved about 10% of the net radiation flux R_n during the hours with intensive solar radiation.

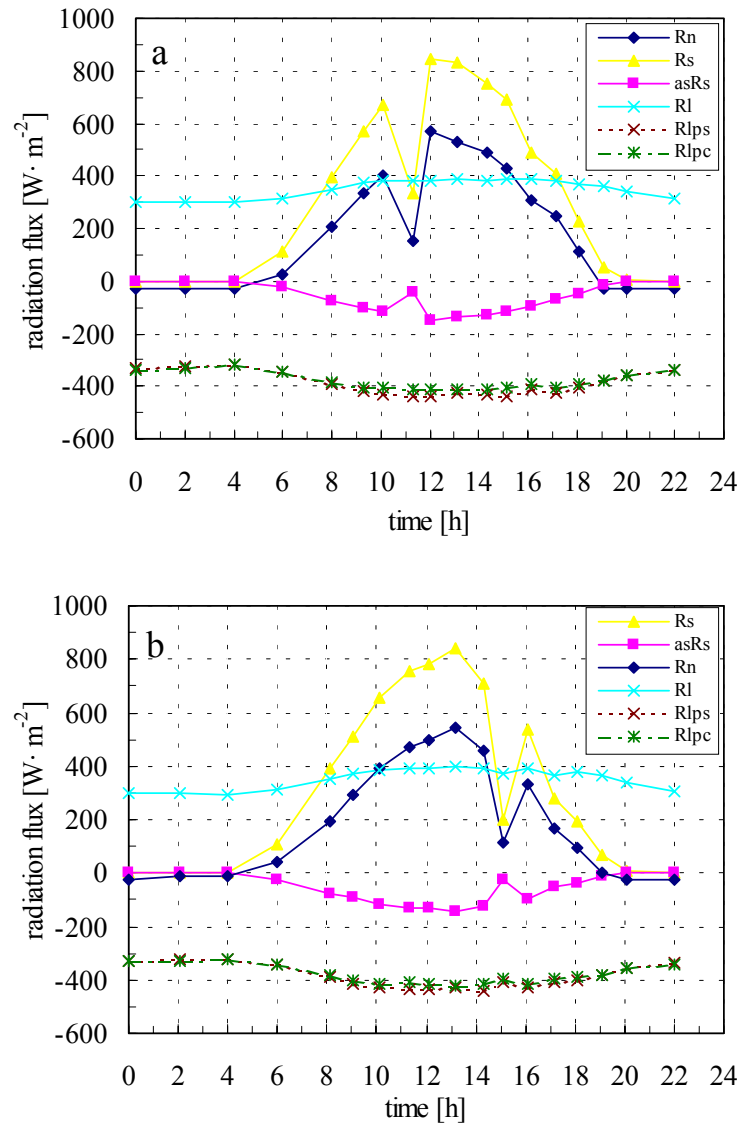


Fig. 36. Daily courses of radiation balance components: R_n – net radiation, R_s – incoming shortwave solar radiation, $\alpha_s R_s$ – reflected shortwave radiation, R_l – longwave radiation of atmosphere, R_{lps} , R_{lpc} – longwave radiation emitted from lysimeters (a–28.07.94. b – 02.08.94)

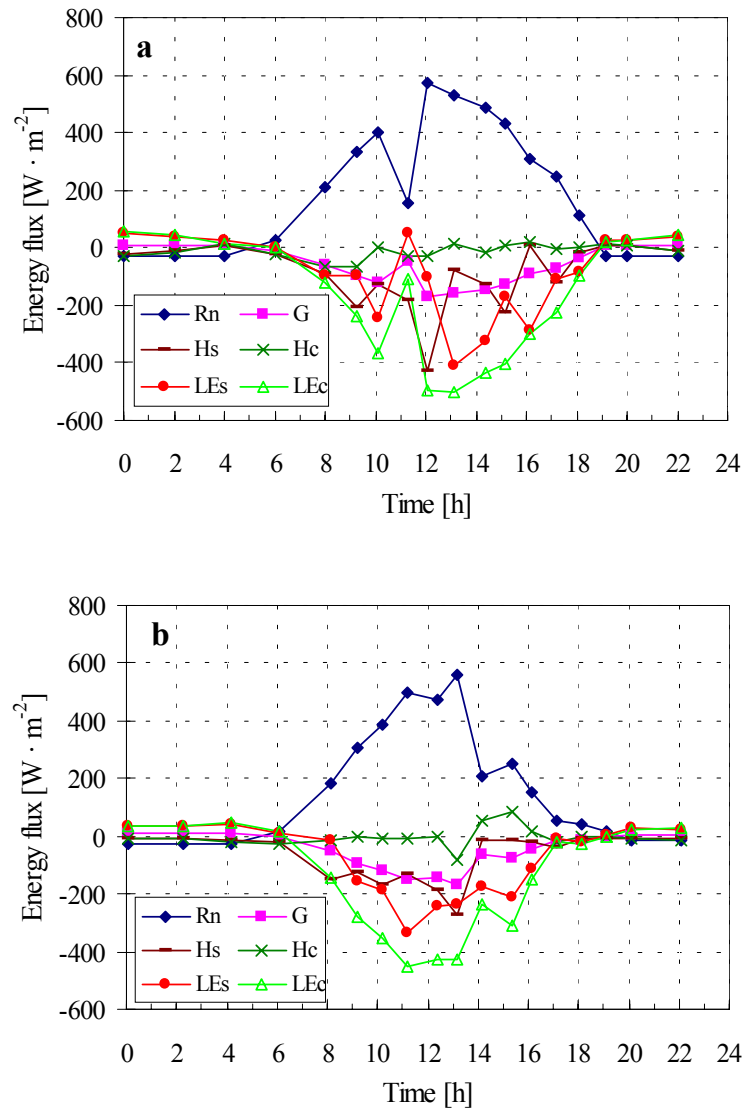


Fig. 37. Daily courses of heat balance components: R_n – net radiation, G – heat flux in the soil, H_s and H_c – sensible heat fluxes from stressed and nonstressed lysimeters, LE_{s+} and LE_c – latent heat fluxes (*a* – 28.07.94. *b* – 02.08.94)

The intensity of evapotranspiration, expressed by the latent heat flux differed significantly for lysimeters with varying soil water conditions. During afternoon hours differences between LE_c and LE_s fluxes reached 200 W m^{-2} . At the same time, it was stated, that rapid changes of the net radiation flux resulted in violent changes of the latent heat flux.

6.5. Comparison of potential evapotranspiration calculated with various methods with actual evapotranspiration any limitation of soil water availability

To analyze the courses of potential and actual evapotranspiration of the studied objects, they were derived using chosen methods. Some examples of twenty-four hours courses of evapotranspiration are presented in Fig. 38. The occurrence of differences of instantaneous values of potential evapotranspiration, derived by three methods, was stated, with exception of night hours and some moments of low intensity of solar radiation, what can be noticed clearly in Fig. 38a at 11 a.m. From the used methods, this based on the Penman equation (67) gave the highest values, especially for the hours with high intensity of solar radiation. Potential evapotranspiration values calculated with two other methods did not differ considerably.

The way of calculation of the aerodynamic diffusive resistance influenced to some extent its values and therefore the obtained values of actual evapotranspiration. The use of the method based on semiempirical equations (81-91) resulted in obtaining lower instantaneous values of actual evapotranspiration for lysimeters with comfort and stress water conditions than corresponding values obtained with the use of Jackson's method (equations 92-95). The comparison of twenty-four hours courses of actual evapotranspiration obtained with both methods at the background of potential evapotranspiration courses is presented in Fig. 39.

It can be stated by analyzing twenty-four hour courses of potential evapotranspiration calculated with various methods and actual evapotranspiration with aerodynamic resistance calculated from equation (81-91), that hourly values of actual evapotranspiration in lysimeters with comfort water conditions were nearest the values obtained by Penman-Monteith and Kimberly-Penman's methods, and for lysimeters with stress water conditions they were considerably lower.

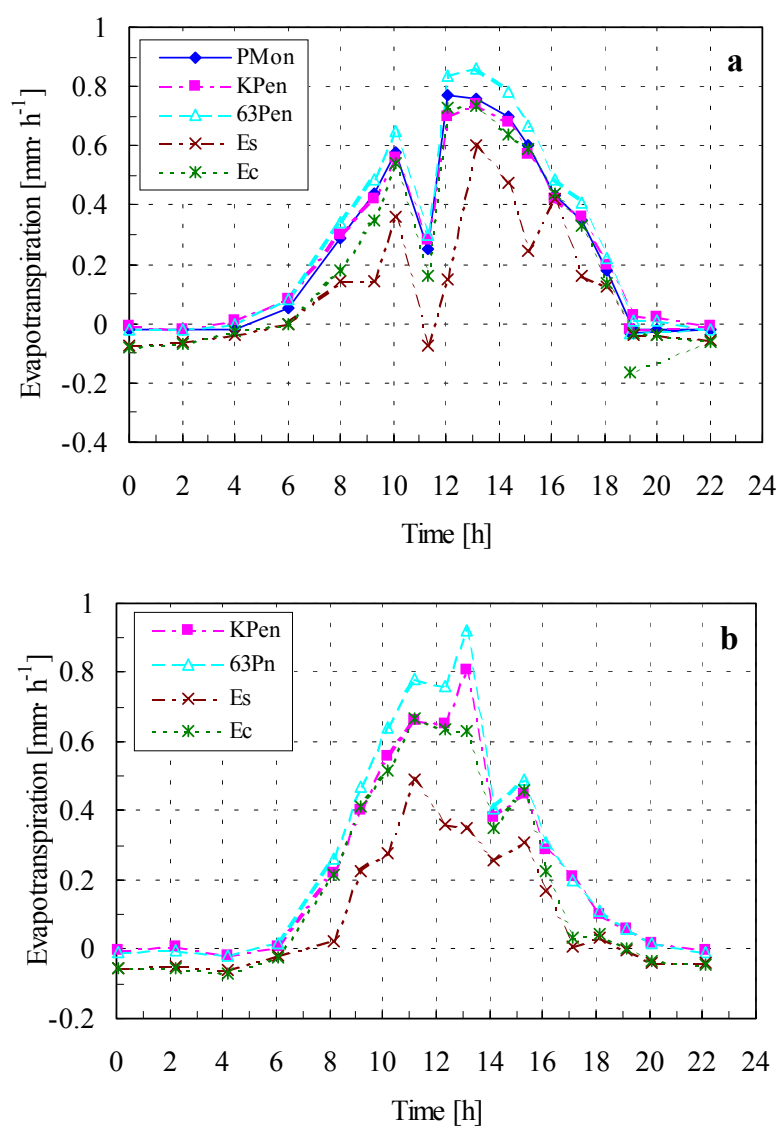


Fig. 38. Daily courses of potential and actual evapotranspiration calculated with different methods (a– 28.07.94, b – 02.08.94): PMon – Penman-Monteith method, KPen – Kimberly-Penman method, 63Pn – 1963 Penman equation, E_s – actual evapotranspiration (water stress), E_c – actual evapotranspiration (water comfort)

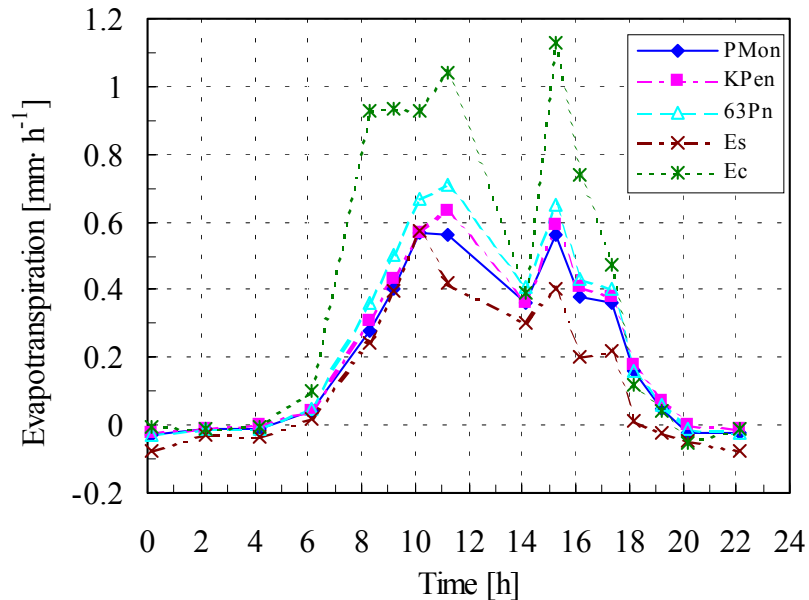


Fig. 39. Comparison of actual evapotranspiration calculated with Jackson method and potential evapotranspiration calculated with different methods for a pair lysimeters with organic soil: PMon – Penman-Monteith method, KPen – Kimberly-Penman method, 63Pn – 1963 Penman equation, Es – actual evapotranspiration (water stress), Ec – actual evapotranspiration (water comfort)

The instantaneous values of actual evapotranspiration with aerodynamic resistance calculated by Jackson's method for lysimeters with comfort water conditions, presented in Fig. 39, are much higher for hours of intensive solar radiation than potential evapotranspiration values calculated with each of three chosen methods. It can speak for necessity of correction of empirical coefficients for Polish conditions for possible future application of this method.

Figure 39 presents day and night values of actual evapotranspiration for lysimeters with unlimited availability of soil water, weight losses of water from lysimeters and twenty four hour values of potential evapotranspiration calculated with Penman-Monteith's method for chosen measuring days. The actual evapotranspiration, which was calculated with the use of formulas for aerodynamic resistance (81-91) for organic soil was for most days a little bit higher than for mineral soil. Day and night values of potential evapotranspiration for most measuring days were close to the actual evapotranspiration from

lysimeters with organic soil. It also results from this figure that weight losses of water from lysimeters were up to 25% higher from the potential evapotranspiration calculated from Penman-Monteith formula and from the actual evapotranspiration for lysimeters with comfort soil water conditions.

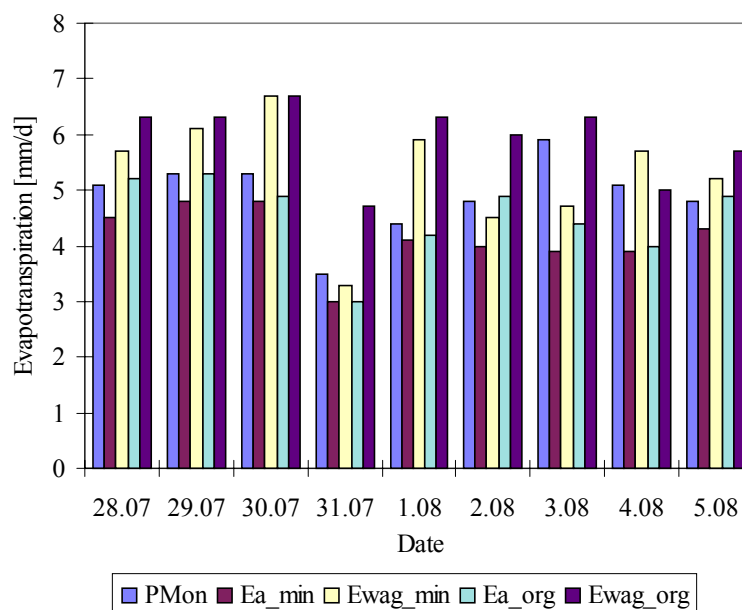


Fig. 40. Comparison of daily values of actual evapotranspiration for lysimeters with unlimited soil water (Ea_min – mineral soil, Ea_org – organic soil), weighed lost of water from lysimeter (Ewag_min – mineral soil, Ewag_org – organic soil) and daily values of potential evapotranspiration calculated with Penman-Monteith (Pmon) for several chosen measuring days

A plot comparing day and night values of actual evapotranspiration in lysimeters with limited availability of soil water with water losses from lysimeters for both soils and the same measuring days is presented in Fig. 41. The actual evapotranspiration in conditions of limited availability of soil water was higher for the organic soil than for the mineral soil. In the mineral soil after complete removing of gravitational water the slowing down of evapotranspiration process occurred earlier than in case of the organic soil. In the final stage of the drying cycle, the difference of actual evapotranspiration between lysimeters with mineral and organic soils exceeded 200%.

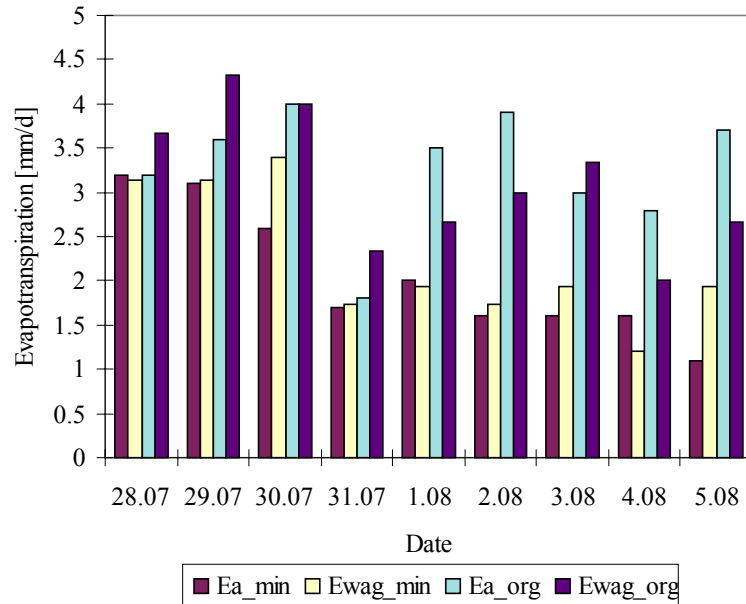


Fig. 41. Comparison of daily values of actual evapotranspiration in lysimeters with limited soil water (Ea_min – mineral soil, Ea_org – organic soil) with daily weighed lost of water from lysimeter (Ewag_min – mineral soil, Ewag_org – organic soil)

It was noticed, when comparing the weight loses of water from lysimeters with gravitational water carried away with daily values of actual evapotranspiration, that both for mineral and organic soils the weight loses for some days were higher and for the others lower than the values of actual evapotranspiration, which was not stated in case of lysimeters with comfort water conditions.

6.6. Determination of crop water stress index CWSI on the base of radiation temperature of plant cover as well as actual and potential evapotranspiration

Determined instantaneous and daily values of actual and potential evapotranspiration were the base for calculation of the crop water stress index CWSI. This index was calculated for the hours of high solar radiation, when the maximum differences of actual evapotranspiration for lysimeters with varying soil water content were stated.

On the base of equation (96), which assumes a linear relation between the temperature difference: air – evaporating crop surface and the water vapour pressure deficit, a linear regression of this relation was derived, separately for measuring values for lysimeters of stress and comfort water availability conditions (look at Fig. 42). The measuring data considered in this analysis concerned measurements conducted under net radiation values exceeding 500 W m^{-2} .

High dispersion of measuring data for the lysimeters with stress water conditions was noticed ($R^2=0.10$) as compared with the data for the lysimeters with comfort soil water conditions ($R^2=0.75$). Basing on eq. (98), the upper limit of the crop-air temperature difference was found, representing the complete restrain of evapotranspiration ($r_c \rightarrow \infty$) and from eq. (99), the lower limit of this difference, which corresponds to the case of wet plants acting as free water surface ($r_c=0$). The regression line obtained for plants growing in conditions of unlimited availability of the soil water had parameters nearing the line corresponding to the lower limit of $T_c - T_a$. The regression line for plants being in water stress had parameters close to the line appointing the upper limit. Upper and lower limits of $T_c - T_a$ in Fig. 42 were derived for the net radiation of 500 W/m^2 the turbulent aerodynamic resistance 90 s m^{-1} for stressed plant cover and 68 s m^{-1} for plants in comfortable water conditions and for the air temperature 30°C .

The courses of CWSI for hours of intensive radiation and the courses of the crop surface temperature during the twenty-four hours for a pair of lysimeters are presented in Fig. 43. The CWSI was calculated from equation (97). The potential evapotranspiration was calculated from Penman-Monteith formula and actual evapotranspiration from the heat balance equation with aerodynamic resistance, which was calculated according to formulas (81-91). Considerable differences of CWSI were noticed in particular pairs of lysimeters. In conditions of plant water comfort the CWSI did not exceed 0.3, whereas for conditions of limited availability of soil water it changed from 0.3 to 1.0, what confirmed high differentiation of the evapotranspiration intensity for both lysimeters of particular pairs.

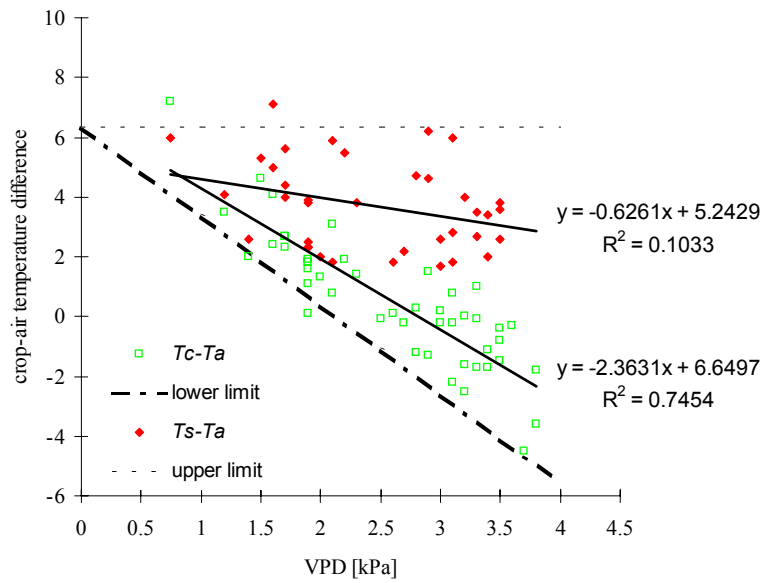


Fig 41. Relation between the difference of crop surface temperature – air temperature and water vapour deficit in the air

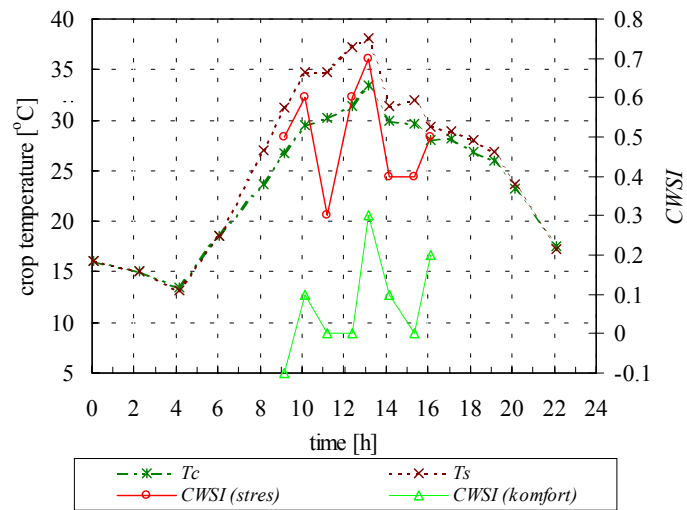


Fig. 43. Changes of CWSI during a day for plants in water stress ($CWSI_s$) and in water comfort conditions ($CWSI_k$) with the courses radiation temperature T_s and T_c

Evapotranspiration intensity is mainly determined by availability of soil water for the rooting system of plants. In particular elements of the soil-plant-atmosphere system high gradients of the water potential exist, enforcing the water movement from soil through plants into atmosphere. The water vapour potential in atmosphere under the relative air humidity of let's say 50%, in air temperature of 20°C is as high as -94.1 MPa. In case of high values of the water vapour pressure deficit in the subsurface layer of atmosphere, the differences of the soil water potential lead to differentiation of the plant water potential and consequently to differentiation of the evapotranspiration intensity.

In Fig. 44 the differentiation of the plant water potential is presented for succeeding measuring days within one pair of lysimeters as well as the averaged daily values of CWSI for this pair. High differences of the plant water potential were observed between lysimeters with varying availability of soil water. In case of plants growing in comfort water conditions, the plant water potential, measured for the hours of the highest intensity of transpiration, maximally reached the value of -3 MPa. However, in conditions of plant water stress, the plant water potential achieved values up to -4.5 MPa. The daily values of CWSI calculated for the same pair of lysimeters for all days achieve higher values in case of stress soil water conditions. It was also stated that CWSI is sensitive to changes of the plant water potential.

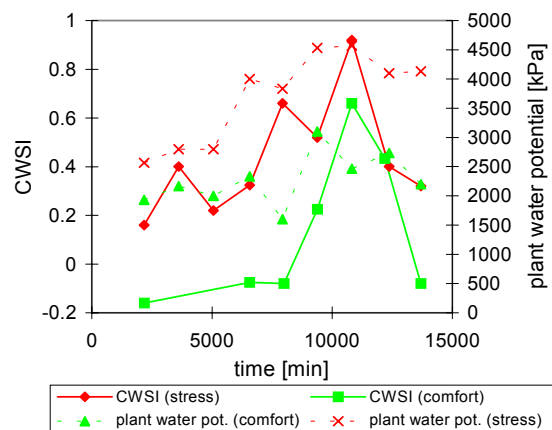


Fig. 44. Changes of plant water potential for succeeding measuring days and respective changes of daily values of CWSI for plants in stress and water comfort

7. SUMMARY

The measurement of radiation temperature as an indicator of the plant water stress and a parameter required for evaluation of the actual evapotranspiration should fulfill the following conditions:

- it should be conducted in such external conditions that they did not limit, except from the soil water conditions, the intensity of transpiration, which is responsible for a distinct temperature effect. Factors not connected with soil, which limit the intensity of transpiration are: high relative air humidity, low air temperature, temporary plant cover temperature below the dew point temperature.
- it should be performed under near to complete cover of soil with plants to eliminate the impact of the radiation temperature of bare soil on averaged temperature of the studied object. The soil temperature is influenced by thermal inertia, which depends on the soil water content and the dynamics of temperature, whereas the plant temperature, according to the assumption, by the intensity of transpiration.
- to eliminate maximally the action of other factors, influencing the measurement of the radiation temperature and to increase the precision of measurement, a method of differences derivation should be applied, *i.e.* the differences between investigated plots and a plot being in comfort soil water conditions should be determined under the same meteorological conditions.

The difference between the radiation temperature of the studied plant cover and the reference plant cover temperature (a plot with comfort soil water conditions), is a good indicator of plant water stress, determined by the soil water potential, as a physical factor which decides of water availability for plants.

The temperature difference in reference to water comfort conditions increases when the soil water potential exceeds pF 3.7 (about 5 bars), what corresponds to the range of water not easily available for plants, reaching its maximum values under pF 4.2 (about 15 bars), what corresponds to the permanent wilting point. This conclusion refers to all variants of experiment.

The measurement of the radiation temperature difference (a studied object – object with comfort water conditions) cannot be used in the whole range of the water content for determination of water stored in soil. It is used to determine a very important from physical point of view value of the soil water content, corresponding to the soil water potential of pF 3.7, under which the limitation of water availability occurs. The soil water content values, corresponding to this

potential of soil water are characteristic for particular soils (for mineral soil it is about 10% and for organic soil about 40%).

The courses of the radiation temperature difference (a studied object – an object with comfort water conditions) in relation to the soil water content and the soil water potential in laboratory and field experiments in two different spectral ranges (3.5-5 μm i 8-13 μm) have an identical character. The longwave infrared range is recommended in field experiments due to the lack of disturbances caused by direct and dispersed solar radiation, which occur in shortwave range.

The altitude of observed radiation temperature difference (a studied object – an object with comfort water conditions) depends on the conditions during the conducted experiment. Higher temperature differences were stated in the field lysimetric experiment. Under inhibition of availability of soil water the differences of 2°C occurred and in conditions of complete unavailability of soil water they increased to about 7°C.

The radiation temperature can be used in the study of the plant water stress from various levels, including airborne and satellite ones, and the measurements should be performed in favourable meteorological conditions. It is recommended to use the temperature difference between the studied area and the area with comfort soil water conditions, treated as a reference plot situated in the area of the thermal imagery in close neighbourhood of natural water-courses or water reservoirs. The stated radiation temperature difference (a studied object – object with comfort water conditions) for grass cultures, achieving values above 2°C (results of field experiment), can indicate the occurrence of water stress.

Performed verification of two variants of the heat balance method of actual evapotranspiration determination, varying with the way of calculation of the aerodynamic resistance for heat transport and using the radiation temperature of plant cover as an input parameter, proved their usefulness in determination of daily and hourly values of evapotranspiration under varying availability of soil water.

Obtained actual evapotranspiration values depend on the way of calculation the diffusive aerodynamic resistance. The use of the method based on semiempirical equations of the transport of water vapour and heat in the subsurface layer of atmosphere resulted in obtaining lower instantaneous values of actual evapotranspiration for lysimeters with comfort and stress water conditions than corresponding values obtained with the use of Jackson's method.

The instantaneous values of actual evapotranspiration with aerodynamic resistance calculated by Jackson's method for lysimeters with comfort water

conditions are much higher for hours of intensive solar radiation than potential evapotranspiration values calculated with use of each of three chosen methods and from water weight losses from lysimeters. It can speak for necessity of correction of empirical coefficients for Polish conditions for possible future application of this method.

The daily values of potential evapotranspiration calculated with various methods show significant differences. The actual evapotranspiration values with the aerodynamic resistance calculated from semiempirical theory of water vapour and heat transport in the subsurface layer of the atmosphere (equations 44-51) for lysimeters with unlimited availability of soil water are nearest the corresponding values of potential evapotranspiration calculated from Penman-Monteith and Kimberly-Penman methods.

For hours of intensive solar radiation, the sensible heat flux for lysimeters with comfort water conditions shows high stability. Its values oscillated around zero $W m^{-2}$ and its sign underwent changes. However, in case of lysimeters with stress water conditions, the sensible heat flux achieves negative values as result of the thermal energy transfer from the evaporating surface to the atmosphere. Values of this heat flux changed considerably during the daily hours.

Combination of the potential evapotranspiration with the actual evapotranspiration, calculated with the use of radiation temperature of plant cover enables to determine the deepness of the plant water stress by application of the crop water stress index (CWSI). In comfort plant water conditions, the CWSI did not exceed 0.3, whereas for the conditions of limited availability of soil water it changed from 0.3 to 1.0.

It was also stated that the CWSI is sensitive to changes of the water potential in plants.

8. REFERENCES

1. **Adamczyk B., Aramowicz B., Gołaszewska K., Olech T.,** Modelowanie procesów dyfuzyjnych w ośrodkach porowatych. *Rocz. Nauk Roln.*, 73-C-4.,175-185, 1978.
2. **Adamenko W.N.,** Wlianieje melioratiwnych wozdiejstwij na tiepłofiziceskije swojstwa i tiepłowej režim poczwuy. *Trudy GGO*, 288, 83–91, 1972.
3. **AGEMA Infrared Systems-**materiały szkoleniowe.
4. **Allen R.G., Jensen M.E., Wright J.L., Burman R.D.,** Operational estimates of reference evapotranspiration. *Agron. J.*, 81, 650-662, 1989.
5. **Allen R.G., Pruitt W.O.,** FAO-24 Reference evapotranspiration factors. *J. of Irrig. Drain. Eng.*, 117, 5, 1991.
6. **Aston A.R., van Bavel C.H.M.,** Soil surface water depletion and leaf temperature. *Agron. J.*, 64, 368-373, 1972.
7. **Axelsson S., Lunden B.,** Experimental results in soil moisture mapping using IR thermography. *ITC Journal*, 1, 43-49, 1986.
8. **Baranowski P., Mazurek W., Walczak R.T.,** Ocena warunków termicznych w uprawie pod osłonami z wykorzystaniem termowizji. *Zesz. Probl. Post. Nauk Roln.* , 429, 37-41, 1996.
9. **Baranowski P., Mazurek W., Walczak R.T.,** Uzyskiwanie, analiza i interpretacja obrazów termalnych. *Materiały VI Letniej Szkoły "Fizyka z elementami agrofizyki"*, Lublin 26-27 września, 127-141, 1994.
10. **Baranowski P., Mazurek W., Walczak R.T.,** Weryfikacja modeli wyliczania ewapotranspiracji w badaniach lizymetrycznych z zastosowaniem pomiaru temperatury radiacyjnej. *Materiały III Ogólnopolskiej Konferencji Termografii i Termometrii w Podczerniewi, Warszawa 27-29 listopada*, 219-224, 1996.
11. **Baranowski P., Mazurek W., Walczak R.T.,** Wykorzystanie techniki zobrazowań termalnych w badaniach rolniczych. *Acta Agrophysica*, 72, 7-14, 2002.
12. **Baranowski P., Mazurek W., Walczak R.T.,** Zastosowanie pomiaru temperatury powierzchni ładu do określania strumienia ciepła jawnego przy zróżnicowanej dostępności glebowej. *Acta Agrophysica*, 34, 9-18, 2000.
13. **Baranowski P., Mazurek W., Walczak R.T.,** Zastosowanie termografii do badania stresu wodnego roślin i ewapotranspiracji rzeczywistej. *Monografia. Acta Agrophysica*, 21, 1999.
14. **Baranowski P., Walczak R.T., Witkowska-Walczak B.,** Rola parametrów struktury gleby w modelach plonowania roślin. *Materiały VIII Szkoły "Fizyka z elementami agrofizyki"*, Lublin 19-20 września, 17-38, 1996.
15. **Baranowski P., Walczak R.T., Witkowska-Walczak B.,** Submodele fizycznych procesów systemu gleba-roślina-atmosfera w modelach plonowania roślin. *Materiały VIII Szkoły "Fizyka z elementami agrofizyki"*, Lublin 19-20 września, 39-50, 1996.
16. **Bartholic J.F., Namken L.N., Wiegand C.L.,** Aerial thermal scanner to determine temperatures of soils and of crop canopies differing in water stress. *Agron. J.*, 64, 603-608, 1972.
17. **Batchelor C.H.,** The accuracy of evapotranspiration estimates with the FAO modified Penman equation. *Irrig. Sci.*, 5, 223-233, 1984.

18. **Ben-Asher J., Phene C.J., Kinarti A.**, Canopy temperature to assess daily evapotranspiration and management of high frequency drop irrigation systems. *Agric. Water Manag.*, 22, 379-390, 1992.
19. **Bowen I.S.**, The ratio of heat losses by conduction and by evaporation from any water surface. *Phys. Rev.*, 27, 779-787, 1926.
20. **Brown K.W.**, Calculation of evapotranspiration from crop surface temperature. *Agric. Meteorol.* 14, 199-209, 1974.
21. **Brutseart W.**, Evaporation into the atmosphere. Kulwer Academic Publishers. 1982,
22. **Businger J.A., Wyngaard J.C, Izumi Y., Bradley E.F.**, Flux profile relationships in the atmospheric surface layer. *J. Atmos. Sci.* 28, 181-189, 1971.
23. **Businger J.A.**, Some remarks on Penman's equation for the evapotranspiration. *Neth. J. Agri. Sci.* 4, 77-80, 1956.
24. **Caselles V., Delegido J.**, A simple model to estimate the daily value of the regional maximum evapotranspiration from satellite temperature and albedo images. *Int. J. Remote Sensing*, 8, 1151-1162, 1987.
25. **Choudchury B.J., Idso S.B.**, An empirical model for stomatal resistance of wheat. *Agric. Forest Meteorol.* 30, 56-59, 1985.
26. **Choudchury B.J.**, Simulating the effects of weather variables and soil water potential on a corn canopy temperature. *Agric. Meteorol.* 29, 169-182, 1983.
27. **Choudhury B.J., Idso S.B.**, Simulating sunflower canopy temperatures to infer root-zone soil water potential. *Agric. Forest Meteorol.*, 31, 69-78, 1984.
28. **Clawson K.L. and Blad B.L.**, Infrared thermometry for scheduling irrigation of corn. *Agron. J.* 74, 311-316, 1982.
29. **Clawson K.L., Jackson R.D., Pinter P.J.**, Evaluating plant water stress with canopy temperature differences. *Agron. J.*, 81, 858-863, 1989.
30. **Czudnowski A.F, Miczurin B.N., Mielnikowa M.K., Moszkow B.S., Pojasow N.P., Wierszynin P.W.**, Podstawy Agrofizyki, PWRiL Warszawa, 1967.
31. **Czudnowski A.F.**, Tiejlofizyckije charakteristiki dispiersnych materialow. Gos. Izd. Fiz. Mat. Lit., Moskwa, 1962.
32. **Dąbrowska-Zielińska K.**, Określenie ewapotranspiracji i wilgotności gleb w strefie korzeniowej roślin metodami teledetekcyjnymi. *Prace Inst. Geod. i Kartogr.* 36, 1-2, 1989.
33. **Dąbrowska-Zielińska K.**, Szacowanie ewapotranspiracji, wilgotności gleb i masy zielonej łąk na podstawie zdjęć satelitarnych NOAA. *Prace Geograficzne IGI PAN*, 165, 1995.
34. **Dąbrowska-Zielińska K.**, Wykorzystanie zdjęć satelitarnych NOAA do oszacowania ewapotranspiracji i wilgotności gleb. *Przeg. Geofiz.* 36, 309-320, 1991.
35. **Davies J.A., Allen C.D.**, Equilibrium, potential and actual evaporation from cropped surfaces in southern Ontario. *J. Appl. Meteorol.* 12, 649-657, 1973.
36. **de Vries D.A.**, A critical analysis of the calorimetric method for determining the heat flux in soils. *Proc. 8-th Int. Heat Transfer Conf. Hemiphen Publ. Corp., Washington*, 2, 473-476, 1986,
37. **de Vries D.A.**, Heat transfer in soils. In *Heat and mass transfer in the biosphere*. de Vries, D.A. and N.A. Afgan (ed.). Washington. 6-28, 1975.
38. **de Vries D.A.**, The theory of heat and moisture transfer in porous media revisited. *Int. J. Heat Mass Transfer*, 30, 7, 1343-1350, 1987.
39. **de Vries D.A.**, Thermal properties of soils. In W.R. van Wijk (ed.) *Physics of plant environment*. North-Holland, Amsterdam, 210-235, 1963.

40. **Doorenbos J., Pruitt W.O.**, Guidelines for predicting crop water requirements. Irrigation and Drainage Paper 24, Food and Agriculture Organization of the United Nations, Rome, 156 p. 1977.
41. **Doorenbos J., Pruitt W.O.**, Guidelines for predicting crop water requirements. Irrigation and Drainage Paper 24, Food and Agriculture Organization of the United Nations, Rome, 179, 1975.
42. **Duchesne J.**, Detection par radiothermometrie d'une attaque de pietin-verse sur cereale. ENSA de Rennes. Chaire de Génie Rural, Hydraulique et Climatologie Agricoles. Rapport 1987.
43. **Eadie W.T., Drijard D., James F.E., Roos M., Sadoulet B.**, Metody statystyczne w fizyce doświadczalnej. PWN. W-wa, 63–64, 1989.
44. **Ehrler W.L.**, Cotton leaf temperatures as related to soil water depletion and meteorological factors. *Agron. J.* 65, 404-409, 1973.
45. **Feddes, R.A.**, Water, heat and crop growth. *Meded. Landbouwhogeschool, Wageningen*, 71, 12, 1971,
46. **Frevert D.K., Hill R.W., Braaten B.C.**, Estimation of FAO evapotranspiration coefficients. *J. Irrig. Drain. Eng.*, 109, 2, 1983.
47. **Fusch M. and Tanner C.B.**, Infrared thermometry of vegetation. *Agron. J.*, 5, 597-601, 1966.
48. **Fusch M.**, Infrared measurement of canopy temperature and detection of plant water stress. *Theor. Appl. Climatol.* 42, 253-261, 1990.
49. **Gates D.M., Tantraporn W.**, The reflectivity of deciduous trees and herbaceous plants in the infrared to 25 microns. *Science*, 115, 613-616, 1952.
50. **Gliński J., Lipiec J.**, Soil physical conditions and plant roots. CRC Press, Boca Raton, FL, 1990.
51. **Gliński J., Stępniewski W.**, Soil aeration and its role for plants. CRC Press Inc., Boca Raton, FL, 1985.
52. **Globus A.M., Arefiew A.W.**, O niektórych zależnościach między gidrofizycznymi i ciepłofizycznymi charakterystykami poczw. *Sb. Trudow. Po Agron. Fiz.* 32, 127–136, 1971.
53. **Góźdź A.**, Modelowanie w fizyce. Skrypt X Szkoły „Fizyka z elementami agrofizyki. Instytut Agrofizyki PAN, 18–19 września 1997, Lublin, 23–29, 1997.
54. **Gupało A.I.**, Tęploty i jego własności poczw w zależności od wilgotności i gęstości. *Poczvov.*, 4, 40–45, 1959.
55. **Hadas A.**, Heat transfer in dry aggregated soil. I. Heat conduction. *Soil Sci. Soc Am. J.*, 41, 1055–1059, 1977.
56. **Hadas A.**, Simultaneous flow of water and heat under periodic heat fluctuations. *Soil Sci. Soc Am. Proc.* 32, 297–301, 1968.
57. **Hajnos M., Sokółowska Z., Alekseev A., Alekseeva T.**, Mechaniczne właściwości materiałów rolniczych. *Mat. Konf. Nauk. LTN –IA PAN* (ed. J. Gliński, R. Dębicki, K. Konstankiewicz), Lublin, 1997.
58. **Halim R.A., Buxton D.R., Hattendorf M.J. and Carlson R.E.**, Crop water stress index and forage quality relationships in alfalfa. *Agron. J.*, 82, 906-909, 1990.
59. **Halim R.A., Buxton D.R., Hattendorf M.J., Carlson R.E.**, Water-deficit effects on alfalfa at various growth stages. *Agron. J.*, 81, 765-770, 1989.
60. **Hanks R.J., Ashcroft G.L.**, *Applied Soil Physics*. Springer-Verlag, Berlin-Heidelberg, 1980.
61. **Hargreaves G.L., Hargreaves G.H., Riley J.P.**, Agricultural benefits for Senegal River Basin. *J. Irrig. Drain. Eng.*, ASCE, 111, 113-124, 1985.

62. **Hatfield J.L.**, Canopy temperatures, The usefulness and reliability of remote measurements. *Agron. J.*, 67, 889-897, 1979.
63. **Hatfield J.L.**, Wheat canopy resistance determined by energy balance techniques. *Agron. J.*, 77, 279-283, 1985.
64. **Hattendorf M.J., Evans D.W., Peaden R.N.**, Canopy temperature and stomatal conductance of water-stressed dormant and nondormant alfalfa types. *Agron. J.*, 82, 873-877, 1990.
65. **Heilman J.L., Heilman W.E., Moore D.G.**, Remote sensing of canopy temperature at incomplete cover. *Agron. J.*, 73, 403-406, 1981.
66. **Heilman J.L., Kanemasu E.T., Rosenberg N.J., Blad B.L.**, Thermal scanner measurement of canopy temperature to estimate evapotranspiration. *Remote Sens. Environ.*, 5, 137-145, 1976.
67. **Hillel D.**, Soil temperature and heat flow. In *Fundamentals of soil physics*, Chapt.12, Academic Press, INC, New York, 287-317, 1980.
68. **Idso S.B., Jackson R.D., Pinter P.J. Jr., Reginato R.J., Hatfield J.L.**, Normalizing the stress-degree-day parameter for environmental variability. *Agric. Meteorol.*, 24, 45-55, 1981.
69. **International Agrophysics**. Vol. 7, No. 2-3, 1993.
70. **Jackson R.D., Idso S.B., Reginato R.J., Pinter P.J.**, Canopy temperature as a crop water stress indicator. *Water Resour. Res.*, 17, 4, 1133-1138, 1981.
71. **Jackson R.D., Moran M.S., Gay L.W., Raymond L.E.**, Evaluating evaporation from field crops using airborne radiometry and ground based meteorological data. *Irrig. Sci.* 8, 324-332, 1987.
72. **Jackson R.D., Pinter P.J., Reginato R.J.**, Net radiation calculated from remote multispectral and ground station meteorological data. *Agric. Forest Meteorol.*, 35, 153-164, 1985.
73. **Jackson R.D., Reginato R.J., Idso S.B.**, Wheat canopy temperature, a practical tool for evaluating water requirements. *Water Resour. Res.* 13, 651-657, 1977.
74. **Jackson R.D.**, Canopy temperature and crop water stress. *Adv. Irrig.*, 1, 43-85, 1982.
75. **Jackson R.D.**, Estimating areal evapotranspiration by combining remote and ground-based data. *Remote Sensing Applications for Consumptive Use (Evapotranspiration)*. AWRA Monograph Series, 6, 13-25, 1986.
76. **Jalali-Farahani H.R., Slack D.C., Kopec D.M. and Matthias A.D.**, Crop water stress index models for bermudagrass turf, a comparison. *Agron. J.*, 85, 1210-1217, 1993.
77. **Jiang L., and S. Islam**, Estimation of surface evaporation map over southern great plains using remote sensing data. *Water Resour. Res.*, 37, 329-340, 2001.
78. **Kasubuchi T.**, The effect of soil moisture on thermal properties in some typical Japanese upland soils. *J. Soil Sci. Plant Nurt.*, 21, 107-112, 1975.
79. **Kędziora A., Ciesielski R.**, Przydatność uproszczonej metody Penmana do określania ewapotranspiracji potencjalnej w zastosowaniu do sterowania nawodnieniami. *Rocz. AR Poznań*, 149, 20-31, 1984.
80. **Kędziora A., Kapuściński J., Moczko J., Olejnik J., Karliński M.**, Struktura bilansu cieplnego pola lucerny. *Rocz. AR Pozn.* 201, Melioracje 8, Mat. Sesji „Mikroklimat i parowanie terenowe”, 31-39, 1989.
81. **Kędziora A., Olejnik J., Kapuściński J.**, Impact of landscape structure on heat and water balance. *Ecology Int. Bull.*, USA, 17, 1-17, 1989.
82. **Kędziora A.**, Micrometeorological and remote sensing methods used in environmental investigation. *Zesz. Probl. Post. Nauk Roln.*, 405, 101-114, 1994.
83. **Kędziora A.**, *Podstawy agrometeorologii*. PWRiL, Poznań, 1995.

84. **Kersten M.S.**, Thermal properties of soils. Bull. 28, University of Minnesota. Inst. Technology, Engineering Experiment Station, 52, 21, 1949.
85. **Kimball B.A., Jackson R.D., Nakayama F.S., Idso S.B., Reginato R.J.**, Soil-heat flux determination, Temperature gradient method with computed thermal conductivities. Soil Sci. Soc. Am. J., 40, 25–28, 1976a.
86. **Kimball B.A., Jackson R.D., Reginato R.J., Nakayama F.S., Idso S.B.**, Comparison of field-measured and calculated soil-heat fluxes. Soil Sci. Soc. Am. J., 40, 18–25, 1976.
87. **Kimes D.S.**, Remote sensing of row crop structure and component temperature using directional radiometric temperatures and inversion techniques. Remote Sens. Environ., 13, 33–55, 1983.
88. **Kohnke H., Nakshabandi A.G.**, Heat transfer in soils. 8-th Int. Congress of Soil Science, Bucharest, 183–193, 1964.
89. **Kossowski J.**, Charakterystyka cieplnych właściwości warstwy ornej gleby pola doświadczalnego Felin. Raport z tematu MR II. 08,02,8, Badanie stosunków cieplnych środowiska glebowego. (Maszynopis w IA PAN, Lublin), 1977.
90. **Kustas W.P., Choudhury B.J., Inoue Y., Pinter P.J., Moran M.S., Jackson R.D., Reginato R.J.**, Ground and aircraft infrared observations over a partially-vegetated area. Int. J. Remote Sensing, 11, 3, 409–427, 1990.
91. **Łabędzki L.**, Evaluating crop water stress using infrared thermometry. Zesz. Probl. Post. Nauk Roln., 419, 69–73, 1995.
92. **Łabędzki L.**, Potrzeby nawadniania użytków zielonych - uwarunkowania przyrodnicze i prognozowanie. Wydawnictwo IMUZ, Falenty, 1997.
93. **Lang C.**, Uber Warmecapacitat der Bodenconstituenten. Forsch. Gebiete Agr. – Phys., 1, 109–145, 1878.
94. **Lipiec J.**, Stan fizyczny gleby i jego wpływ na wzrost i funkcjonowanie korzeni roślin. Wybrane metody badań. X Szkoła „Fizyka z elementami Agrofizyki” nt. „Fizyczne właściwości gleby a rozwój roślin - metody badawcze”, Lublin, 22–23 września 1998.
95. **Lipiec J., Hakansson J., Tarkiewicz S., Kossowski J.**, Soil physical properties and growth of spring barley related to the degree of compactness. Soil Till. Res., 19, 307–317, 1991.
96. **Luchiari A., Jr. and Riha S.J.**, Bulk surface resistance and its effect on evapotranspiration rates in irrigated wheat. Agron. J., 83, 888–895, 1991.
97. **Łukomska I., Rudowski G.**, Wpływ różnych warunków na temperaturę roślin. Biuletyn WAT, Warszawa, 1979.
98. **Malicki M.A., Mazurek W.**, Thermoelectrical thermometer for remote recording of the temperature in the soil profile. Zesz. Probl. Post. Nauk Roln., 281, 139–145, 1982.
99. **Malicki M.A.**, Reflectometric (TDR) meter of moisture content in soils and other capillary-porous materials. Zesz. Probl. Post. Nauk Roln., 388, 107–114, 1987.
100. **Mateos L., Smith R.C.G., Sides R.**, The effect of soil surface temperature on the crop water stress index. Irrig. Sci., 12, 37–43, 1991.
101. **Mazurek W., Walczak R.T., Sobczuk H.A., Baranowski P.**, The model investigation of soil water content and soil water potential impact on radiation temperature of meadow plant cover. Zesz. Probl. Post. Nauk Roln., 436, 93–100, 1996.
102. **Mazurek W., Baranowski P., Walczak R.T., Sobczuk H.**, Zastosowanie pomiaru temperatury radiacyjnej do oceny stresu wodnego roślinności łąkowej. Doświadczenie wazonowe. Materiały III Ogólnopolskiej Konferencji Termografii i Termometrii w Podczerniewi, Warszawa 27–29 listopada, 225–229, 1996.

103. **Mazurek W.**, Temperatura radiacyjna jako wskaźnik stresu wodnego roślin. Praca doktorska wykonana w IA PAN, Lublin, 1998.
104. **Millard J.P., Jackson R.D., Goettelman R.C., Reginato R.J.**, Crop water-stress assesment using an airborne thermal scanner. *Photog. Eng. Remote Sens.*, 44, 77-85, 1978.
105. **Miller E.C., Saunders A.R.**, Some observation on the temperature of the leaves of crop plants. *J. Agric. Res.*, 26, 15-43, 1923.
106. **Molga M.M.**, Meteorologia rolnicza. PWRiL, Warszawa, 1986.
107. **Monteith J.L., Szeicz G., Waggoner P.E.**, Measurement and control of stomatal resistance in the field. *J. Appl. Ecol.*, 2, 345-355, 1965.
108. **Monteith J.L., Szeicz G.**, Radiative temperature in the heat balance of natural surfaces. *Q. J. R. Meteorol. Soc.*, 88, 496-507, 1962.
109. **Monteith J.L.**, Evaporation and surface temperature. *Q. J. R. Meteorol. Soc.*, 107, 1-27, 1981,
110. **Nakayama F.S., Bucks D.A.**, Crop water stress index, soil water, and rubber yield relations for the Guayule plant. *Agron. J.*, 76, 791-794, 1983.
111. **Nielsen D.C., Clawson K.L., Blad B.L.**, Effect of solar azimuth and infrared thermometer view direction on measured soybean canopy temperature. *Agron. J.*, 76, 607-610, 1984.
112. **Nieuwenhuis G.J.A., Smidt E.H., Thunnissen H.A.M.**, Estimation of regional evapotranspiration of arable crops from thermal infrared images. *Int. J. Remote Sensing*, 6, 8, 1319-1334, 1985.
113. **Noborio K., McInnes K.J.**, Thermal conductivity of salt-affected soils. *Soil Sci.Soc.Am. J.*, 57, 329-334, 1993.
114. **Olejnik J., Kędziora A.**, A model for heat and water balance estimation and its application to land use and climate variation. *Earth Surface Processes Landforms*, 16, 601-617, 1991.
115. **Olszta W.**, Simulation of transpiration and leaf temperature for grassland with varying soil moisture condition. Wageningen (The Netherlands). The Winand Staring Centre. Interne mededeling, 6, 1989.
116. **O'Toole J.C. and Hatfield J.L.**, Effect of wind on the crop water stress index derived by infrared thermometry. *Agron. J.*, 75, 811-817, 1983.
117. **Pandey R.K., Herrera W.A., Pendleton J.W.**, Drought response of grain legumes under irrigation gradient, II. Plant water status and canopy temperature. *Agron. J.*, 76, 553-557, 1984.
118. **Paulson C.A.**, The mathematical representation of wind speed and temperature profiles in the unstable atmospheric surface layer. *J. Appl. Meteorol.*, 9, 857-861, 1970.
119. **Penman H.L., Schofield R.K.**, Some physical aspects of assimilation and transpiration. *Sympos. Soc. Exper. Biol.*, 5, 115-129, 1951.
120. **Penman H.L.**, Evaporation, An introductory survey. *Neth. J. Agric. Sci.*, 9, 9-29, 1956.
121. **Penman H.L.**, Natural evaporation from open water, bare soil and grass. *Proc. Roy. Soc. London, A* 193, 120-146, 1948.
122. **Penman H.L.**, Vegetation and hydrology. *Tech. Comm. 53, p.124, Commonwealth Bureau. of Soils, Harpenden, Herts., England, 1963.*
123. **Piotrowski J., Rogalski A.**, Detektory podczerwieni dla urządzeń zobrazowania termalnego. Materiały Sympozjum Naukowego „Technika przetwarzania obrazu”, 22-23 września Warszawa, 215-225, 1988.
124. **Price J.C.**, Estimation of regional scale evapotranspiration through analysis of satellite thermal-infrared data. *IEEE Transactions of Geoscience and Remote Sensing of Environment*, 18, 75-89, 1982.

125. **Price J.C.**, The contribution of thermal data in Landsat multispectral classification. *Photog. Eng. and Remote Sens.*, 47, 229-236, 1981.
126. **Price J.C.**, The potential of remotely sensed thermal infrared data to infer surface soil moisture and evaporation. *Water Resour. Res.*, 16, 787-795, 1980.
127. **Qiu, G.Y., H. Shimizu, Y. Gao, K. Omasa, and K. Tobe**, Estimation of aerodynamic and soil resistance using temperature related approach. *Proc. of Annual Meeting of the Society of Agricultural Meteorology of Japan*, 191, 2001.
128. **Qiu, G.Y., J. Ben-Asher, T. Yano, and K. Momii**, Estimation of soil evaporation using the differential temperature method. *Soil Sci. Soc. Am. J.*, 63, 1608-1614, 1999.
129. **Qiu, G.Y., S. Sase, P. Shi, G. Ding**, . Theoretical analysis and experimental verification of a remotely measurable plant transpiration transfer coefficient. *JARQ-Japan Agricultural Research Quarterly*, 37, 141-149, 2003.
130. **Qiu, G.Y., T. Yano, and K. Momii**, An improved methodology to measure evaporation from bare soil based on comparison of surface temperature with a dry soil. *J. Hydrol.*, 210, 93-105, 1998.
131. **Reginato R.J., Jackson R.D., Pinter P.J.**, Evapotranspiration calculation from remote multispectral and ground station meteorological data. *Remote Sens. Environ.*, 18, 75-89, 1985.
132. **Reginato R.J.**, Field quantification of crop water stress. *Transactions of ASAE*, 26, 772-775, 1983.
133. **Rewut I.B.**, *Fizyka gleby*, PWRiL, Warszawa, 1980.
134. **Rudowski G., Pietrzak E.**, *Opracowanie metody określania wpływu atmosfery na mierzoną temperaturę radiacyjną. Sprawozdanie IGiK*, Warszawa, 1986.
135. **Rudowski G.**, *Termowizja i jej zastosowanie*. WKiŁ, Warszawa, 1978.
136. **Ryszkowski L., Kędziora A.**, Impact of agricultural landscape structure on energy flow and matter cycling. *Landscape Ecology*, 1(2), 85-94, 1987.
137. **Sala A.**, *Radiacyjna wymiana ciepła*. WNT, Warszawa, 1982.
138. **Sawicki J.**, *Kierunki sukcesji zbiorowisk roślinnych w zależności od sposobu i intensywności gospodarowania w warunkach wieloletniego użytkowania kośnego i pastwiskowego. Sprawozdanie końcowe z projektu badawczego nr 5 S312 030 04, Katedra Łąkarstwa Wydział Rolniczy AR w Lublinie*, 1996.
139. **Seguin B., Brunet Y., Perrier A.**, Estimation of evaporation, a review of existing methods and recent developments. *E.G.S. Meeting Symposium on Evaporation*, Leeds, August 1982.
140. **Seguin B., Itier B.**, Using midday surface temperature to estimate daily evaporation from satellite thermal I.R. data. *Int. J. Remote Sens.*, 4, 371-384, 1983.
141. **Sharma M.L.**, *Estimating evapotranspiration. Advances in Irrigation*. Academic Press, New York, 213-281, 1985.
142. **Sikora E.**, *Zależność właściwości cieplnych zagregowanych próbek glebowych od wielkości agregatów i uwilgotnienia. Praca doktorska*. AR Lublin, 1983.
143. **Słownik fizyczny**. Praca zbiorowa. WP, Warszawa, 1984.
144. **Soczyńska U.**, *Podstawy hydrologii dynamicznej*. Wyd. UW, Warszawa, 1993.
145. **Soer G.J.R.**, Estimation of Regional Evapotranspiration and soil moisture conditions using remotely sensed crop surface temperatures. *Remote Sens. Environ.*, 9, 27-45, 1980.
146. **Soer G.J.R.**, The TERGRA model - a mathematical model for the simulation of the daily behaviour of crop surface temperature and actual evapotranspiration. *NIWARS publ.* 46, Delft, 1977.
147. **Sokolowska Z.**, *Informacja prywatna*, 1998.

148. **Staniszewski B.**, Wymiana ciepła. PWN, Warszawa, 1979.
149. **Steinmetz S., Lagouarde J. Delecolle R., Guerif M., Seguin B.**, Evapotranspiration and water stress using thermal infrared measurements. A general review and a case study on winter durum wheat in southern France. Materials of International Symposium on „Physiology / Breeding of winter cereals for mediterranean environments”, Mountpellier, France, July 3-6, 1989.
150. **Stewart R.B., Rouse W.R.**, A simple method for determining the evaporation from shallow lakes and ponds. *Water Resour. Res.* 12, 623-628, 1976.
151. **Stockle C.O. and Dugas W.A.**, Evaluating canopy temperature-based indices for irrigation scheduling. *Irrig. Sci.*, 13, 31-37, 1992.
152. **Stoll A.M., Hardy J.D.**, A method for measuring radiant temperatures of the environment. *J. Appl. Physiol.*, 5, 117-124, 1952.
153. **Stone L.R., Horton M.L.**, Estimating ewapotranspiration using canopy temperatures, Field evaluation. *Agron. J.*, 66, 450-454, 1974.
154. **Sugita M., Brutsaert W.**, Daily evaporation over a region from lower boundary layer profiles measured with radiosondes. *Water Resour. Res.*, 27, 5, 747-752, 1991.
155. **Suleiman, A.A., and J.T. Ritchie.** Modeling soil water redistribution during second-stage evaporation. *Soil Sci. Soc. Am. J.*, 67, 377-386, 2003.
156. **Suleiman, A.A., and R. Crago,** Hourly and daytime evapotranspiration from grassland using radiometric surface temperature. *Agron. J.*, 96, 484-390, 2004.
157. **Szeicz G., Long I.F.**, Surface resistance of canopies. *Water Resour. Res.*, 5, 622-633, 1969,
158. **Tanner S.B.**, Plant temperatures. *Agron. J.*, 55, 210-211, 1963.
159. **Thofelt L.**, Studies on leaf temperature recorded by direct measurement and by thermography. *Acta Universitatis Upsaliensis*, Uppsala 1975.
160. **Thom A.S., Oliver H.R.**, On Penman’s equation for estimating regional evaporation. *Quart. J. R. Met. Soc.*, 103, 345-357, 1977.
161. **Tubaileh A.S., Sammis T.W. and Lugg D.G.**, Utilization of thermal infrared thermometry for detection of water stress in spring barley. *Agric. Water Management.*, 12, 75-85, 1986.
162. **Turski R., Domżał H., Borowiec J., Flis-Bujak M., Misztal M.**, Gleboznawstwo – ćwiczenia dla studentów wydziałów rolniczych. AR, Lublin, 1997.
163. **Turski R., Hetman J., Słowińska-Jurkiewicz A.**, Podłoża stosowane w ogrodnictwie szklarniowym *Rocz. Nauk Rol.*, 180, Seria D, 1–88, 1980.
164. **Turski R., Martyn W.**, Heat capacity of chernozms and brown soils formed from loesses of the Lublin Upland. *Polish. Soil Sci.*, 8, 2, 131–136, 1975.
165. **Usowicz B.**, Application of themocouples for the recording of air humidity and temperature profile and soil temperature. *Zesz. Probl. Post. Nauk Roln.*, 346, 133-140, 1987.
166. **Usowicz B.**, Ciepłne właściwości wybranych podłoży ogrodniczych. *Zesz. Probl. Post. Nauk Roln.*, 429, 305–313, 1996.
167. **Usowicz B.**, Evaluation of methods for soil thermal conductivity calculations. *Int. Agrophysics*, 9(2), 109–113, 1995.
168. **Usowicz B.**, Modelowe badania wpływu wilgotności gleby na kształtowanie się temperatury w profilu glebowym. Praca doktorska. AR Lublin, 1991.
169. **Usowicz B.**, Soil Thermal Properties Software Package. Copyright Institute of Agrophysics PAS, Lublin, 1992a.
170. **Usowicz B.**, Statistical - physical model of thermal conductivity in soil. *Polish J. Soil Sci.*, XXV/1, 25–34, 1992.

171. **Usowicz B.**, Statistical-physical model of thermal conductivity in soil. *Polish J. Soil Sci.*, XXV/1, 27-34, 1992.
172. **Usowicz B.**, Time and space variability of soil thermal properties in cultivated fields. *Proc. 16th World Congress of Soil Science, Montpellier, France, 20–26 August 1998.*
173. **Usowicz B.**, Estimation of soil thermal properties. *Acta Agrophysica*, 72, 135-165, 2002.
174. **Uziak, S., Bogda A., Chodak T., Cieśla W., Komornicki T., Stach L., Wilgat M.**, Clay minerals of selected loess soils. *Rocz. Gleb.*, 3, 59–77, 1987.
175. **Van Bavel C.H.M., Ehrler W.L.**, Water loss from sorghum field and stomatal control. *Agron. J.*, 60, 84-86, 1968.
176. **Van Bavel C.H.M.**, Potential evaporation, the combination concept and its experimental verification. *Water Resour. Res.*, 2 (3), 455-464, 1966.
177. **Van de Griend A.A., Owe M. Groen M. and Stoll M.P.**, Measurement and spatial variation of thermal infrared surface emissivity in a savanna environment. *Water Resour. Res.*, 27, 371-379, 1991.
178. **Walczak R., Reszetin O.L., Czachor H.**, Transport of water and heat in soil. *Polish J. Soil Sci.*, VII, 1, 134, 1974.
179. **Walczak R.**, Basic problems of mass and energy transfer in the soil-plant-atmosphere system. *Zesz. Probl. Post. Nauk Roln.*, 346, 11–22, 1987.
180. **Walczak R.T., Mazurek W., Baranowski P.**, Teledetekcja w badaniach agrofizycznych. *Materiały III Letniej Szkoły "Fizyka z elementami agrofizyki"*, Lublin 23-25 września 1991, 1-24.
181. **Walczak R.T., Baranowski P., Mazurek W.**, The impact of meteorological conditions on radiation temperature (range 8-13 μm) of plant cover under different water conditions. *5th International Conference on Physical Properties of Agricultural Materials*, Paper No. 93-1008, Bonn, 1993.
182. **Walczak R.T., Sławiński C., Sobczuk H.A., Gliński J.**, Aspekt hydrologiczny w modelu EURO-ACCESS (Agroclimatic Change and European Soil Suitability). *Acta Agrophysica* 9, 1998.
183. **Walczak R.T.**, Modelowe badania zależności retencji wodnej od parametrów fazy stałej gleby. *Problemy Agrofizyki* 41, 1984.
184. **Walczak R.T.**, Określenie zależności między wilgotnością gleby a temperaturą radiacyjną pokrywającej ją roślinności łąkowej na podstawie laboratoryjnych badań wazonowych. (Temat objęty planem koordynacyjnym CPBP nr 01,20 "Rozwój i wykorzystanie badań kosmicznych" podprogramu 4 "Teledetekcja", poz. 4,2,2,6) - I i II etap prac w latach 1987-1988, Instytut Agrofizyki PAN, Lublin.
185. **Walczak R.T.**, Struktura bilansu promieniowania i stosunki termiczno-wilgotnościowe gleby. *Projekt badawczy nr PB 1679/5/91*, Instytut Agrofizyki PAN, Lublin 1994.
186. **Walker G.K., Hatfield J.L.**, Stress measurement using foliage temperatures. *Agron. J.*, 75, 623-629, 1983.
187. **Wanjura D.F., Kelly C.A., Wendt C.W. and Hatfield J.L.**, Canopy temperature and water stress of cotton crops with complete and partial ground cover. *Irrig. Sci.*, 5, 37-46, 1984.
188. **Wiegand C.L., Namken L.N.**, Influence of plant moisture stress, solar radiation, and air temperature on cotton leaf temperatures. *Agron. J.*, 58, 582-586, 1966.
189. **Wierchoś J.**, Analiza fizykochemicznych warunków tworzenia się i trwałości struktury glebowej. *Praca doktorska. IUNG Puławy*, 1989.

190. **Witkowska-Walczak B.**, Evaporation from aggregates of a podzolic, a light brown and a chernozem soil. *Int. Agrophysics*, 9, 49-54, 1995.
191. **Wright G.G. and Morrice J.G.**, Potato crop distribution and subdivision on soil type and potential water deficit. An integration of satellite imagery and environmental spatial database. *Int. J. Remote Sens.*, 9, 683-699, 1988.
192. **Wright J.L.**, New evapotranspiration crop coefficients. *J. Irrig. Drain.*, 108, 57-74, 1982.
193. **Zhang, X., D. Pei, and C. Hu**, Conserving groundwater for irrigation in the North China Plain. *Irrig. Sci.*, 21, 159-166, 2003.

9. SUPPLEMENT

9.1. A procedure of preparation of basic input data for the model

The procedure of preparation of input data for the model consists in measurement or determination of basic physical parameters of the soil, *i.e.* the mineralogical composition of the soil, the granulometric composition, the density of the solid phase, the soil bulk density, the organic matter content, the temperature, the soil water potential, the water content corresponding to the field water capacity or to the wilting point of plants, gas pressure in the soil, the soil water content and the soil salinity. This complete set of data enables to determine thermal properties of soil, which take into account the heat flow by conduction through the components of the solid, liquid and gaseous phases as well as by convection. If temperature and potential gradients in the soil are small, it can be assumed that any heat flow takes place by conduction. In this case, the number of input data can be limited to the mineralogical composition of the soil, the density of the solid phase, the soil bulk density, the organic matter content, the soil temperature and the soil water content. Prepared data from measurement should be transmitted into a computer and written to a file in ASCII code. The data are separated using space sign [169].

The mineralogical composition is derived using X-ray diffraction method [19] or can be roughly evaluated from the grain-size distribution, assuming that soil fractions larger than 0.02 mm contain mainly quartz particles. It is assumed that fractions smaller than 0.02 mm contain other materials. The evaluation of the mineralogical composition from the grain size distribution has its justification in performed comparative measurements [167,172]. It should be noticed that the specific surface is a good indicator for this kind of determination of the mineralogical composition, however its values shouldn't exceed $50 \text{ (m}^2\text{g}^{-1}\text{)}$ [147]. Some methods of measurement and determination of other physical parameters in soil are presented in the manuscript of Turski *et al.* – exercises for the students of agricultural universities [162].

The input data formats, accepted by the program, which calculates the thermal properties of the soil are presented in Tables 4. 5. 6. The first two cells of the first line in the upper left corners of these tables contain the numbers of data and numbers of columns, respectively. The second lines of the Tables contain the abbreviations referring to the number of data, the depth and basic physical

parameters of the soil, succeeding lines contain the input data. The explanation of abbreviations included in the second lines of the Tables:

Abbreviation Unit Explanation of abbreviations

INDE - - number of data

DEPTH (m) - depth

TEMPE ($^{\circ}\text{C}$) – soil temperature

PARDE (Mg m^{-3}) – bulk density of solid phase

BULDE (Mg m^{-3}) – bulk density of soil

%_QUA (%) – percent content of quartz in unit volume

%_MIN (%) – percent content of other minerals in unit volume

%_ORG (%) – percent content of organic matter in unit volume

WATER ($\text{m}^3 \text{m}^{-3}$) – content of water in unit volume of soil

ORGAN ($\text{m}^3 \text{m}^{-3}$) – content of organic matter in unit volume of soil

SOLID ($\text{m}^3 \text{m}^{-3}$) – content of solid phase in unit volume of soil

GAS_PR (kPa) – gas pressure in soil (equal to atmospheric pressure)

WAT_PR (kPa) – water potential in soil

WILT ($\text{m}^3 \text{m}^{-3}$) – water content corresponding to the field water capacity or to the wilting point of plants.

The zero values in the last three columns of Tables 4. 5. 6 mean, that the heat conduction by convection is not considered to determine the thermal conductivity of soil.

Table 4. Format of input data. 100% organic matter (data from de Vries study, [39])

12	8						
INDE	DEPTH	TEMPE	ORGAN	WATER	WILT	WAT_PR	GAS_PR
1	0	5	0.21	0.79	0	0	0
2	0	5	0.292	0.676	0	0	0
3	0	5	0.171	0.66	0	0	0
4	0	5	0.244	0.614	0	0	0
5	0	5	0.169	0.399	0	0	0
6	0	5	0.248	0.38	0	0	0
7	0	5	0.087	0.322	0	0	0
8	0	5	0.169	0.25	0	0	0
9	0	5	0.095	0.229	0	0	0
10	0	5	0.088	0.135	0	0	0
11	0	5	0.256	0.032	0	0	0
12	0	5	0.164	0.023	0	0	0

Table 5. Format of input data. Mineral soil (data from de Vries study, [39])

INDE	DEPTH	TEMPE	SOLID	%_QUA	%_MIN	%_ORG	WATER	WILT	WAT_PR	GAS_PR
1	0	5	0.66	60.6	39.4	0	0.212	0	0	0
2	0	5	0.71	60.6	39.4	0	0.203	0	0	0
3	0	5	0.632	60.6	39.4	0	0.184	0	0	0
4	0	5	0.705	60.6	39.4	0	0.117	0	0	0
5	0	5	0.665	60.6	39.4	0	0.112	0	0	0
6	0	5	0.691	60.6	39.4	0	0.102	0	0	0
7	0	5	0.631	60.6	39.4	0	0.101	0	0	0
8	0	5	0.71	60.6	39.4	0	0.05	0	0	0
9	0	5	0.665	60.5	39.4	0	0.047	0	0	0
10	0	5	0.631	60.6	39.4	0	0.043	0	0	0
11	0	5	0.727	60.6	39.4	0	0.026	0	0	0
12	0	5	0.705	60.6	39.4	0	0.025	0	0	0
13	0	5	0.665	60.6	39.4	0	0.024	0	0	0
14	0	5	0.631	60.6	39.4	0	0.021	0	0	0
15	0	5	0.71	60.6	39.4	0	0.004	0	0	0
16	0	5	0.665	60.6	39.4	0	0.004	0	0	0
17	0	5	0.629	60.6	39.4	0	0.003	0	0	0

Table 6. Format of input data. Mineral soil with organic matter

INDE	DEPT	TEMP	PARD	BULD	WATE	%_QU	%_MI	%_OR	WIL	WAT_P	GAS_P
1	0	25	2.65	1.18	0.123	66	32	2	0	0	0
2	0	25	2.65	1.27	0.156	66	32	2	0	0	0
3	0	25	2.65	1.33	0.172	66	32	2	0	0	0
4	0	25	2.65	1.37	0.185	66	32	2	0	0	0
5	0	25	2.65	1.48	0.207	66	32	2	0	0	0
6	0	25	2.65	1.53	0.220	66	32	2	0	0	0
7	0	25	2.65	1.50	0.210	66	32	2	0	0	0
8	0	25	2.65	1.48	0.197	66	32	2	0	0	0
9	0	25	2.65	1.46	0.193	66	32	2	0	0	0
10	0	25	2.65	1.43	0.190	66	32	2	0	0	0
11	0	25	2.65	1.44	0.194	66	32	2	0	0	0

10. ELABORATION OF ALGORITHM OF THE PROGRAMME FOR ESTIMATION OF THERMAL PROPERTIES OF SOIL AND GROUND

Each calculating program is written according to a specific algorithm, *i.e.* a rule or a procedure of solving a considered problem. A graphical form of the program for estimation of the thermal properties of soil and ground is presented in Fig. 8. It shows the network of the program's realization. This program presents the information chart, it opens the data file from a disk, reads them, places data into appropriate formulas and data matrices, which are used for further calculations or for checking the conditions, it conducts calculations according to the mathematical formulae, derived theoretically, calculating the thermal conductivity, the heat capacity and the thermal diffusivity. To consider the heat conduction by convection, the thermal conductivity of the water vapor is taken into account to derive the thermal conductivity of the air λ_a . After calculation, the data are displayed on the screen and written into the computer disk.

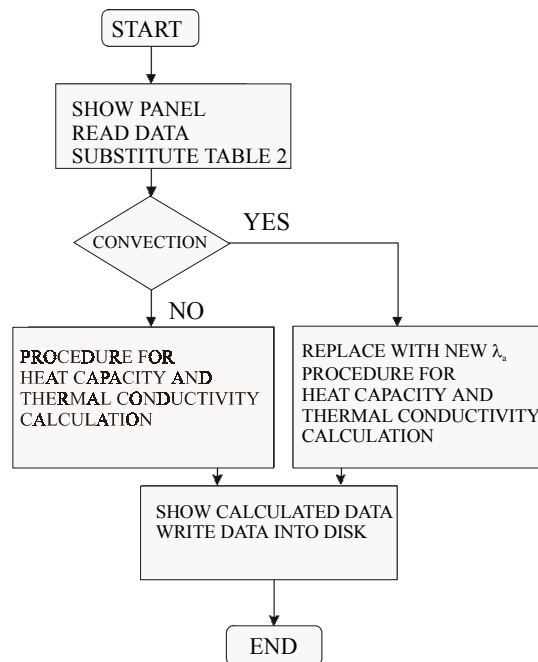


Fig. 45. Scheme of realization of the program for determination of thermal properties of soil.

11. ELABORATION OF COMPUTER PROGRAMME FOR CALCULATION OF THERMAL PROPERTIES OF SOIL AND GROUND

The computer program for estimation of thermal properties of soil and ground: „SOIL THERMAL PROPERTIES SOFTWARE – 2.0” has been written on the base of the previous version of „SOIL THERMAL PROPERTIES SOFTWARE” program [169], which had been elaborated in frame of the international research project: "ASSESSMENT OF SOIL STRUCTURE IN AGRICULTURAL SOIL" realized by Austria, Czech Republic, Poland, Slovakia and Hungary (International Agrophysics, 1993). In the programme: „SOIL THERMAL PROPERTIES SOFTWARE – 2.0” the procedures were changed of determination of the radii of spheres and calculation of the thermal conductivity for given values of soil saturation.

The computer programme for calculation of thermal properties of soil and ground was written in Turbo Basic programme for DOS. The programme was compiled and written to a file called thermal.exe. This programme is available at the author’s private site: <http://www.ipan.lublin.pl/~usowicz/>

11.1. Maintenance of thermal.exe programme.

The program can be started from a floppy disk or a hard disk. To start this programme the name of the executable file should be typed, e.g a:\thermal.exe followed by pressing the Enter key. The folder with basic information about the programme will be displayed. After pressing any key, the next page will be displayed with proposition of typing the name of reading file, e.g. "INPUT NAME OF READING FILE " sand.dat. After typing the file name the Enter key should be pressed. The program will ask if the flow of heat as water vapor is to be included: "INCLUDE THERMAL VAPOR DIFFUSIVITY, IF YES – PRESS (Y), IF NO – PRESS ANY KEY". If the key “Y” is pressed, an encouragement is displayed to choose the formula for water vapor diffusivity calculation „BY – de VRIES; PRESS (V)” or "BY – DORSEY; PRESS (D)". An appropriate formula is selected by choosing „V” or „D” key. From that moment the programme starts to calculate the thermal properties. A page is displayed, informing about the number of steps: "WAIT "; R; " STEPS", the actually realized step: "NOW IS "; X; " STEP" and the value of the sphere radius: „RK =”. After completing all the steps

of calculation, the programme ask if the calculated data are to be displayed, if yes press „Y”, if not press any other key "DO YOU WANT TO SEE DATA, IF YES – PRESS (Y), IF NO – PRESS ANY KEY". If the number of data is too large to be fitted on the screen, the prompt for continuation is displayed, if yes press any key, if not press “N” key: STRIKE ANY KEY TO CONTINUE OR (N) TO STOP. After the data overview is stopped or after all the data are overviewed, a prompt appears to give the name of the file to which the calculated data will be stored on a hard disk or a floppy disk, *e.g.* "INPUT NAME OF OUTPUT FILE " C:\sand.the, which should be followed by pressing the Enter key. A note will appear informing that the data are store to the file sand.the on disk C:\: "DATA IS WRITING TO FILE " C:\sand.the.

When any key is pressed after the question is displayed if to consider the heat flow through the water vapour: "INCLUDE THERMAL VAPOR DIFFUSIVITY, IF YES – PRESS (Y), IF NO – PRESS ANY KEY", the programme starts to calculate the thermal properties and shows a page with number of steps. In this case other procedures of program realization are the same as presented before.

Some cases of incorrect conduct of thermal.exe programme can occur when reading the input data. An incorrect name of data will cause stopping the programme and the announcement about the error will be displayed. In this case the whole process of programme execution should be repeated. It can occur that during reading the input data from a file, the program stops reading this file. Such behaviour of the programme informs us about the error in the input data. It can be a letter, a comma, empty lines or other signs which do not fit the format of input data. In this case the input data should be corrected and the calculation process of thermal properties should be repeated from the beginning.

The data format displayed on the screen is as follows:

```
INDE DEPTH TEMPE SOLID QUART MINER ORGAN WATER AIR CONDOC CAPACITY DIFFUSI
##### #.### ##.## #.### #.### #.### #.### #.### #.### ##.### #.###^# #.###^#
1 0.000 5.00 0.660 0.400 0.260 0.000 0.212 0.128 2.239 2.210E+06 1.013E-06
2 0.000 5.00 0.710 0.430 0.280 0.000 0.203 0.087 2.463 2.273E+06 1.084E-06
3 0.000 5.00 0.632 0.383 0.249 0.000 0.184 0.184 2.055 2.037E+06 1.009E-06
4 0.000 5.00 0.705 0.427 0.278 0.000 0.117 0.178 2.284 1.904E+06 1.200E-06
5 0.000 5.00 0.665 0.403 0.262 0.000 0.112 0.223 2.004 1.802E+06 1.112E-06
Abbreviation Unit Explanation of abbreviations
```

INDE - - number of data
 DEPTH (m) - depth
 TEMPE ($^{\circ}\text{C}$) – soil temperature
 SOLID ($\text{m}^3 \text{m}^{-3}$) – content of solid phase in unit volume of soil
 QUART ($\text{m}^3 \text{m}^{-3}$) – content of quartz in unit volume
 MINER ($\text{m}^3 \text{m}^{-3}$) – content of other minerals in unit volume
 ORGAN ($\text{m}^3 \text{m}^{-3}$) – content of organic matter in unit volume
 WATER ($\text{m}^3 \text{m}^{-3}$) – content of water in unit volume of soil
 AIR ($\text{m}^3 \text{m}^{-3}$) – content of air in unit volume of soil
 CONDUCT ($\text{Wm}^{-1}\text{K}^{-1}$) – thermal conductivity
 CAPACITY ($\text{Jm}^{-3}\text{K}^{-1}$) – heat capacity
 DIFFUSI (m^2s^{-1}) – thermal diffusivity

The data stored into the disk have ASCII format, this format is in agreement with the format of GEOEAS, VARIOWIN, GEOPACK programme packages and is presented in the following example:

Sand.the

12

INDEX NUMBER

DEPTH (m)

TEMPERA (C)

SOILD (Mg/m^3)

QUATRZ (m^3/m^3)

MINERAL (m^3/m^3)

ORGANIC (m^3/m^3)

WATER (m^3/m^3)

AIR (m^3/m^3)

CONDUCT (W/mK)

CAPACITY ($\text{J}/\text{m}^3\text{K}$)

DIFFUSION (m^2/s)

```

1 0.000 5.00 0.660 0.400 0.260 0.000 0.212 0.128 2.239 2.210E+06 1.013E-06
2 0.000 5.00 0.710 0.430 0.280 0.000 0.203 0.087 2.463 2.273E+06 1.084E-06
3 0.000 5.00 0.632 0.383 0.249 0.000 0.184 0.184 2.055 2.037E+06 1.009E-06
4 0.000 5.00 0.705 0.427 0.278 0.000 0.117 0.178 2.284 1.904E+06 1.200E-06
5 0.000 5.00 0.665 0.403 0.262 0.000 0.112 0.223 2.004 1.802E+06 1.112E-06
  
```

Explanation of abbreviations:

line 1: file title

line 2: number of variables

lines from 3 to 14: names of variables

next lines: data matrix

Abbreviation Unit Explanation of abbreviations

INDEX- - number of data

DEPTH (m) - depth

TEMPERA ($^{\circ}\text{C}$) – soil temperature

BULDE (Mg m^{-3}) – bulk density of soil

SOLID ($\text{m}^3 \text{m}^{-3}$) – content of solid phase in unit volume of soil

QUARTZ ($\text{m}^3 \text{m}^{-3}$) – content of quartz in unit volume

MINERAL ($\text{m}^3 \text{m}^{-3}$) – content of other minerals in unit volume

ORGANIC ($\text{m}^3 \text{m}^{-3}$) – content of organic matter in unit volume

WATER ($\text{m}^3 \text{m}^{-3}$) – content of water in unit volume of soil

AIR ($\text{m}^3 \text{m}^{-3}$) – content of air in unit volume of soil

CONDUCT ($\text{W m}^{-1}\text{K}^{-1}$) – thermal conductivity

CAPACITY ($\text{J m}^{-3}\text{K}^{-1}$) – heat capacity

DIFFUSION (m^2s^{-1}) – thermal diffusivity

Addresses of the Authors:

Piotr Baranowski

Bogusław Usowicz

Ryszard T. Walczak

Wojciech Mazurek

Instytut Agrofizyki im. Bohdana Dobrzańskiego PAN

ul. Doświadczalna 4. 20-290 Lublin

e-mail: pbaranow@demeter.ipan.lublin.pl